AD-A072 057 ATLANTIC SCIENCE CORP INDIAN HARBOUR BEACH FL F/G 17/2.1
AN INVESTIGATION INTO THE NOISE INTERFERENCE PROBLEMS AT LOGAN --ETC(U)
APR 79 B J LIPOFSKY, R B BENT, S K LLEWELLYN DOT-FA77WAI-774
UNCLASSIFIED FAA-RD-79-58 NL

1 OF 2
AD A072057

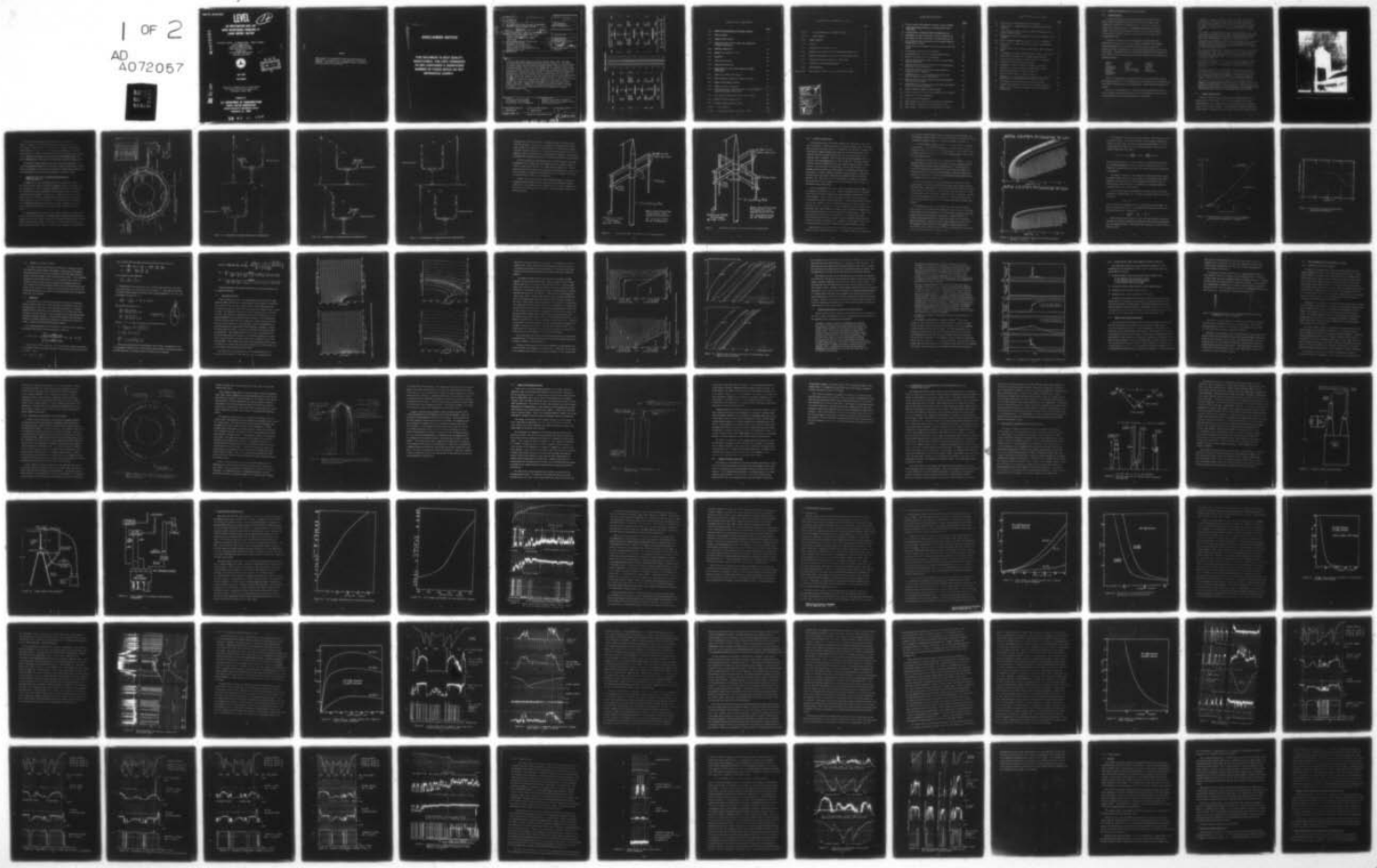

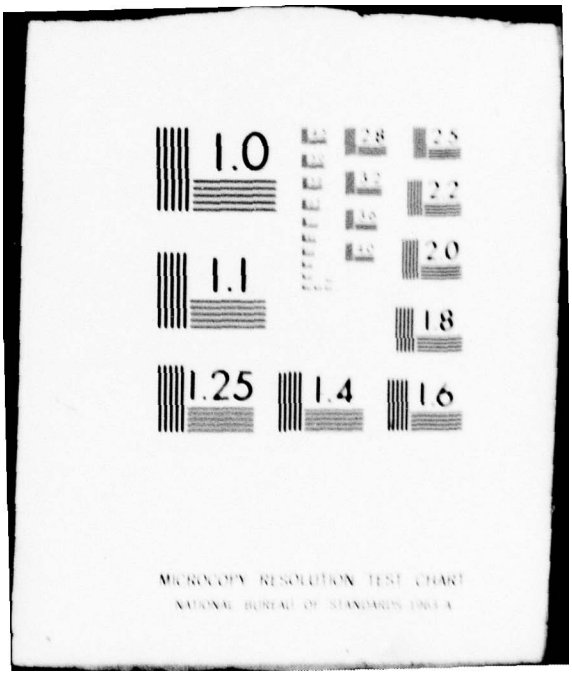
1.0
1.1
1.25
1.4
2.8
2.5
2.2
2.0
1.8
1.6
MICROCOPY RESOLUTION TEST CHART
NATIONAL BUREAU OF STANDARDS 1963-A

Report No. FAA RD-79-58

LEVEL

B.S. 12

AN INVESTIGATION INTO THE NOISE INTERFERENCE PROBLEMS AT LOGAN AIRPORT, BOSTON

Dr. Barton J. Lipofsky Dr. Rodney B. Bent Sigred K. Llewellyn
Office of Naval Research
Atlantic Scientific Corporation
Indian Harbour Beach, Fla. 32937
and Jack Leahy
FAA New England Regional Office
Burlington, Mass. 01803

Harbor

April 1979

Final Report

Prepared for

U.S. DEPARTMENT OF TRANSPORTATION
FEDERAL AVIATION ADMINISTRATION
Systems Research & Development Service
Washington, D.C. 20590

NOTICE

This document is disseminated under the sponsorship of the Department of Transportation in the interest of information exchange. The United States Government assumes no liability for its contents or use thereof.

DISCLAIMER NOTICE

THIS DOCUMENT IS BEST QUALITY PRACTICABLE. THE COPY FURNISHED TO DDC CONTAINED A SIGNIFICANT NUMBER OF PAGES WHICH DO NOT REPRODUCE LEGIBLY.

Technical Report Documentation Page

1. Report No.	2. Government Accession No.	3. Recipient's Catalog No.
FAA-RD-79-58		196 p.

4. Title and Subtitle
AN INVESTIGATION INTO THE NOISE INTERFERENCE PROBLEMS AT LOGAN AIRPORT, BOSTON.

5. Report Date
April 1979

6. Performing Organization Code

7. Author(s)
Barton J. Lipofsky, Rodney B. Bent, Jack K. Llewellyn and Leahy D.

8. Performing Organization Report No.

9. Performing Organization Name and Address
Office of Naval Research
Atlantic Science Corporation
1901 N. A1A
Indian Harbour Beach, Florida 32937

10. Work Unit No. (TRAIS)

11. Contract or Grant No.
DOT-FA77WA1-774

12. Sponsoring Agency Name and Address
Department of Transportation
Federal Aviation Administration
Systems Research & Development Service
Washington, DC 20590

13. Type of Report and Period Covered
Final report,
Aug 1977 - Apr 1979

14. Sponsoring Agency Code
ARD-350

15. Supplementary Notes

16. Abstract

A severe noise problem exists at many air traffic control tower locations in the VHF receivers during certain severe weather conditions. The problem has theoretically been investigated for Boston Logan Airport and has been found to be most likely related to corona discharge from air terminals close to the receiving antennas. The effect of the charge that can accumulate on the radome has not yet been well identified. The charge from raindrops transferred to the antennas seems unlikely as a noise source. Elimination techniques using static dischargers at some ATCT locations have been analyzed and are criticized. A detailed experimental study of the effect of corona noise on voice communications has been carried out using receivers and antennas which are representative of equipment in current use at air traffic control centers. In this part of the investigation a controlled discharge was induced at a sharp point in order to simulate the corona noise problems which have been reported during severe weather conditions. Suggestions for possible corrective procedures include relocation of the air terminals or placing corona balls over the tips of the air terminal. The latter modifications will also enhance the lightning protection capabilities.

17. Key Words	18. Distribution Statement
lightning, corona discharge, air terminals, VHF antennas, corona noise, static dischargers	Document is available through the National Technical Information Service Springfield, VA 22151

19. Security Classif. (of this report)	20. Security Classif. (of this page)	21. No. of Pages	22. Price
UNCLASSIFIED	UNCLASSIFIED	105	

Form DOT F 1700.7 (8-72) Reproduction of completed page authorized

METRIC CONVERSION FACTORS

Approximate Conversions to Metric Measures

Symbol	When You Know	Multiply by	To Find	Symbol
	LENGTH			
in	inches	*2.5	centimeters	cm
ft	feet	30	centimeters	cm
yd	yards	0.9	meters	m
mi	miles	1.6	kilometers	km
	AREA			
in^2	square inches	6.5	square centimeters	cm^2
ft^2	square feet	0.09	square meters	m^2
yd^2	square yards	0.8	square meters	m^2
mi^2	square miles	2.6	square kilometers	km^2
	acres	0.4	hectares	ha
	MASS (weight)			
oz	ounces	28	grams	g
lb	pounds	0.45	kilograms	kg
	short tons (2000 lb)	0.9	tonnes	t
	VOLUME			
tsp	teaspoons	5	milliliters	ml
Tbsp	tablespoons	15	milliliters	ml
fl oz	fluid ounces	30	milliliters	ml
c	cups	0.24	liters	l
pt	pints	0.47	liters	l
qt	quarts	0.95	liters	l
gal	gallons	3.8	liters	l
ft^3	cubic feet	0.03	cubic meters	m^3
yd^3	cubic yards	0.76	cubic meters	m^3
	TEMPERATURE (exact)			
°F	Fahrenheit temperature	5/9 (after subtracting 32)	Celsius temperature	°C

*1 in = 2.54 (exactly). For other exact conversions and more detailed tables, see NBS Misc. Pub. 286, Units of Weights and Measures, Price $2.25, SD Catalog No. C13.10:286.

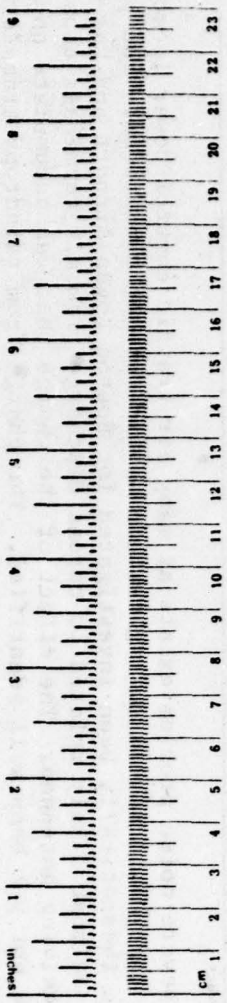

Approximate Conversions from Metric Measures

Symbol	When You Know	Multiply by	To Find	Symbol
	LENGTH			
mm	millimeters	0.04	inches	in
cm	centimeters	0.4	inches	in
m	meters	3.3	feet	ft
m	meters	1.1	yards	yd
km	kilometers	0.6	miles	mi
	AREA			
cm^2	square centimeters	0.16	square inches	in^2
m^2	square meters	1.2	square yards	yd^2
km^2	square kilometers	0.4	square miles	mi^2
ha	hectares (10,000 m^2)	2.5	acres	
	MASS (weight)			
g	grams	0.035	ounces	oz
kg	kilograms	2.2	pounds	lb
t	tonnes (1000 kg)	1.1	short tons	
	VOLUME			
ml	milliliters	0.03	fluid ounces	fl oz
l	liters	2.1	pints	pt
l	liters	1.06	quarts	qt
l	liters	0.26	gallons	gal
m^3	cubic meters	35	cubic feet	ft^3
m^3	cubic meters	1.3	cubic yards	yd^3
	TEMPERATURE (exact)			
°C	Celsius temperature	9/5 (then add 32)	Fahrenheit temperature	°F

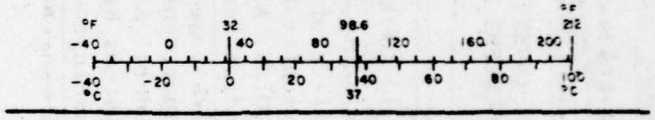

TABLE OF CONTENTS

TABLE OF CONTENTS (con't)

LIST OF FIGURES

LIST OF FIGURES (con't)

1.0 NOISE INTERFERENCE PROBLEM AREAS

1.1. Noise Problem

A severe noise problem exists at numerous Air Traffic Control Tower (ATCT) locations in the VHF/UHF receivers during certain rainstorms, snowstorms or thunderstorms. The noise is often continuous and is characterized by a high pitched hissing or screaming sound. It can last for many tens of minutes and be so intense that the controllers are unable to receive communications from aircraft for a considerable period.

A number of airports are investigating the problem while other airports have carried out certain questionable solutions to the problem. Static dischargers have been purchased to alleviate the radio interference, but these dischargers are considered to play no part in correcting the problem. The Midway Tower in Chicago purchased ten such dischargers in the Fall of 1975 and since that time, the devices have been installed at the following airports:

Midway	Bismark	Atlanta
Flint	Pueblo	Louisville
Youngstown	Minot	Stanford
Indianapolis	Colorado Springs	Tampa
Darwin	Denver-Arapaho	Parkesburg
Rhinelander		
Fairmont		

There are undoubtedly many more facilities in these and other regions with similar problems. The investigation performed provides recommendations to all ATCT locations which, when carried out, would eliminate this potential hazard.

Electrical breakthrough on the VHF receivers has occurred at various times at Logan International Airport, Boston, and to illustrate the problem, excerpts from an internal memorandum are reproduced.

"On Sunday, August 1, at 1500Z, the tower reported electrical breakthrough on main 119.1RX, which is located on the 21st floor of the tower with its antenna above the cab. They switched to standby 119.1RX, which is presently in the equipment room of the old tower building with its antenna on the old tower building roof.

The weather conditions at this time were misty and overcast, with electrical storm cells in a line approximately 4 miles wide and 25 miles long stretching north and south. This line was located 10 miles west of the airport moving in an easterly direction.

During the period 1500Z to 1529Z, both receivers were monitored at the jack panel on the 6th floor. The ratio of short bursts of electrical static breakthrough on the main 119.1RX to the standby 119.1RX was approximately 3:1.

The electrical storm cell reached the airport at 1530Z. Electrical breakthrough became more frequent and longer in duration on the main 119.1RX. The standby 119.1RX continued to have short electrical breakthrough similar to when the storm was 10 miles west of the airport.

At 1531Z, the main 119.1RX seemed to go into oscillations which lasted nearly 1 minute. The standby 119.1RX continued to have short burst of electrical breakthrough. Rain was very heavy at this time.

During 1532Z to 1533Z, the main 119.1RX went into oscillations again (caused by electrical discharge). This time the RF gain was decreased to eliminate the oscillation. At this gain setting, 5μV from a signal generator (HP-608D) was necessary to break the squelch. The receiver was then returned to 2μV squelch break.

The electrical storm had dissipated some over Boston, and by 1540Z it was approximately 2 to 4 miles at sea. Our main 119.1RX during the period 1532Z to 1540Z returned to normal operation, with electrical breakthrough decreasing in duration. The standby 119.1RX also decreased in electrical breakthrough during this period."

1.2 Logan Airport Layout

The new control tower at Logan Airport, shown in Figure 1, is approximately 301 feet high. The receiving antennas for aircraft communications are on top of the tower and spaced around a walkway which circumscribes a radome. A lightning rod is placed on top of the radome and other lightning rods are spaced around the walkway parapet.

Figure 1. The air traffic control tower at Boston's Logan Airport.

The layout of the antennas and lightning rods is shown in Figure 2. Figures 3a-3c show the approximate positions of some of the antennas relative to the air terminals and the approximate distances to the probable corona source at the tip of the lightning rod. Antenna mount number six shows a VHF antenna only 18 1/2 inches from a corona source, and other antennas are spaced not too much further away from other lightning rods. The nearest UHF antenna is some 35 inches away.

The parapet, radome framework and air terminals appear to be excellently grounded with all lines being inter-connected before the grounding system is reached. It was, however, difficult to decide if the coaxial lines from the antennas were grounded at both ends or just at one end.

1.3 Reduction of the Noise Problem by Installation of Static Dischargers

In September of 1976 the Midway Tower, Chicago successfully reduced their corona problem with the installation of static dischargers on the lightning rods. Other locations installed similar devices and the overall results were usually significant. Chicago indicate about an 80-90% reduction in the occasions of corona noise, although the devices gave no improvement at Fairmont. Logan Airport installed them in mid August which seemed to improve the sitcation, since during some local storms in the following month no noise problems existed. However, noise was monitored again during snowstorm and high wind conditions during the winter.

The static dischargers used at most of these facilities are primarily for aircraft use where they offer a controlled path to bleed off the accumulated charge on an aircraft. They attenuate the resultant broadband radio frequency noise by approximately 50db, as compared to a discharge from the tip of a wing without dischargers installed, because more frequent low amplitude dis-

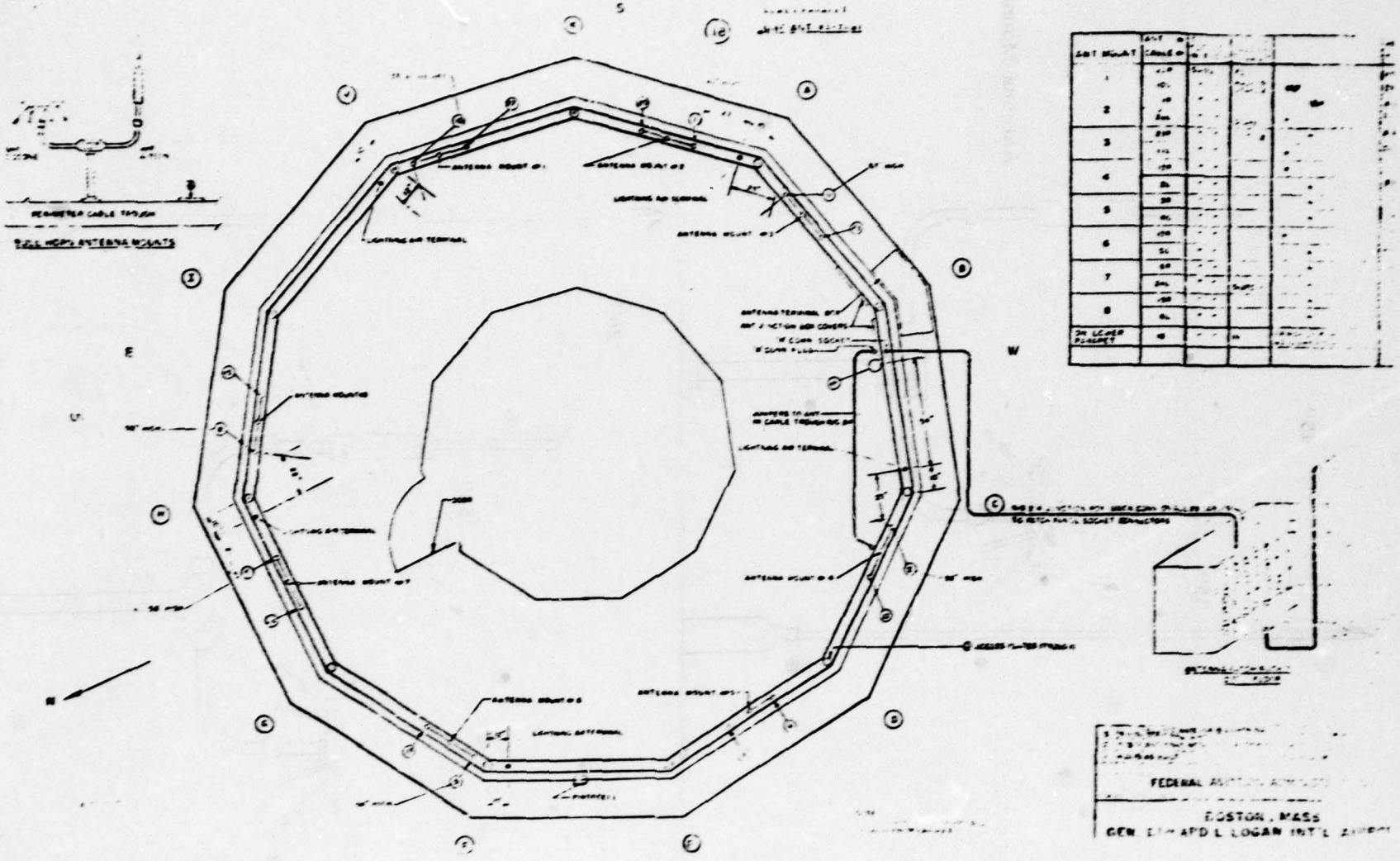

Figure 2. Logan International Airport Air Traffic Control Tower, Roof Antenna Layout

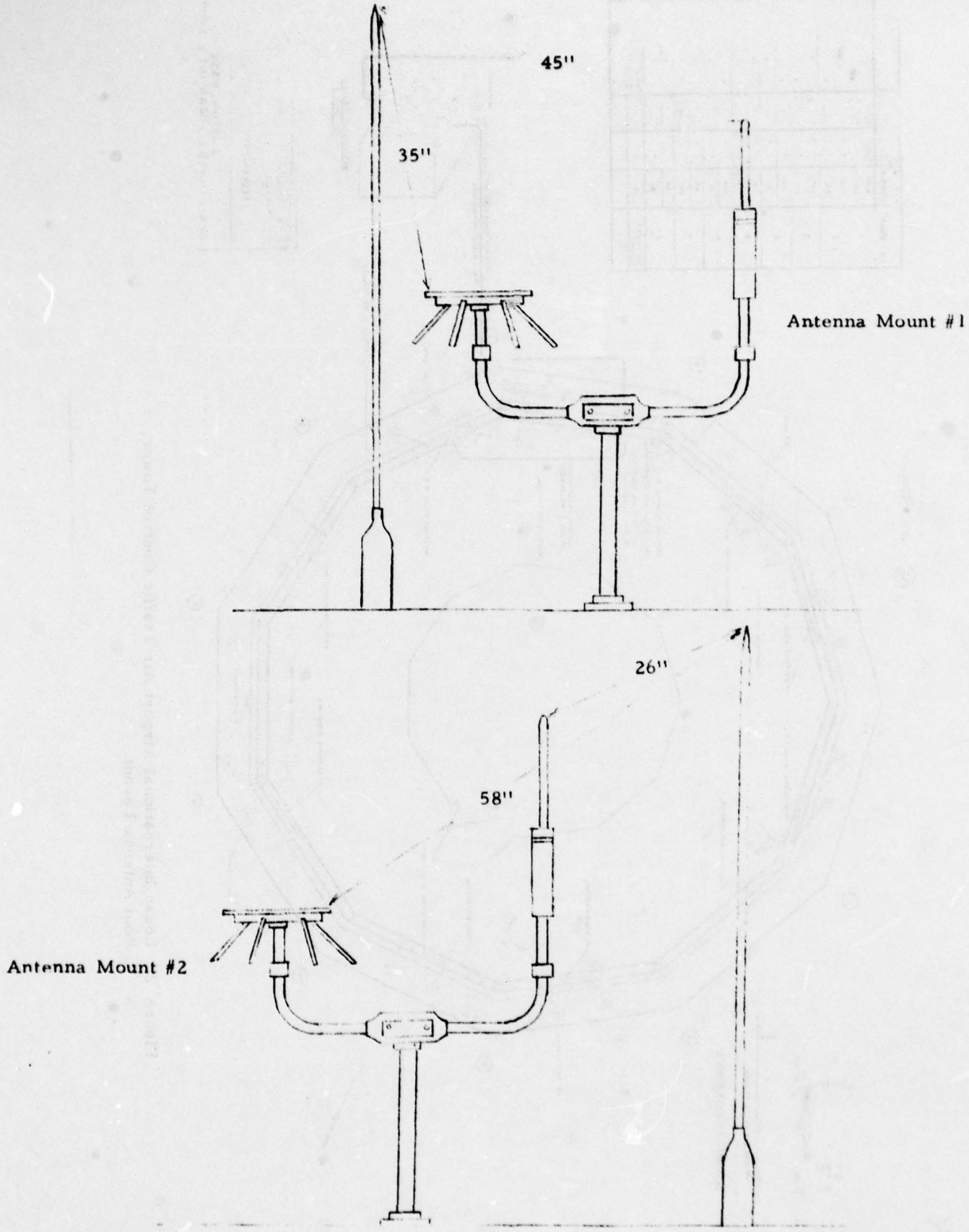

Figure 3a. Configurations of Antenna Mounts and Lightning Rods

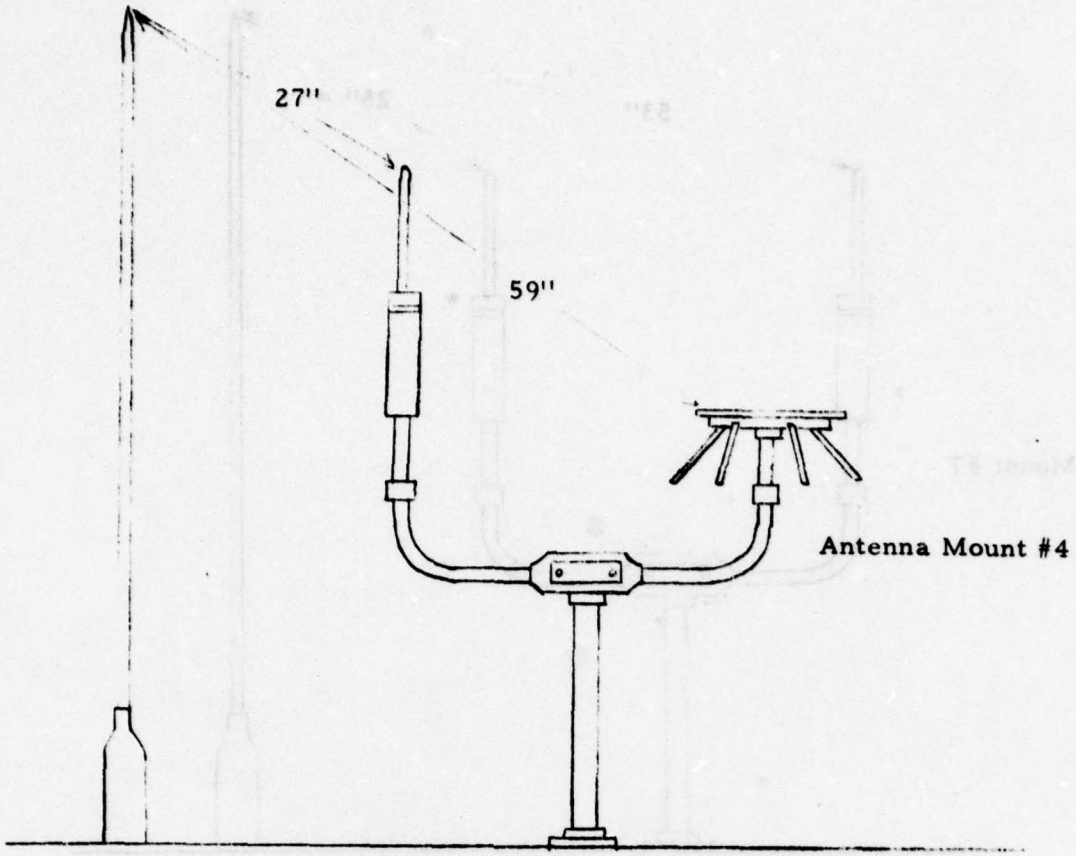

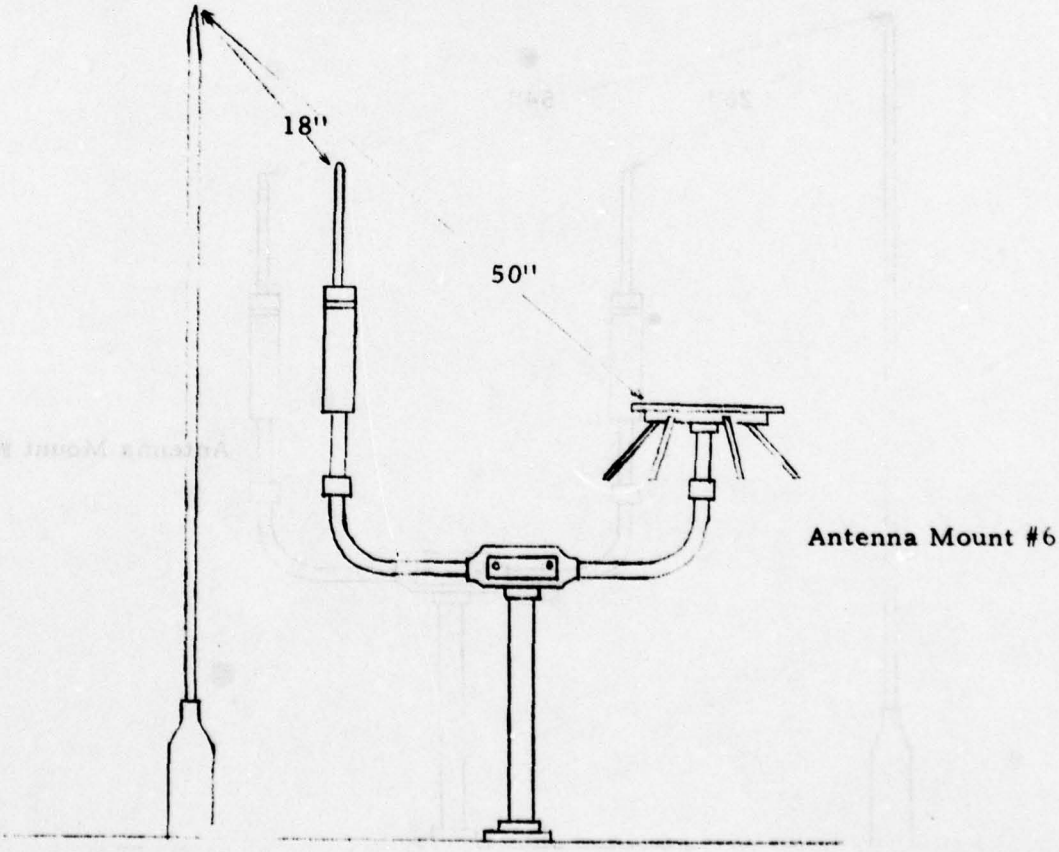

Figure 3b. Configurations of Antenna Mounts and Lightning Rods

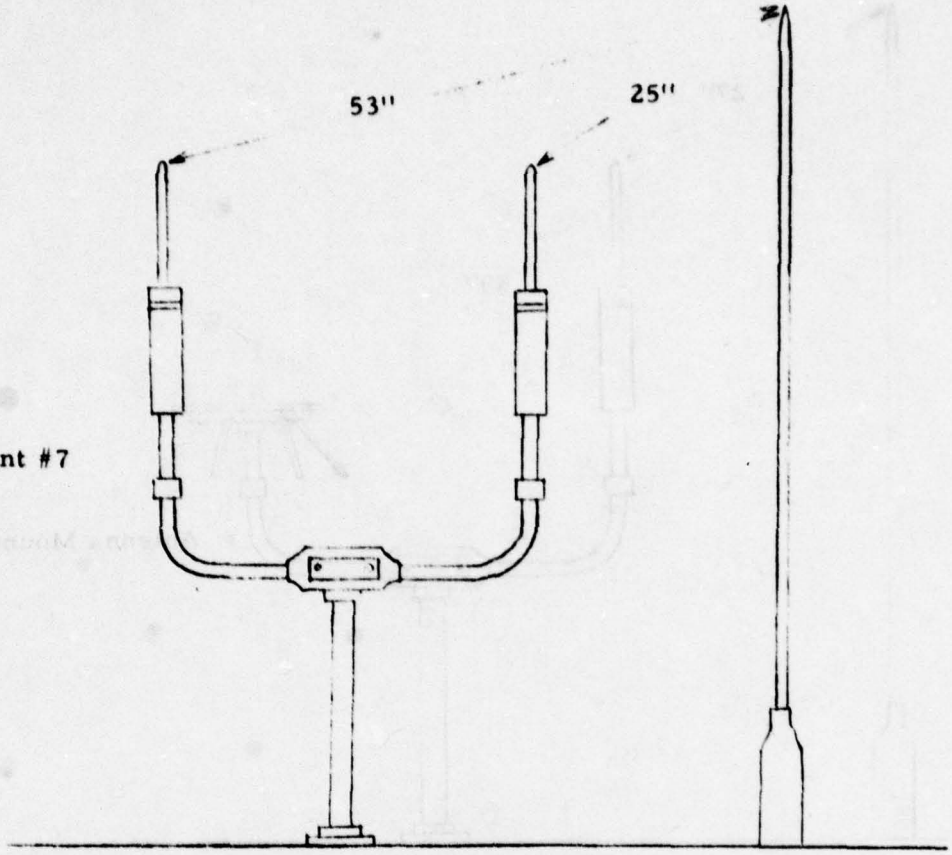

Antenna Mount #7

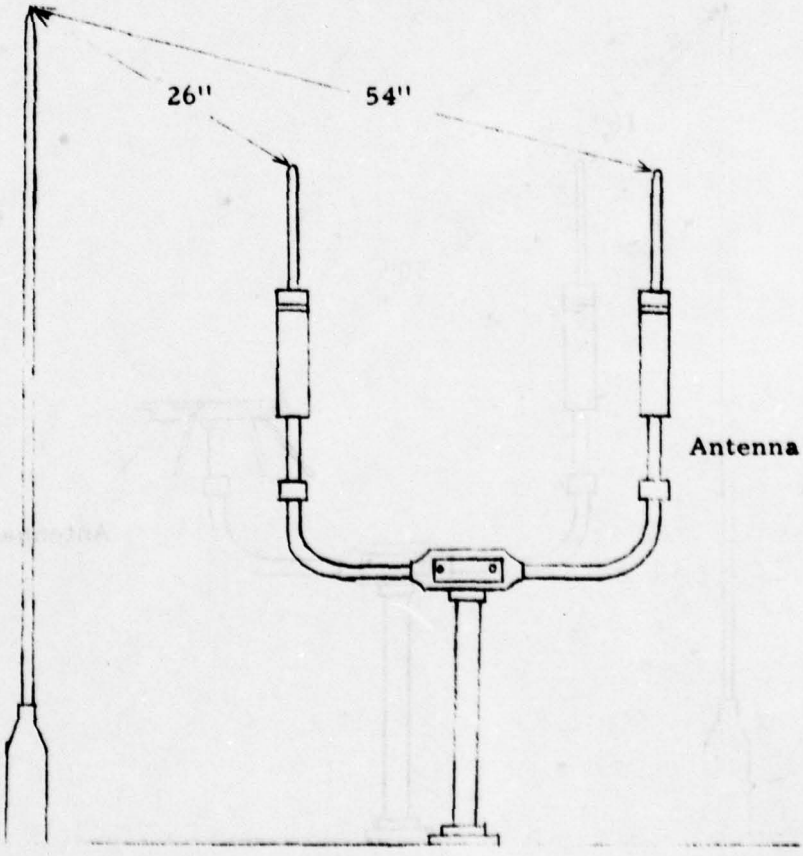

Antenna Mount #8

Figure 3c. Configurations of Antenna Mounts and Lightning Rods

charge pulses will occur with the small points of the dischargers than with larger points. In effect, they attempt to bring the potential of the body on which they stand to the potential of their surroundings using the principle of point-discharge over many thousands of special four micron diameter wires to reduce the noise coupling to the aircraft. Such devices no doubt work extremely well on the aircraft for which they were designed.

For the purposes of reducing the noise at ATCT locations, the static dischargers were connected to the lightning rods, as shown in Figures 4 and 5, utilizing 3/4" x 3/4" x 16" angle iron to support them. These figures show that the static discharging wires point downward, which, due to the mounting configuration of the lightning rods, is always in a region of reduced field over the surrounding area.

It will be shown later that the static discharges play no role in the reduction of the RF noise, but that the associated installation hardware reduces the corona at the tip of the lightning rod. In order to understand the source of the noise, it is necessary to explain the physical process of corona discharge.

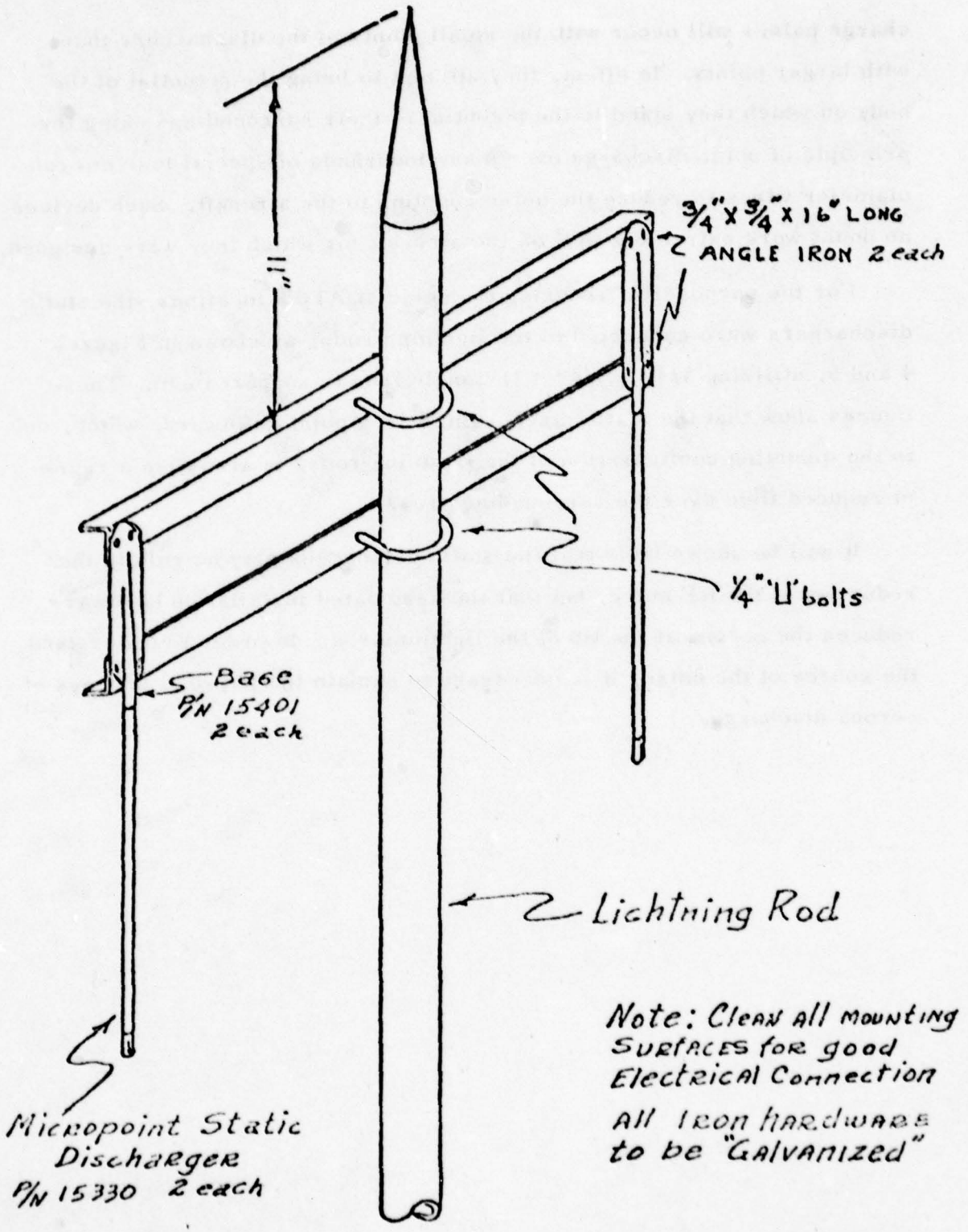

Figure 4. Installation of Static Discharger on ATCT Lightning Rod

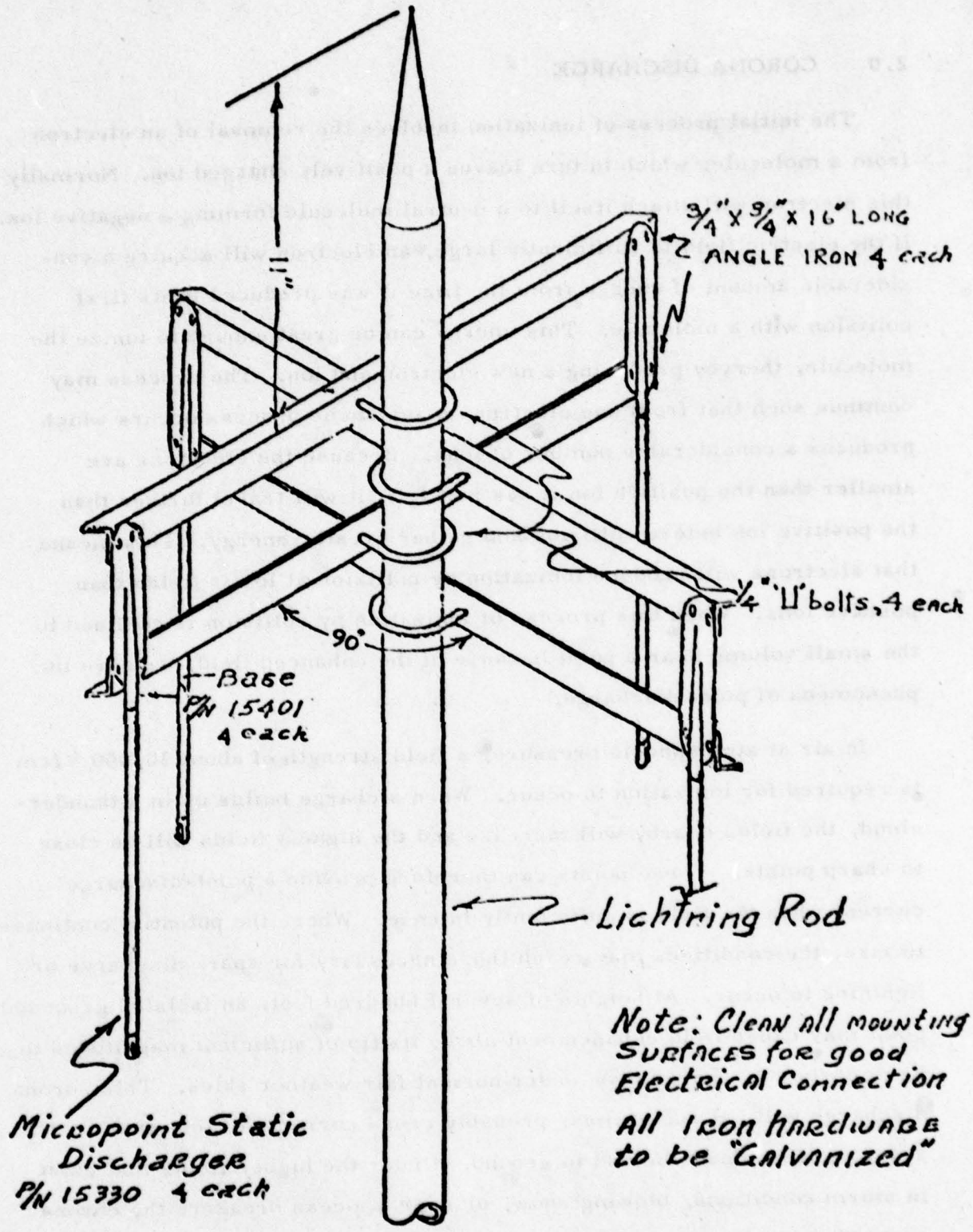

Figure 5. Installation of Static Discharger on RCAG Lightning Rod

2.0 CORONA DISCHARGE

The initial process of ionization involves the removal of an electron from a molecule, which in turn leaves a positively charged ion. Normally this electron will attach itself to a neutral molecule forming a negative ion. If the electric field is sufficiently large, an electron will acquire a considerable amount of energy from the time it was produced to its first collision with a molecule. This energy can be great enough to ionize the molecule, thereby producing a new electron and ion. The process may continue such that from one electron an avalanche process occurs which produces a considerable number of ions. Because the electrons are smaller than the positive ion it has just left, it will travel further than the positive ion before collision and gather greater energy. This means that electrons will produce ionization by collision at lower fields than positive ions. When this process of ionization by collision is confined to the small volume near a point because of the enhanced field, we have the phenomena of point discharge.

In air at atmospheric pressure, a field strength of about 30,000 V/cm is required for ionization to occur. When a charge builds up in a thundercloud, the fields nearby will increase and the highest fields will be close to sharp points. These points can therefore provide a point-discharge current when the field is sufficiently intense. Where the potential continues to rise, the conditions may reach those necessary for spark discharge or lightning to occur. At heights of several hundred feet, an isolated grounded point may cause field enhancement above its tip of sufficient magnitudes to be in corona discharge even under normal fair weather skies. This corona discharge will, at such times, probably cause currents of less than 1/4 μA to flow down the rod to ground. Under the higher fields that exist in storm conditions, blowing snow, or near to ocean breakers the corona current may approach values of 100 μA for periods of about a minute.

Significant levels of corona current can also occur on much lower structures under high field conditions. Basically corona current magnitude

is a function of point height, radius of curvature and wind speed. The field enhancement or exposure factor at the tip for a 30 m tower is shown in Figure 11, and for structures of different heights in Figure 12.

Corona discharge will, therefore, occur in the air above elevated sharp points. The breakdown from these extremities occurs not as a continuous flow of charge, but as a series of pulses with roughly 10 nsec risetime and 200 nsec duration, and it therefore generates radio noise over a broad spectrum.

The effects of wind on corona are illustrated in Figure 6. In this approach only horizontal winds are considered neglecting any updrafts as might exist before and during thunderstorms. The last 2 m of a pointed 30 m high tower are plotted in a storm field of -10,000 V/m. Ionization along the rod surface will take place only where the field is enhanced to values greater than the breakdown potential gradient which is roughly assumed at 1 million V/m.

First, to determine the outermost boundary of a possible space charge cloud, consider the simple picture where space charge does not effect the field. Two cases for winds of about 10 and 30 knots are shown. Under effect of the field the ions move upward and out to the sides, and the wind adds an extra horizontal component to their movement, creating a sort of concentrated line charge as the ions travel around the tower. The ion speed right at the tower is very high and drops off radidly with distance.

The situation can now be considered with space charge limiting. Once corona is formed and starts moving out from the tower, its charge would reduce the field around the tower to below the breakdown potertial gradient, and corona discharge would cease. Within a fraction of a second the wind would blow the charge clear of the tower, exposing it again to high fields, and ions would be formed again etc. This causes the corona currents to be given off in bursts, as first observed by Trichel[1] in 1938. Chalmers and Ette[2] have reported some interesting cases of this phenomena at a negative point.

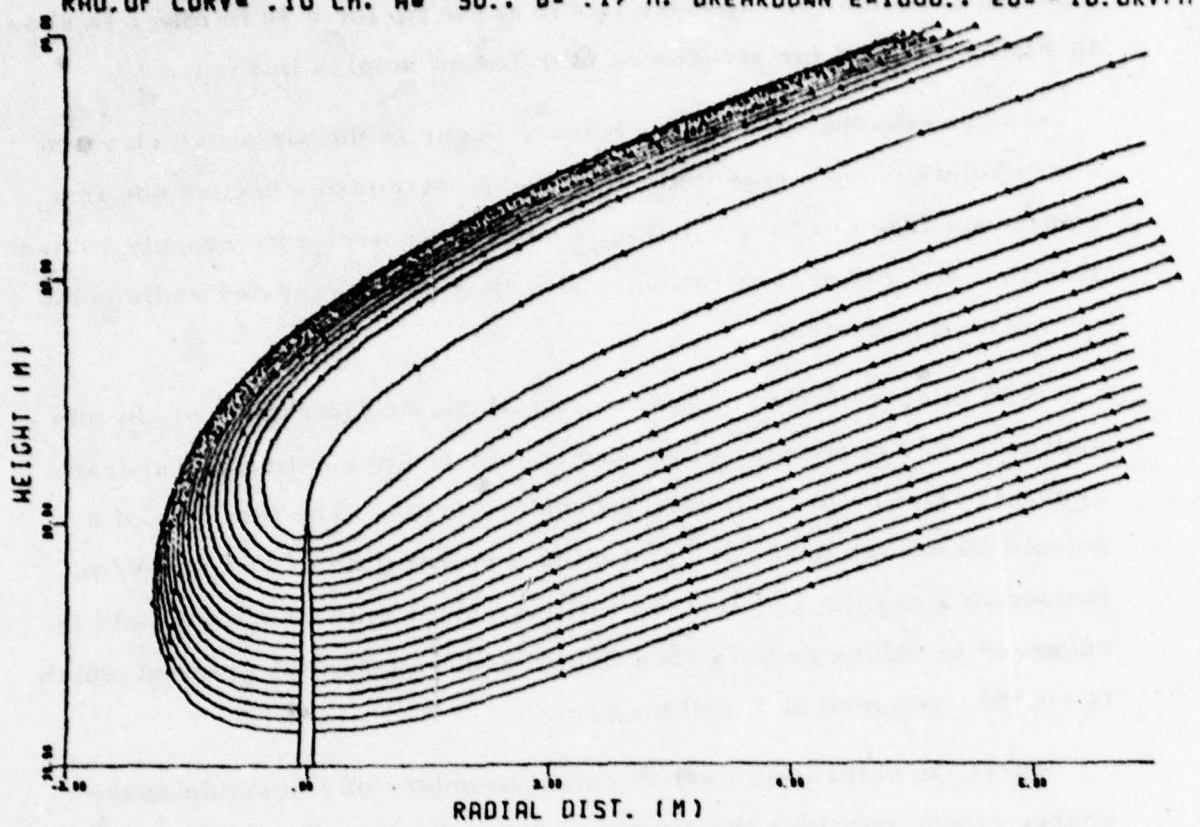

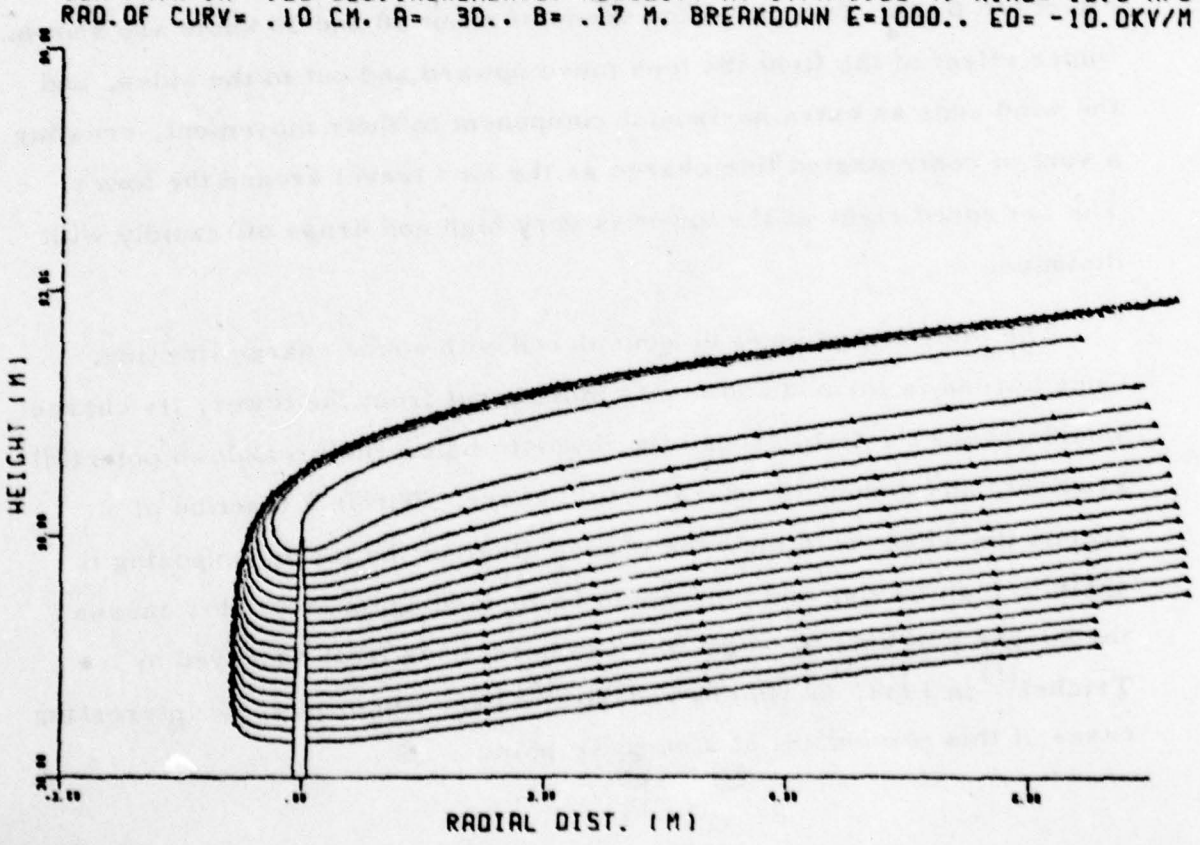

Figure 6. Ion movement under horizontal winds showing maximum boundary of ion cloud.

The magnitude of the corona current increases with rising wind speed, as shown in Figure 7, for 0 and 35 knots. In the equation relating the corona current i to the wind speed v and the point potential V, V_0 is the starting potential, D/D_0 is the ratio of the atmospheric density to the standard, and k the ion mobility.

$$i = 1.315\ \epsilon_0\ v\ (V - V_0)\left(\frac{D_0}{D}\right)^{.91} + 1.785\ \epsilon_0\ k\left(\frac{D_0}{D}\right)\ V\ (V - V_0)$$

Since the point geometry such as the radius of curvature does not enter the equation explicitly but is inherent in the coefficients and V_0, it is difficult to compute theoretical values of corona current for a particular configuration.

The degree to which the radio frequency noise generated by corona discharge couples into electronic systems is determined by the relative locations of the noise source, and the antenna via which the noise is coupled into the affected system. In addition, the coupling depends on frequency and the size of the antenna.

It can be shown that individual pulses associated with a corona discharge can be approximated by a decaying exponential with zero rise time, as follows:

$$F(t) = Ae^{-\alpha t}$$

where A is the pulse amplitude and α is the pulse decay constant. The noise spectrum produced by ν such pulses occurring each second as a function of frequency ω is given by,

$$P = A\left(\frac{\nu}{\pi}\right)^{\frac{1}{2}} \left(\omega^2 + \alpha^2\right)^{-\frac{1}{2}}$$

Figure 8 shows the relative noise-current spectral density plotted as a function of frequency indicating a rapid drop in the spectrum magnitude with increasing frequency. The effects will, therefore, be much lower at UHF than VHF.

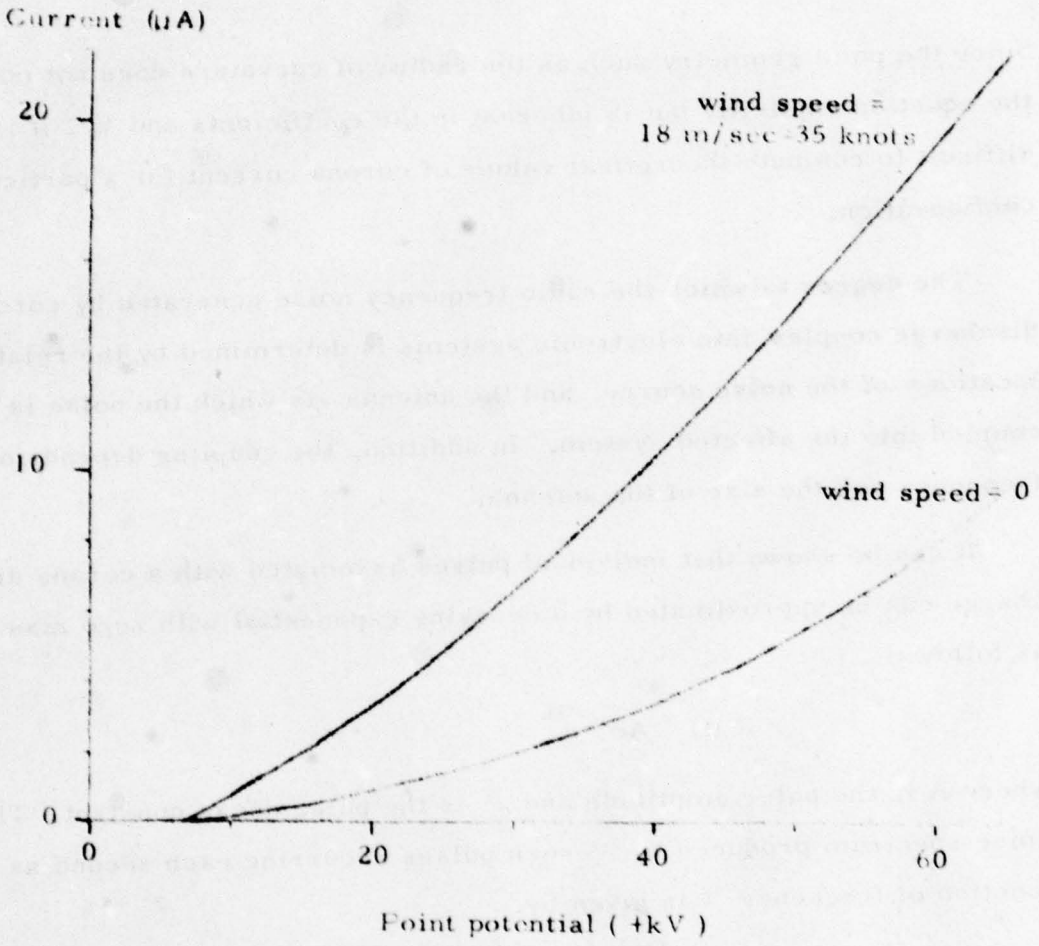

Figure 7. Corona current as a function of the point potential and wind speed. (adapted from Chapman [2])

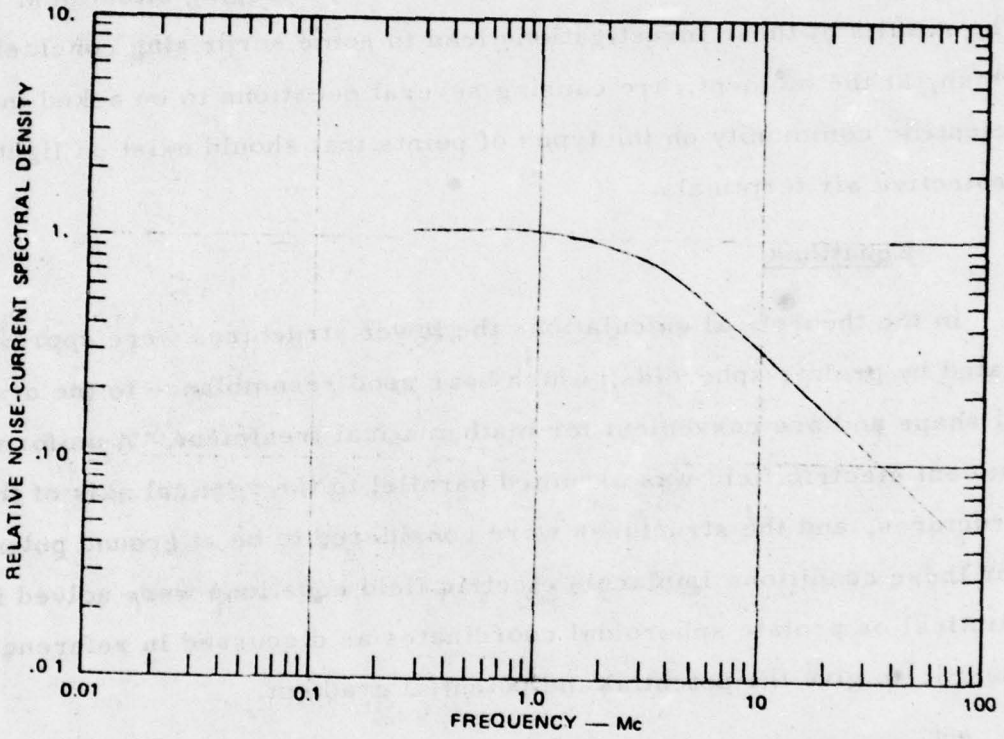

Figure 8. Corona noise spectrum characteristics. (adapted from reference 3)

3.0 SHARP VS. BLUNT POINTS

In order to better understand the atmospheric conditions around structures of various shapes and heights, a theoretical investigation was performed of the corona currents given off from sharp and blunt points, and of the electric fields influencing the corona. Very simplified situations of static field conditions were examined, from which conclusions could be drawn about the dynamically changing situations. The results of these investigations lead to some surprising conclusions which, at the moment, are causing several questions to be asked in the scientific community on the types of points that should exist on lightning protective air terminals.

3.1 Equations

In the theoretical calculations the tower structures were approximated by prolate spheroids, which bear good resemblance to the overall shape and are convenient for mathematical treatment. A uniform ambient electric field was assumed parallel to the vertical axis of the structures, and the structures were considered to be at ground potential. For these conditions Laplace's electric field equations were solved in elliptical or prolate spheroidal coordinates as discussed in references 5 and 6, to give the potential and potential gradient.

The resulting equation for the potential as a function of the elliptical coordinate ξ with major and minor half axes a and b is,

$$\varphi = \varphi_0 + (\varphi_s - \varphi_0)\frac{\int_{\xi}^{\infty} \frac{d\xi}{\xi\,(\xi + a^2)^{3/2}(\xi + b^2)}}{\int_{0}^{\infty} \frac{d\xi}{(\xi + a^2)^{3/2}(\xi + b^2)}} = \varphi_0 + (\varphi_s - \varphi_0)\frac{I_1}{I_2}$$

The potential at the surface $\varphi_s = 0$, because the conducting ellipsoid is grounded, and the potential at height h in the unperturbed parallel field E_o is $\varphi_0 = -E_o h$.

$$\varphi = -E_o h \left(1 - \frac{I_1}{I_2}\right)$$

The vertical and horizontal components of the electric field are,

$$E_v = -\frac{\partial \varphi}{\partial h} = E_0 \left(1 - \frac{I_1}{I_2}\right) - \frac{E_0 h}{I_2} \frac{\partial \xi}{\partial h} \frac{\partial I_1}{\partial \xi}$$

$$E_H = -\frac{\partial \varphi}{\partial r} = -\frac{E_0 h}{I_2} \cdot \frac{\partial \xi}{\partial r} \frac{\partial I_1}{\partial \xi}$$

The equation of the ellipsoid,

$$\frac{x^2}{\xi + a^2} + \frac{y^2}{\xi + b^2} + \frac{z^2}{\xi + c^2} = 1$$

is simplified for the symmetrical case of the prolate spheroid, where the semimajor axis is a, the two semiminor axes b = c, the radial coordinate is the horizontal distance from the center of the ellipsoid $r^2 = y^2 + z^2$, and the height coordinate h = x;

$$\frac{h^2}{\xi + a^2} + \frac{r^2}{\xi + b^2} = 1 \quad \text{and} \quad \xi = f(h, r)$$

The partial derivatives are,

$$\frac{\partial \xi}{\partial h} = \frac{2h\,(\xi + b^2)}{2\xi + a^2 + b^2 - r^2 - h^2}$$

$$\frac{\partial \xi}{\partial r} = \frac{2r\,(\xi + a^2)}{2\xi + a^2 + b^2 - r^2 - h^2}$$

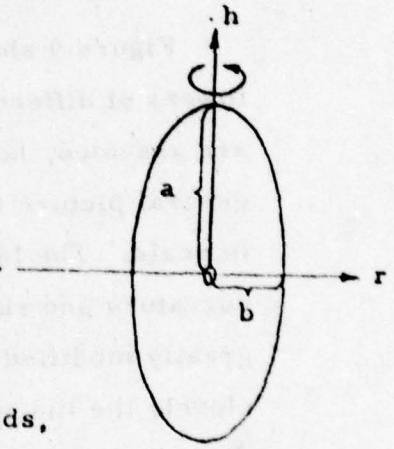

Setting $c = a^2 - b^2$, the evaluation of the integrals yields,

$$I_1 = -\frac{2}{c^2\sqrt{\xi + a^2}} - \frac{1}{c^3} \ln \frac{\sqrt{\xi + a^2} - c}{\sqrt{\xi + a^2} + c}$$

$$I_2 = -\frac{2}{ac^2} - \frac{1}{c^3} \ln \frac{a - c}{a + c}$$

$$\frac{\partial I_1}{\partial \xi} = -\frac{1}{(\xi + a^2)^{3/2}(\xi + b)^2}$$

Hence the equations for the potential φ, the vertical component E_v and the horizontal component E_H of the electric field around a conducted grounded prolate spheroid in a parallel electric field E_0 are as follows:

$$\varphi(h,r) = \varphi\left[h,\ \xi(h,r)\right] = -E_0 h\left(1 - \frac{\frac{2}{\sqrt{\xi + a^2}} + \frac{1}{c}\ln\frac{\sqrt{\xi + a^2} - c}{\sqrt{\xi + a^2} + c}}{\frac{2}{a} + \frac{1}{c}\ln\frac{a-c}{a+c}}\right)$$

$$E_V = -\frac{\varphi}{h} - \frac{2E_0 h^2}{\left(\frac{2}{ac^2} + \frac{1}{c^3}\ln\frac{a-c}{a+c}\right)\cdot(\xi + a^2)^{3/2}(2\xi + a^2 + b^2 - r^2 - h^2)}$$

$$E_H = -\frac{2E_0 hr}{\left(\frac{2}{ac^2} + \frac{1}{c^3}\ln\frac{a-c}{a+c}\right)\sqrt{\xi + a^2}\ (\xi + b^2)\ (2\xi + a^2 + b^2 - r^2 - h^2)}$$

These equations were programmed and a variety of conditions were computed and plotted.

3.2 Theoretical Results

Figure 9 shows two cases of equipotential lines around 30 m high towers of different diameter. Fair weather field conditions of 200 V/m are assumed, however, the equipotential line distribution gives the general picture for any value of the ambient field, requiring only a change in scale. The left plot is of a pointed tower having a 3.3 cm radius of curvature and shows the equipotential lines just around the tower are greatly modified from the parallel field situation. It is striking how closely the lines follow the tower along the vertical structure and how they are concentrated just around the top. But just a short distance away from the tower the parallel field situation is regained. Around the blunt structure with 3.3 m radius of curvature, the picture looks quite different. The equipotential lines are not as closely gathered around the blunt structure as they are around the pointed one, but the field is effected more at greater distances as is apparent by the line concentration. This implies that under appropriate high fields corona ionization occurs only in the immediate vicinity of the sharp point, but over a larger volume around the blunt point.

The field lines run perpendicular to the equipotential lines as represented in Figure 10. The collection area is marked off, for

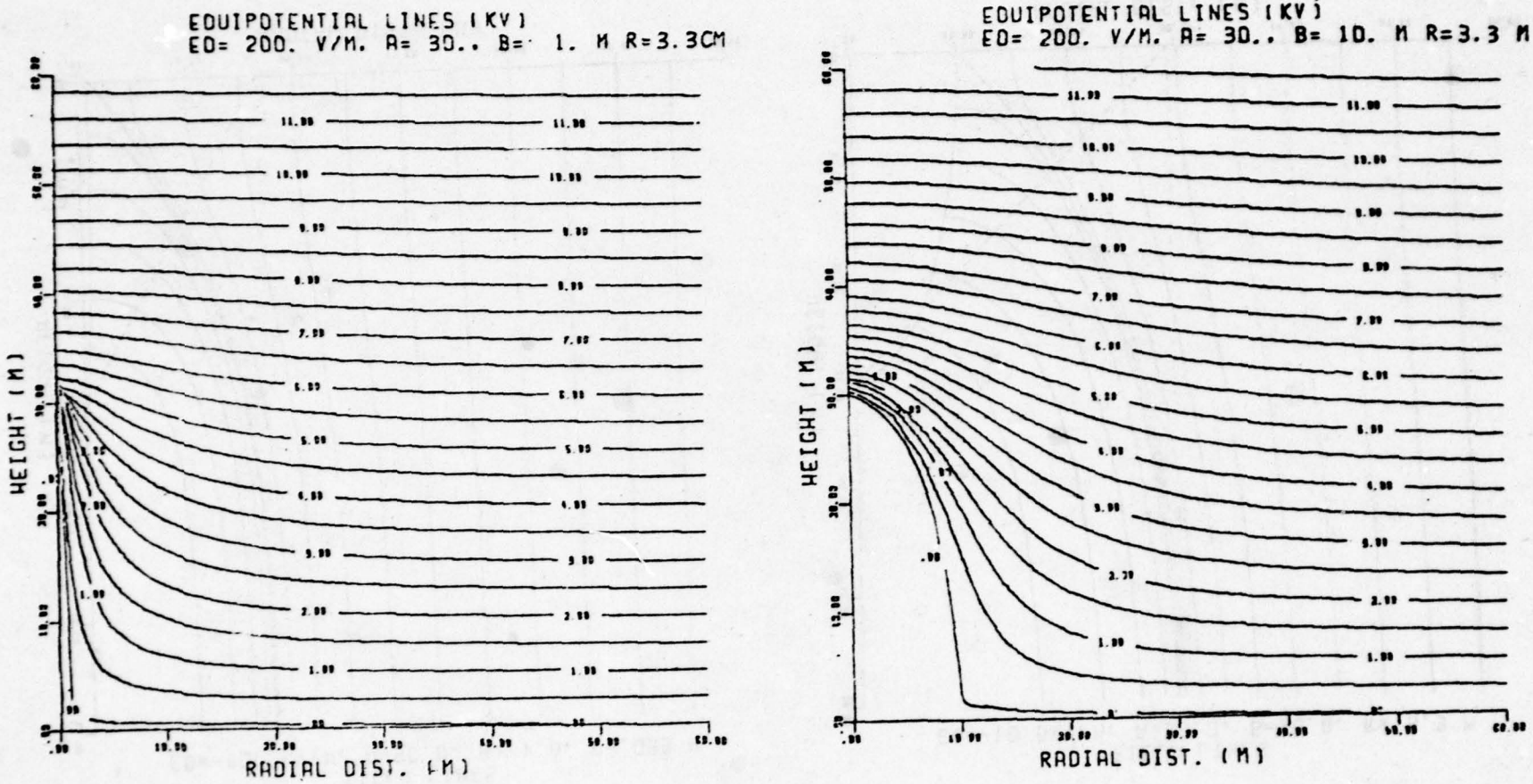

Figure 9. Equipotential lines around pointed and blunt towers.

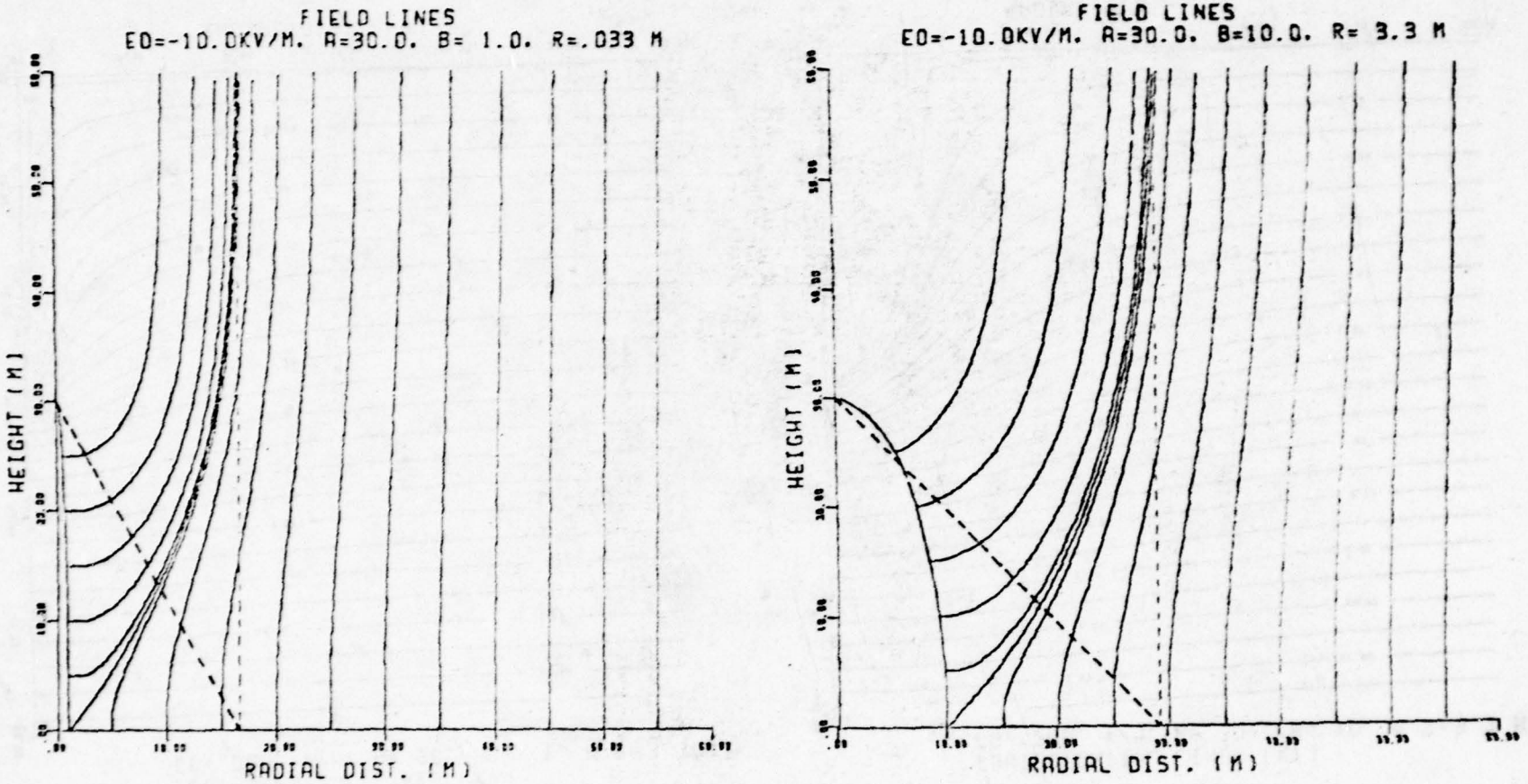

Figure 10. Electric field lines and collection area.

which the field lines terminate on the tower. If a lightning leader was coming down, and the phenomena was assumed very weak, then theoretically it would follow one of the field lines. But of course the high charge carried in a downcoming leader modifies the entire field line pattern.

The exposure factors help determine how soon and out to what distance a tower will go into corona. Figure 11 shows two 30 m high towers with radius of curvature of $\frac{1}{10}$ mm and 10 cm. Lines of equal value were drawn for the exposure factors in an area around the top of the towers, using double logarithmic scales to show detail near and far. Starting from the tower top upward, conditions were examined $\frac{1}{10}$ mm, 1mm, 1cm, 10cm, 1m above the tower; the same was done going down from the top and going outward from the center. The discontinuity in the center of the graph, where the data sets are merged, is insignificant. The enhancement at the tip is of the order of 10,000 for the sharp point, but only 100 for the blunt point. This means that only fields of the order of 100 V/m are required for the sharp point to be in corona, which is in agreement with experimental results from a sharp point giving up to $\frac{1}{4}$ u amp current in fair weather fields. For the blunt point however, conditions of 10,000 V/m are required before corona is given off. It should be noted that the enhancement for the sharp point drops off rapidly with distance, it is down to a factor of 10 only 30 cm above the tip. The enhancement of the blunt point is larger at these distances and drops down to 10 only at twice this distance, or 60 cm above the top.

The sharp point goes into corona in low fields and just immediately around the tip, the blunt point goes into corona only in high fields but out to greater distances from the tower.

In Figure 12 the exposure factors are plotted versus height for two values of radius of curvature, 1mm and 3.3 cm. This data can be useful in correlating measurements from different heights, or for determining

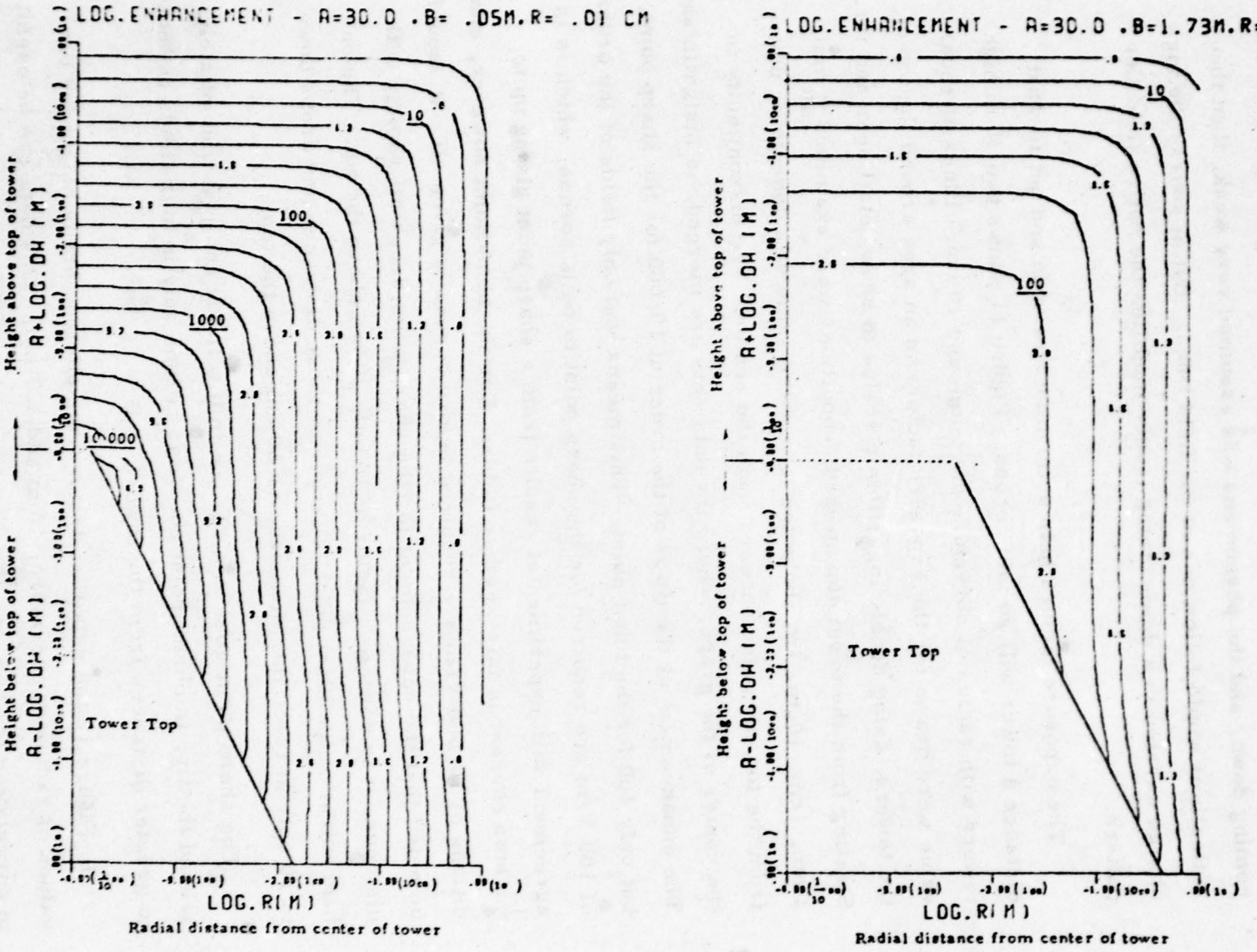

Figure 11. Lines of equal value for exposure factors around sharp and blunt structures.

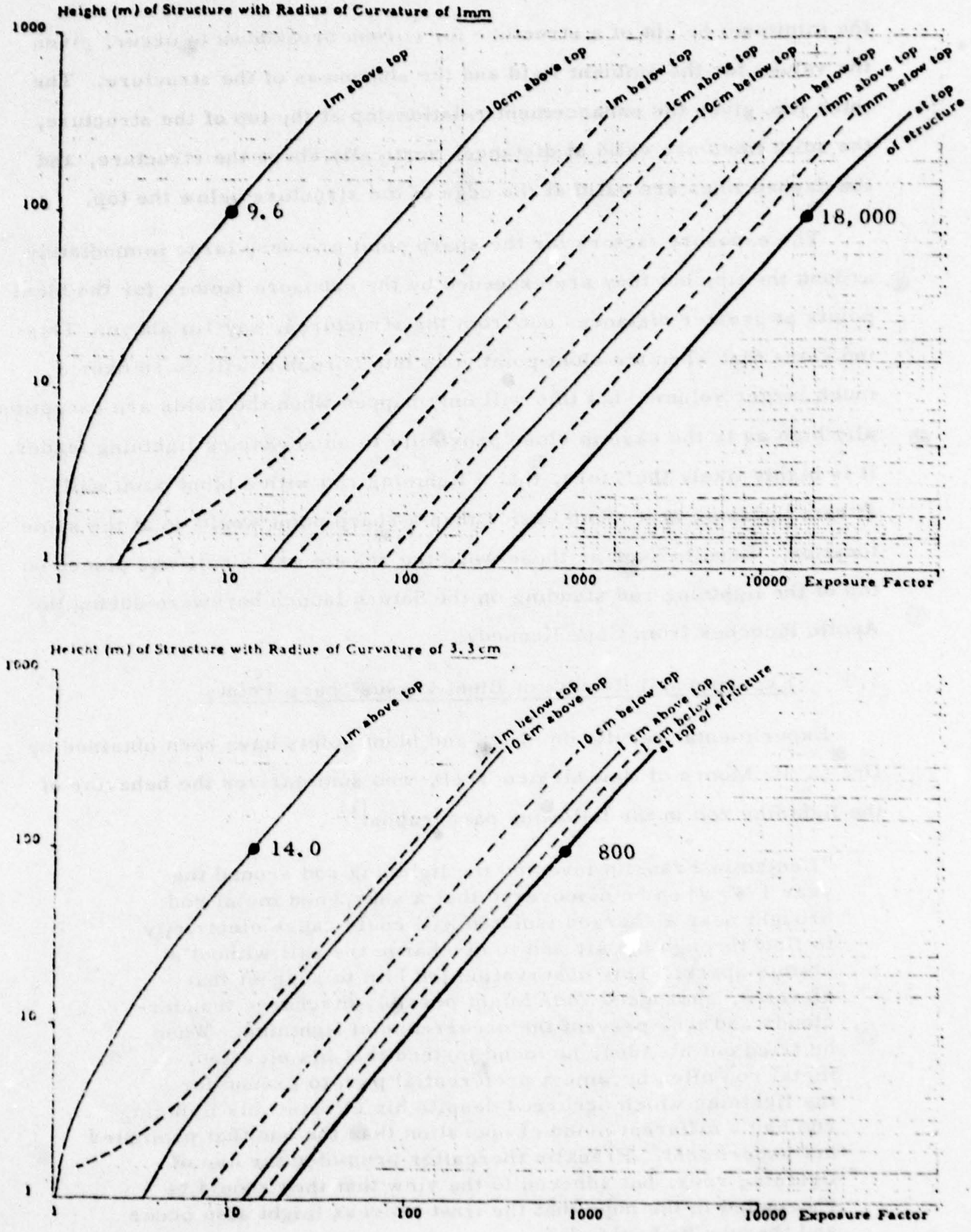

Figure 12. Exposure factors at top of structures, vertically above, and below at side of structures.

the minimum height of a structure for corona breakdown to occur, given the values for the ambient field and the sharpness of the structure. The thick line gives the enhancement relationship at the top of the structure, the solid lines are valid at distances vertically above the structure, and the dashed lines are valid at the edge of the structure below the top.

The exposure factors for the sharp point are very large immediately around the tip, but they are exceeded by the exposure factors for the blunt points at greater distances out from the structures, say 1m above. This indicates that when the blunt point goes into corona it will do so over a much larger volume, but this will only happen when the fields are exceptionally high as is the case in close proximity to an advancing lightning leader. It is highly likely therefore, that a lightning rod with a blunt point will attract lightning to it much easier than a sharp point would do at the same location. Results such as these were the reason why a ball was placed on top of the lightning rod standing on the Saturn launch hardware during the Apollo launches from Cape Kennedy.

3.3 Experimental Results of Blunt versus Sharp Points

Experimental results on sharp and blunt points have been obtained by Dr. C. B. Moore of New Mexico Tech, who summarizes the behavior of the lightning rod in the following paragraphs:[7]

> "Benjamin Franklin invented the lightning rod around the year 1749 when he discovered that a sharpened metal rod brought near a charged isolated ball could cause electricity to flow through the air and to discharge the ball without a visible spark. This observation led him to suggest that elevated, sharpened rods might possibly discharge thunderclouds and thus prevent the occurrence of lightning. When he tried out his idea, he found instead that his elevated, metal rod often became a preferential path to ground for the lightning which occurred despite his efforts: his lightning rod had a different mode of operation than the one that prompted his experiment. Franklin thereafter promoted the use of lightning rods, but adhered to the view that they should be sharpened in the hope that the first process might also occur and thereby be beneficial.

Two schools of thought subsequently developed: one favored Franklin's sharpened rod for lightning protection and the other, the English school led by Benjamin Wilson and George III, urged the use of blunt lightning rods on the basis that sharpened rods might promote the striking of lightning when otherwise a discharge would not have occurred. Contemporary American practice is to use sharpened lightning rods, but appreciable evidence exists that objects within the nominal "cone of protection" of a sharpend rod can be struck by lightning and no explanation for this behavior has been suggested.

We have modelled lightning rods both numerically and experimentally to determine their response to an approaching lightning streamer. Our results indicate that lightning can be induced to 'strike' any surface, but that a sharpened rod is much less likely to be 'struck' than a blunt one. Sharpened rods seem to protect themselves appreciably by the copious emission of point discharge ions so that they are poorer candidates to launch an upward-going return streamer when lightning approaches than is a blunt rod which is passive until the field becomes very strong. When the electric field becomes sufficiently strong over a blunt rod, dielectric breakdown of the air occurs at the blunt tip and a streamer propagates upward and often participates in a major discharge. For these reasons it appears that a blunt rod may be a better protector of a structure than is a sharpened one which may protect itself but leave other objects in its vicinity vulnerable.

Perhaps more attention should have been given to the opinions of George III!"

An example of experimental results by Standler[8] is given in Figure 13, where the current and charge release of a blunt and sharp rod are presented that were obtained in response to two close lightning strokes monitored by the electric field. The blunt rod emitted +11μ coulomb in less than 10 msec from the first field pulse received from the lightning flash, while the sharp rod released only +2.2μ coulomb. During the first 460 msec of this flash the charge transfer for blunt and sharp rods are +25 and -8.3 coulomb respectively. The corona current graphs also illustrate that under the extremely high fields of close lightning much more current is given off by the blunt rod than by the sharp one.

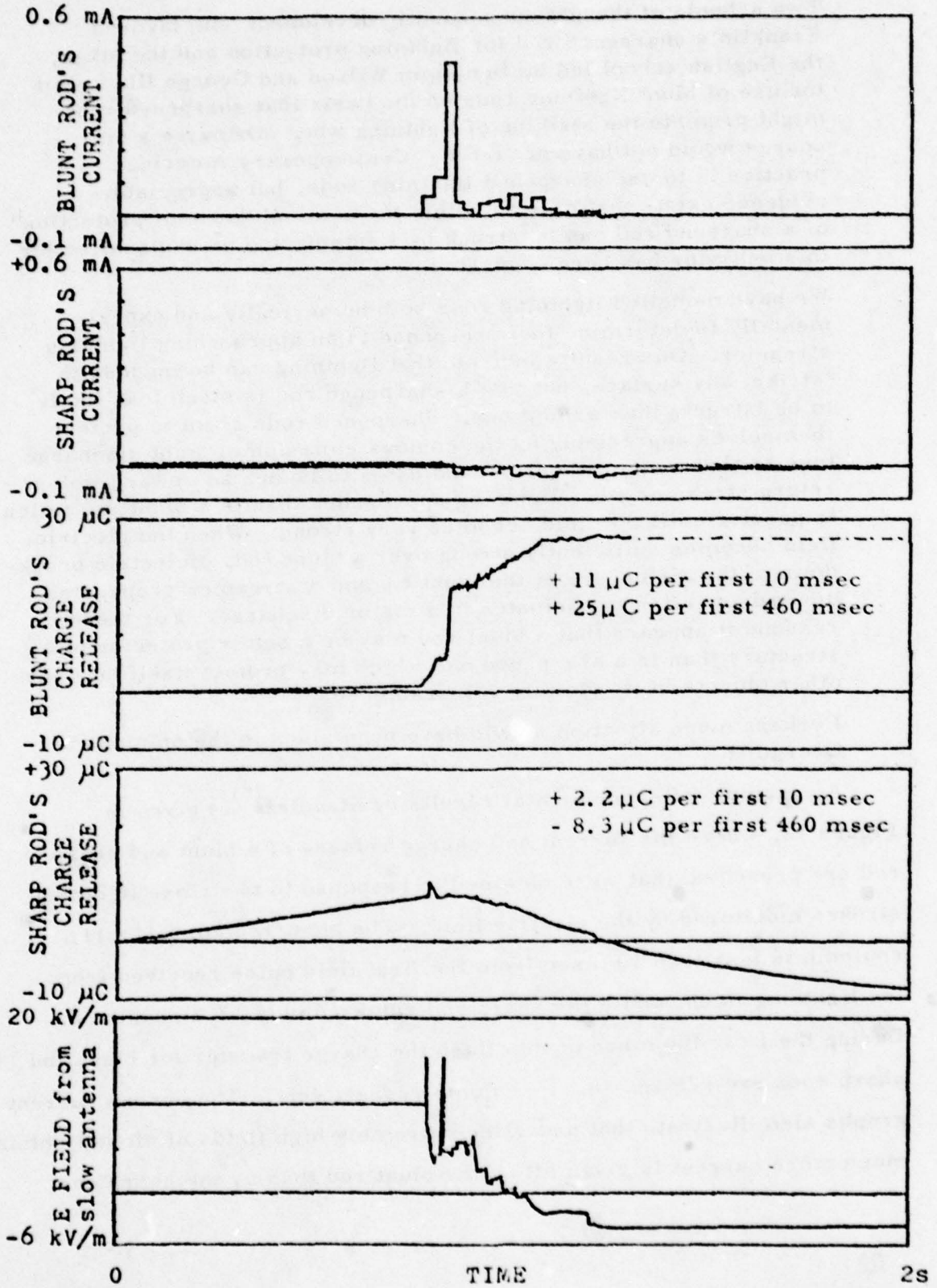

Figure 13. Lightning (0.4 km distant) at 1142:12.00, 18 Aug 1974.

4.0 ANALYSIS OF THE LOGAN AIRPORT NOISE PROBLEM

The radio noise that occurs under high field conditions at VHF frequencies and occasionally on UHF receivers can be generated from one of several sources:

1) Corona discharge under high ambient field conditions from,
   a) the lightning rod on top of the radome.
   b) the lightning rods around the parapet.
   c) the antennas around the parapet.
2) Corona discharge in high fields due to the radome charge.
3) Streamer noise from the radome surface.
4) Charge transfer to the antenna rods from rain.

In order to attempt to determine the specific source of noise and to deduce the onset conditions, measurements of electric field and corona current were taken at Logan Airport, theoretical calculations were performed, and the results of both were correlated with their effect on voice communications as a function of distance between antenna and corona point, and other factors which influence the noise interference problem.

4.1 Effect of the Static Dischargers

It is necessary first to analyze the corrective procedures which have been carried out at several ATCT locations with a certain amount of success, namely the use of the P-static dischargers. The devices are designed to bring the potential of the structure on which they are fastened to the potential of their surroundings. In this case, the lightning rod is at the potential of the control tower and ground, and there is absolutely no way that one can dissipate the charge on the grounded elevated structure to bring it to the potential of its surroundings. Apart from this, it is unlikely that corona will occur at the P-static dischargers which are installed in an area of reduced field underneath the grounded cross-member. Corona discharge

only occurs in high field areas. No matter how many P-static dischargers were connected to the tower, the lightning rods would still remain at ground potential, the field above would be unchanged and corona would still form there.

The question remains, therefore, as to what caused the improvement when the devices were attached to the lightning rods? The answer is quite simple and can be explained again by looking at Figure 9. Around the sharp point the equipotential lines hug the structure. If we now introduce a grounded horizontal cross-member, which subtends an angle of almost 90° at the top of the lightning rod, then the equipotential lines must pass around it in a way similar to that shown in Figure 14.

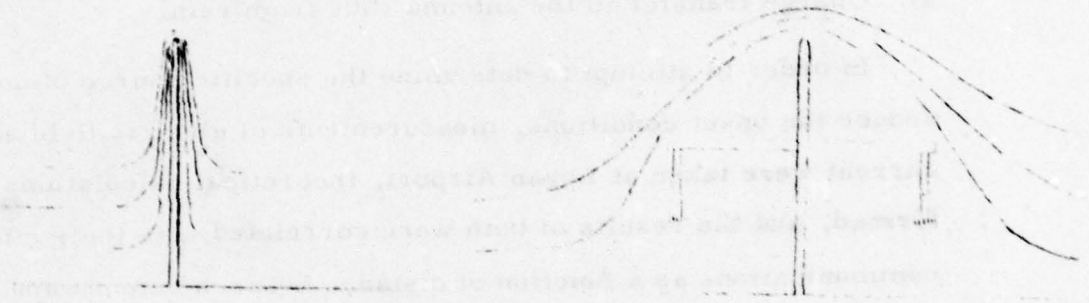

Figure 14. Equipotential Lines around Lightning Rod before and after Installation of Static Dischargers

The effect is to lower the potential gradient at the tip by making the structure look electrically more like a rounded object. This reduced potential gradient makes it necessary for a much larger electric field to be present before corona breakdown is initiated.

Placing the cross-member lower would mean that corona would occur earlier as the field at the tip would increase; placing it higher delays the onset of corona until the electric field is exceptionally high. Care must be taken, however, not to lift the horizontal member too high to avoid corona being formed on its extremities. The above figure shows that no corona will be forthcoming from the P-static dischargers, owing to its environment being a low field condition.

4.2 Determinations of Electric Field and Corona

4.2.1 Lightning Rod on Top of Radome

Theoretical estimates can be made of the fields under which the highest lightning rod on top of the radome will go into corona. Verifications with measurements could unfortunately not be obtained because the top was inaccessible due to high winds during the brief test period. For an air terminal with a radius of curvature of 1mm, which is not particularly sharp, placed on top of a very narrow grounded structure of the height of the control tower of about 300 ft, an enhancement of about 18,000 above the ambient electric field can be determined at the tip of the rod from Figure 12. As a result of the radome and the wide grounded structure below it, however, the exposure factor at the tip of the air terminal on top of the radome is much lower.

Calculations were performed to approximate the Logan tower situation. A 4 ft rod with 1/2 mm radius of curvature was considered, placed on top of a rounded structure with a 19 ft diameter at the top and 112 ft at the bottom. The exposure factor at the tip of the rod was determined as 1,700. For Logan Airport this figure is representative for the field enhancement at the top, but for other similar control towers without a radome and with an effectively higher lightning rod, the field enhancement could be very much higher.

Under fair weather fields of say 200 V/m, the field at the tip of the highest Logan Airport lightning rod will be over 1,700 x 200 V/m, or above 340,000 V/m which is not enough for corona breakdown. Assuming a starting potential of 10^6 V/m for corona, we need a field of 600 V/m at ground level to cause breakdown at the point. Such a value will occur prior to thunderstorm onset, and later in the storm the fields may reach values in excess of 10,000 V/m. With these fields more current will flow and the radio noise will reach a level above the receiver noise level.

The onset of corona can be delayed by modifying the radius of curvature of the rod. By placing a 10 cm diameter corona ball over the

tip of the air terminal, the exposure factor on top would be reduced by a factor of about 8 to around 210, and ambient fields of at least 4,800 V/m are then required instead of the low 600 V/m fields to cause corona breakdown. This modification, however, will not eliminate corona. Removing the rod altogether will result in an enhancement of 23 over the ambient field right on top of the radome, a figure low enough to suppress corona breakdown even under storm conditions. Only the fields of an approaching lightning leader would then be large enough to cause corona, however, the tower would be without lightning protection.

4.2.2 Lightning Rods and Antennas around Parapet

It is difficult to theoretically come up with reasonable enhancement figures for the complex layout of lightning rods and antennas around the parapet, hence it was necessary to take measurements to determine these values. Two field mills were run simultaneously, by one at ground level and one on the parapet around the radome. This gave a calibration for the enhancement over the ambient field at the second field mill location. Then two field mills were run simultaneous, one at the calibrated reference location on the parapet, and with the other one measurements were taken at the locations and heights of the lightning rods and antennas around the radome. From these data the enhancements over the ambient field were computed at the rod locations in the presence of the field mill which resembles a blunted object. With the aid of theoretical calculations, correction factors were applied to these numbers to determine the exposure factors at the tips of the air terminals and antennas unmodified by the presence of the field mill.

These results are shown in Figure 15. The exposure factors are largest for high rods with small radius of curvature well separated from other rods and field reducing structural features. The highest electric fields are above the sharp points of the 6 ft air terminals. The fields are significantly lower above the blunt, 1" diameter VHF antennas which are

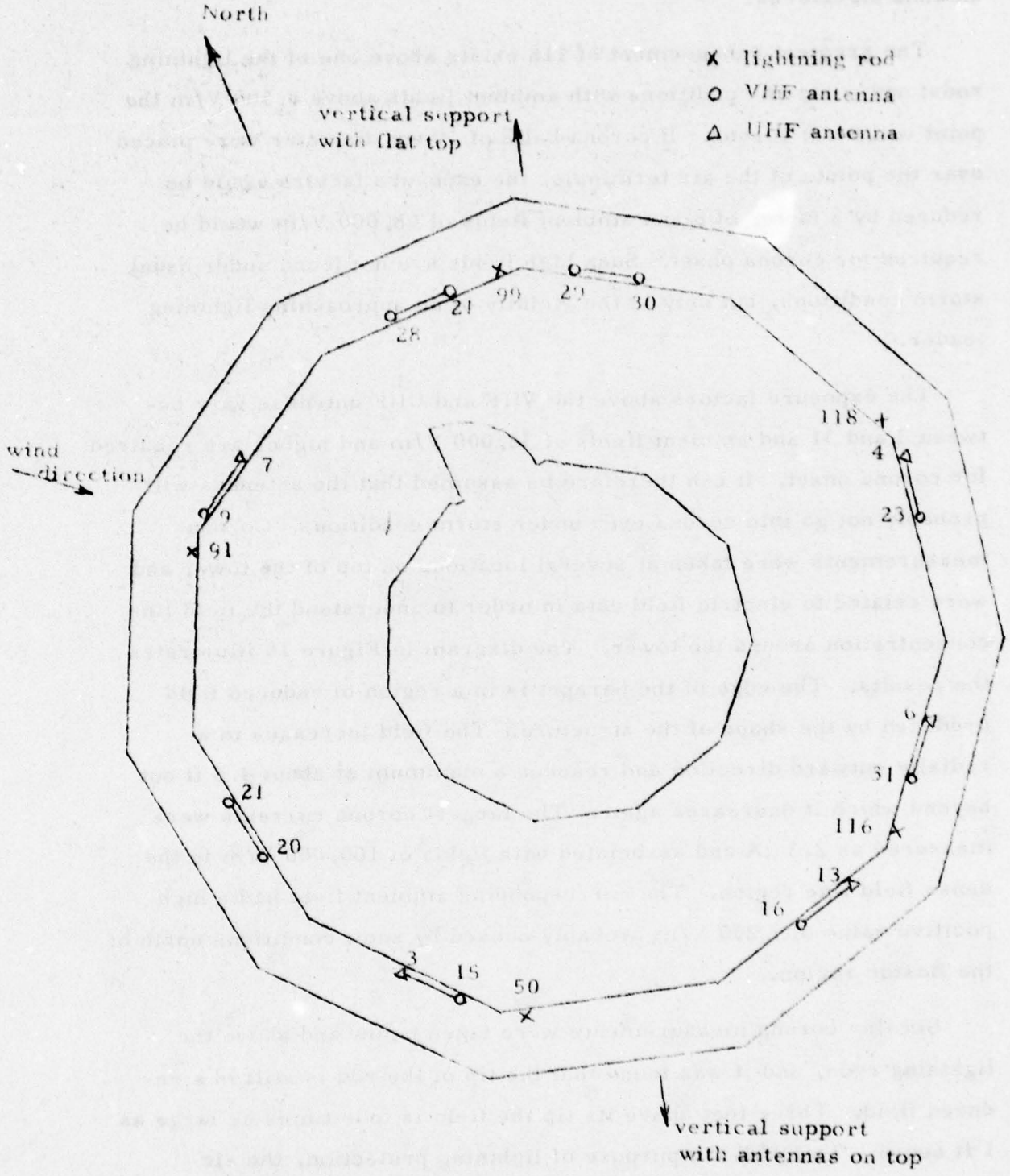

Figure 15. Exposure factors versus ground on top of the lightning rods and VHF antennas on the Logan International Airport air traffic control tower.

nearly 5 ft high, and even much lower above the wide 3 ft high UHF antenna structures.

The greatest enhancement of 118 exists above one of the lightning rods; under storm conditions with ambient fields above 8,500 V/m the point will be in corona. If corona balls of 10 cm diameter were placed over the points of the air terminals, the exposure factors would be reduced by a factor of 8 and ambient fields of 68,000 V/m would be required for corona onset. Such high fields are not found under usual storm conditions, but only in the vicinity of an approaching lightning leader.

The exposure factors above the VHF and UHF antennas vary between 3 and 31 and ambient fields of 32,000 V/m and higher are required for corona onset. It can therefore be assumed that the antennas will probably not go into corona even under storm conditions. Corona measurements were taken at several locations on top of the tower and were related to electric field data in order to understand the field line concentration around the tower. The diagram in Figure 16 illustrates the results. The edge of the parapet is in a region of reduced field produced by the shape of the structure. The field increases in a radially outward direction and reaches a maximum at about 4.5 ft out beyond which it decreases again. The largest corona currents were measured as 2.3 μA and associated with fields of 100,000 V/m in the dense field line region. The corresponding ambient field had a high positive value of 1,200 V/m probably caused by snow conditions north of the Boston region.

Similar corona measurements were taken below and above the lightning rods, and it was found that the tip of the rod is still in a reduced field. Three feet above its tip the field is four times as large as 1 ft above. To fulfill the purpose of lightning protection, the air terminals must have a minimum height of 6 ft, which is just 1 ft above

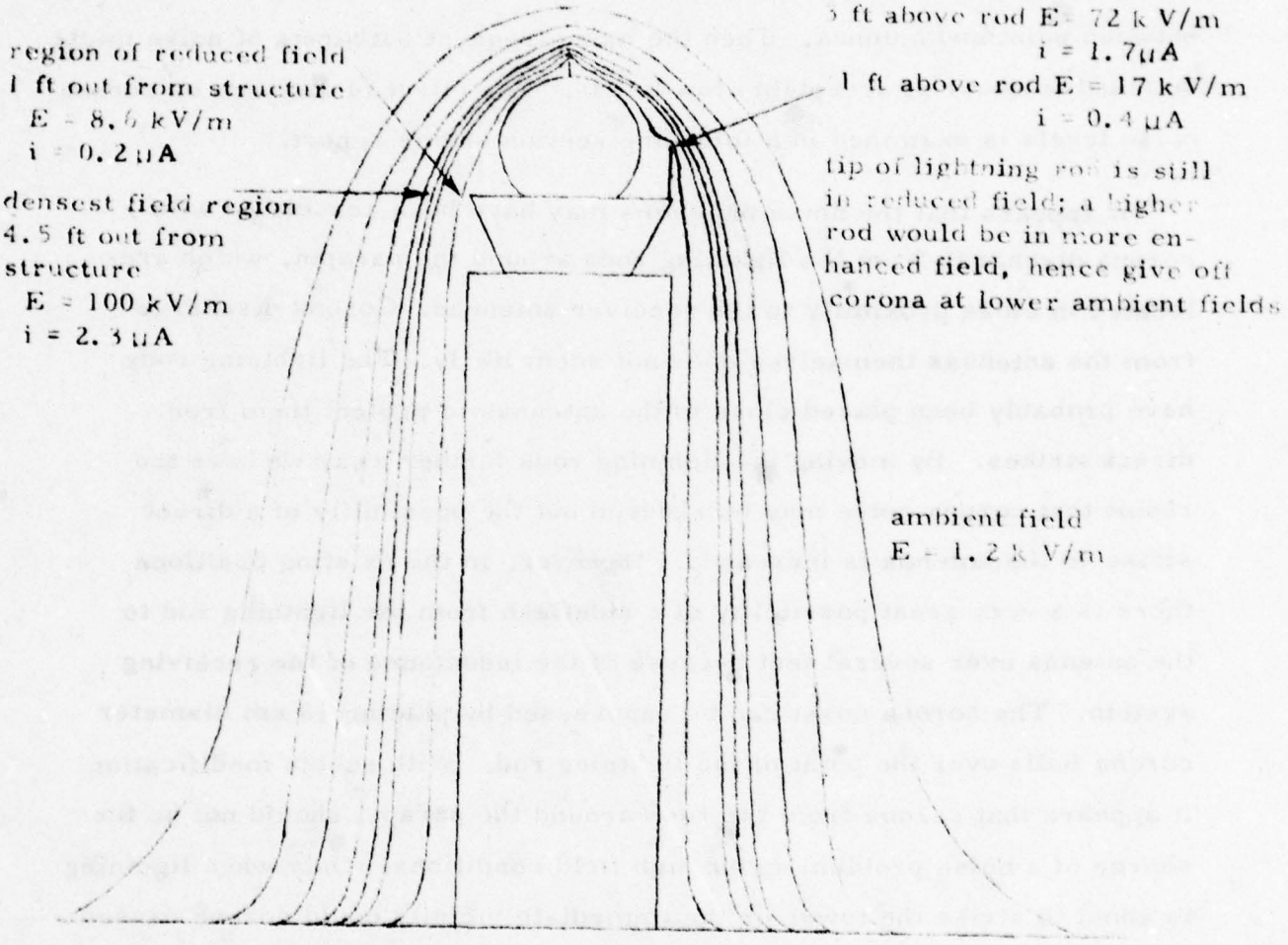

Figure 16. Equipotential lines around structure go through enhanced density 4.5 ft out from structure as determined from corona current (i) measurements.

the height of the VHF antennas. If the lightning rods, however, were much higher, then their points would be in a more concentrated field line region, and corona onset and associated noise problems could be much more frequent and persistent. However, a moderately effective trade-off might result if raising the tip of the lightning rod produced a sufficient increase in distance between point and antenna. Then the more frequent outbursts of noise might be found to occur at acceptably low levels. The effect of distance on corona noise levels is examined in a following section of this report.

It appears that the noise problems may have been associated with corona discharge from the lightning rods around the parapet, which are located in close proximity to the receiver antennas. Corona discharge from the antennas themselves does not seem likely. The lightning rods have probably been placed close to the antennas to protect them from direct strikes. By moving the lightning rods further away we have the result that corona noise may be reduced but the possibility of a direct strike to the antenna is increased. However, in the existing positions there is a very great possibility of a sideflash from the lightning rod to the antenna over several feet because of the inductance of the receiving system. The corona onset can be suppressed by placing 10 cm diameter corona balls over the point of the lightning rod. With such a modification it appears that corona from the rods around the parapet should not be the source of a noise problem under high field conditions. Only when lightning is about to strike the tower or the immediate vicinity could corona caused noise problems be experienced.

4.3 Effect of the Radome Charge

Under severe snow and blowing conditions a very large potential difference may occur between the dielectric surface of the radome and the surrounding structures. If this surface has an electric field intensity that is sufficiently high to cause voltage breakdown across the plastic surface, then a streamer discharge may occur which can generate serious radio interference. Near the ocean where high charges exist due to charge separation in breaking waves, such charges may be transported in a high wind and may cause rapid buildup on the radome. Driving snow will also cause a charge buildup. Hence, the possibility that the radome can become sufficiently charged to cause streamer discharges has to be considered.

The charge accumulated on the radome may have a second effect. It may create high enough fields to cause corona discharge from points in its vicinity such as the lightning rods which are about 4 ft away or the sharp edges of the ladder only 1ft away.

To investigate the magnitude of the charge that may reside on the dielectric surface, electric field measurements were taken a short distance away from some radome panels that were charged by rubbing with a glove. The results are shown in Figure 17. The radome was charged to -29,000 V creating an electric field of -24,000 V/m at a distance of 4 ft at the tips of the lightning rods around the papapet as well as on top of the radome. Since an enhancement of 12 above the ambient field exists 4 ft above the radome in the absence of the air terminal, the charged radome would, at the distance of 4 ft, have an effect equivalent to a change in the ambient field of -2 000 V/m. Whatever the effect is, it would persist for extended periods of time, as it was found that the charge remained on the radome beyond the duration of the experiment and did not drain off.

The field of the charged radome may reinforce or counteract the existing ambient field. It is difficult to estimate the effect on corona formation above the rods, as the equipotential lines there are not normal

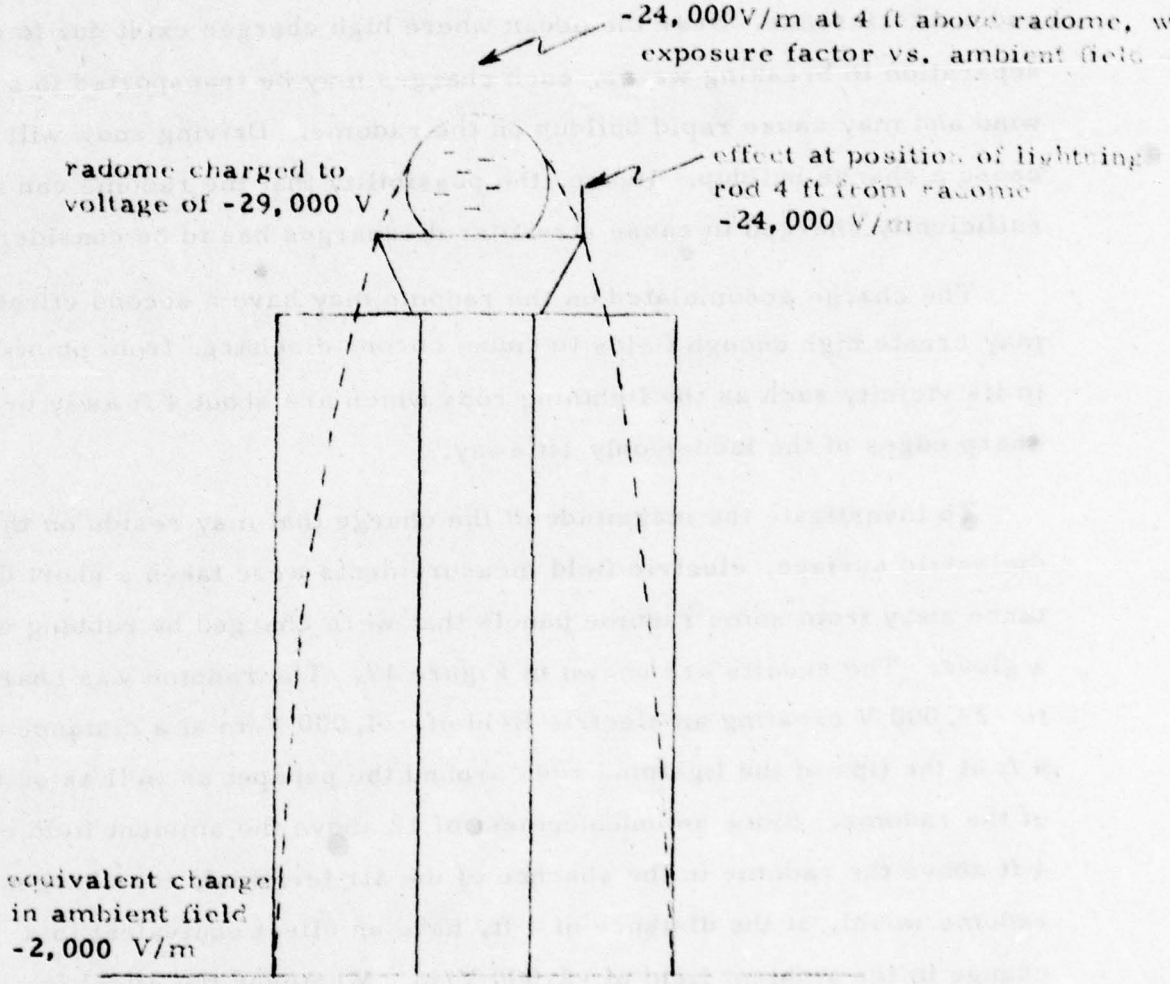

Figure 17 . Effect of radome charge on electric field.
(distorted scale)

to the rods, hence their effect is reduced. To understand this problem would require involved computations and additional measurements. At the location of the ladder about 1ft away from the radome the fields, due to the radome charge, are even much higher of the order of -95,000 V/m, and at the ladder support and the bottom of the highest lightning rod the field might be so high that there exists continuous corona discharge. Furthermore, the potential of the radome could reach values much higher than those we caused with a fur glove.

Charge deposited on a dielectric surface such as the radome is bound there because the surface is an insulator. As a result , under precipitation charging conditions, it is possible for a potential difference of tens of kilovolts or more to exist between a dielectric surface and the neighboring structural parts. As charge continues to accumulate on the dielectric, the potential to the structural parts rises until the electric field intensity at the dielectric surface becomes sufficiently high that voltage breakdown or streamer discharge occurs across the plastic surface. A surface streamer involves the rapid transfer of charge over a substantial distance, and also generates serious radio frequency interference.

The degree to which the radio frequency noise generated by corona and streamer discharges couples into electronic systems is determined by the relative locations of the noise source, and the receiving antennas via which the noise is coupled into the affected system. In addition, the coupling depends on frequency and the size of the antennas. These subjects are examined in the final sections of this report.

4.4 Charge Transfer from Rain

The charge on rain hitting the receiver antennas will cause a current to flow to ground through the receiving circuit that might be of the same order of magnitude as the normal signals and hence produce noise interference. To investigate this hypothesis, a maximum charge on a single raindrop was assumed as -2.3×10^{-12}C $= -1.4 \times 10^{7}$ electrons from Chalmers.[9] If 100 such raindrops fell on the antenna per second trans-

ferring their charges, a current of 2.3×10^{-4} μA would be flowing. This would result in a voltage of 1.2×10^{-2} μV across the receiver impedance of 50Ω, at a power of 2.6×10^{-18} Watt.

The receivers operate at a signal level of 2.5 to 3 μV with a normal ambient noise level of 1 μV, which is about two orders of magnitude greater than the noise attributed to the charge transferred from rain. It is therefore unlikely to be a source of the noise. If, however, the assumed figures of number of drops per second and charge per raindrop do not represent maximum values, then radio interference from charged rain might still be possible. This is more likely to be the case above the Logan tower where the rain may gather an enormous charge due to excessive corona in that environment. The fact that UHF communications have had no noise problems with their antenna's in the same vicinity indicates that charged rain is not a problem.

5.0 EXPERIMENTAL EXAMINATION OF INTERFERENCE DUE TO CORONA DISCHARGE

The study of the factors which influence noise interference due to corona discharge has been carried out with an experimental arrangement which used equipment similar to that found at an air traffic control center. Two types of VHF communications receivers, three antennas, and two corona discharge devices were employed in this study and effects of corona current and distance were examined. As predicted in previous sections of this report, corona discharge could be suppressed by placing a metal sphere on top of the corona point. The initial phase of the study was concerned with finding an objective means to measure noise levels which would closely correspond to the subjective impressions of a listener. It was found that the automatic volume control (AVC) circuit of one of the receivers produced a voltage which could serve as a measure of noise level and incoming signal strength as well. By recording this voltage level, it was possible to make direct comparisons of noise level and RF signal strength. The use of a pair of receivers tuned to the same VHF channel made it possible to document cases in which a voice signal heard in one receiver was totally masked by noise in the other receiver. However, careful inspection of the recorded traces is necessary to distinguish noise from voice signals. This is made possible by the comparisons of the AVC and AGC traces from the pair of receivers. The presence of noise would increase the baseline of an AVC trace while a voice signal would be seen as a roughly rectangular increase above the noise level, if the voice was not totally masked by the noise. In addition, the event marker of the strip chart recorder was used to indicate those voice signals which could be clearly heard through a receiver's loudspeaker output. This marker is seen in many of the following chart records as a straight line at the bottom of the chart, which drops down by about 1 mm whenever the listener heard a voice signal and actuated the marker control.

Noise from positive and negative point discharges was studied since both of these polarities can be naturally induced. However, the physical processes involved are quite different for the two different polarities. The positive point attracts negative electrons toward itself where the electric field strength is highest. As the electrons accelerate toward the point, their collisions with air molecules

produce new ions and secondary electrons which then add to the avalanche of electrons accelerating toward the point. Meanwhile, the positive ions which move very slowly compared to electrons are being repelled by the positive point and are moving outward. This process continues until this space charge weakens the original field and the avalanche stops. Thus, the corona current is not steady but consists of a series of pulses. The negative point discharge also consists of pulses, but the electrons and ions move oppositely. The positive ions are slowly drawn into the region of high field strength near the point, while the fast moving electrons are repelled and move outward. Consequently, it is expected that the relation between noise and corona current will be different for the two point polarities. The magnitude of corona current is also affected by the wind speed which removes the charge being repelled by the point and allows another corona pulse to occur.

5.1 Description of Equipment used for Noise Tests

Two types of VHF fixed-tuned receivers were used to monitor interference with voice communication due to noise from the electrical discharge at a sharp point. The RV-12B is a tube-type receiver which has a single crystal controlled channel (124.1 MHz) and is equipped with automatic noise limiter, delayed and amplified automatic volume control (AVC) and a carrier-operated squelch. The AN/GRR-23 is a solid state receiver which is also crystal controlled and is equipped with noise filtering circuitry and an automatic gain control (AGC). Three vertical dipole antennas of various design were used, all manufactured by the Technical Appliance Corporation. The simplest of the three is the D-2216, a halfwave dipole enclosed in a fiberglass radome with a height of 54.50 inches. The D-2213 has a height of 84.25 inches and contains a UHF section (not used) in addition to its multiple collinear dipole array for VHF. The D-2212 has a height of 152.25 inches and contains two independently operating VHF dipole arrays of which only one was used with each receiver. The position of the point discharge apparatus, relative to these antennas is shown in Figure 18, and further details are in Appendix A.

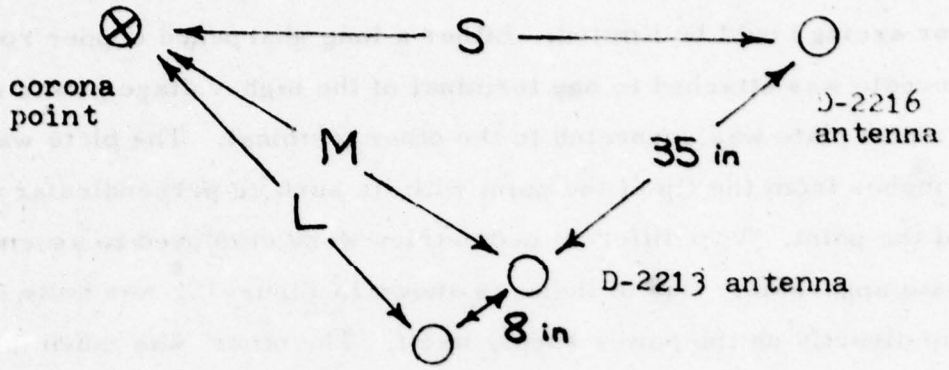

(A) Top view, distances S, M, and L are variable

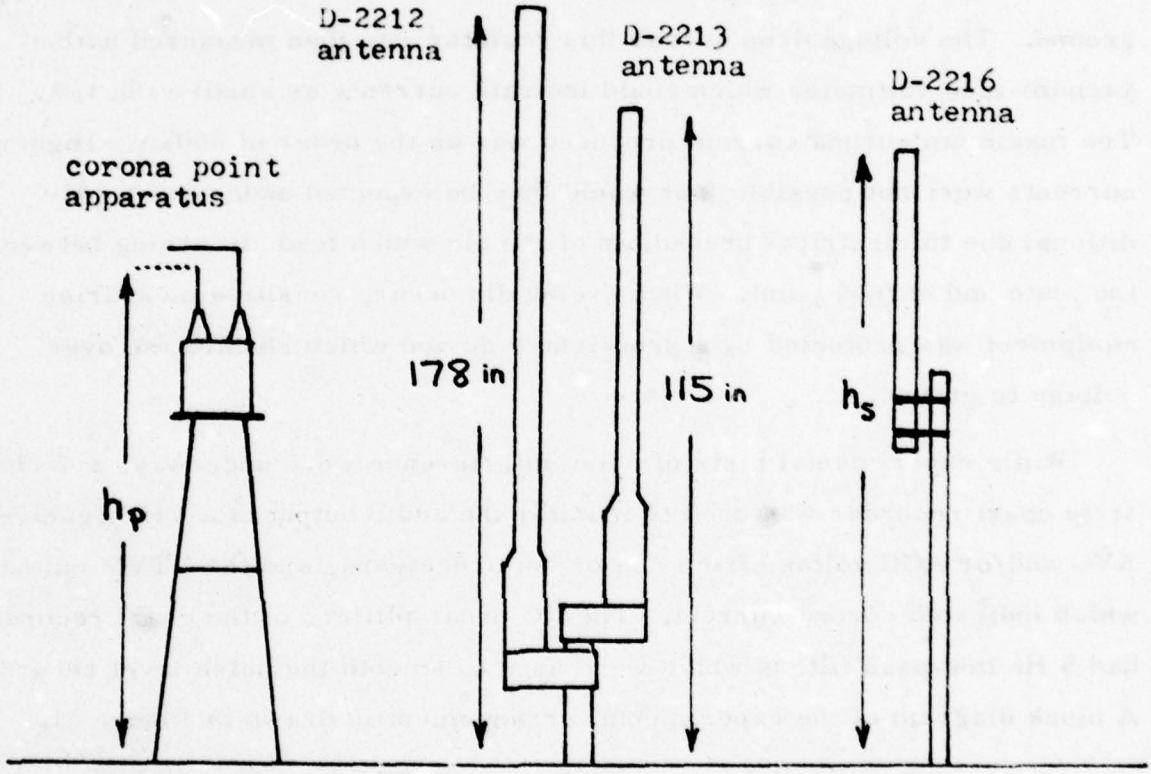

(B) Side view, h_p and h_s are variable

Figure 18. Relative positions of corona point apparatus and antennas

Electrical discharge at a sharp point (corona) was produced using a 50KV D.C. power supply with a variable input voltage so that electrical breakdown or arcing could be limited. Either a long sharpened copper rod or a steel needle was attached to one terminal of the high-voltage power supply and a flat metal plate was connected to the other terminal. The plate was positioned a few inches from the tip of the point with its surface perpendicular to the long axis of the point. Two different geometries were employed to assemble the point and plate apparatus. One of these, as shown in Figure 19, was quite compact, being built up directly on the power supply itself. The other was much larger and was supported by a metal tripod with the power supply placed approximately 10 feet away and is shown in Figure 20. The large unit was used to study dimensional and geometric effects on the coupling of corona noise to the receiver input while the compact unit provided necessary portability for the study of effects due to varying antenna to corona point distance. In order to determine the corona current, a 100 ohm resistor was placed in series between the point and the power supply ground. The voltage drop across this resistor was then measured with a vacuum-tube voltmeter which could indicate currents as small as 0.1μA. The maximum corona current produced was on the order of 500μA. Higher currents were not possible (nor would they be expected under most conditions) due to electrical breakdown of the air which leads to arcing between the plate and corona point. When arcing did occur, sensitive measuring equipment was protected by a proprietary device which shunted the over voltage to ground.

While experimental tests of noise interference were underway, a 4-channel strip chart recorder was used to monitor the audio output of a VHF receiver, AVC and/or AGC voltage from one or both receivers, and the VTVM output which indicated corona current. The DC preamplifiers of the chart recorder had 5 Hz low-pass filters which were used to smooth the noise level recordings. A block diagram of the experimental arrangement is drawn in Figure 21.

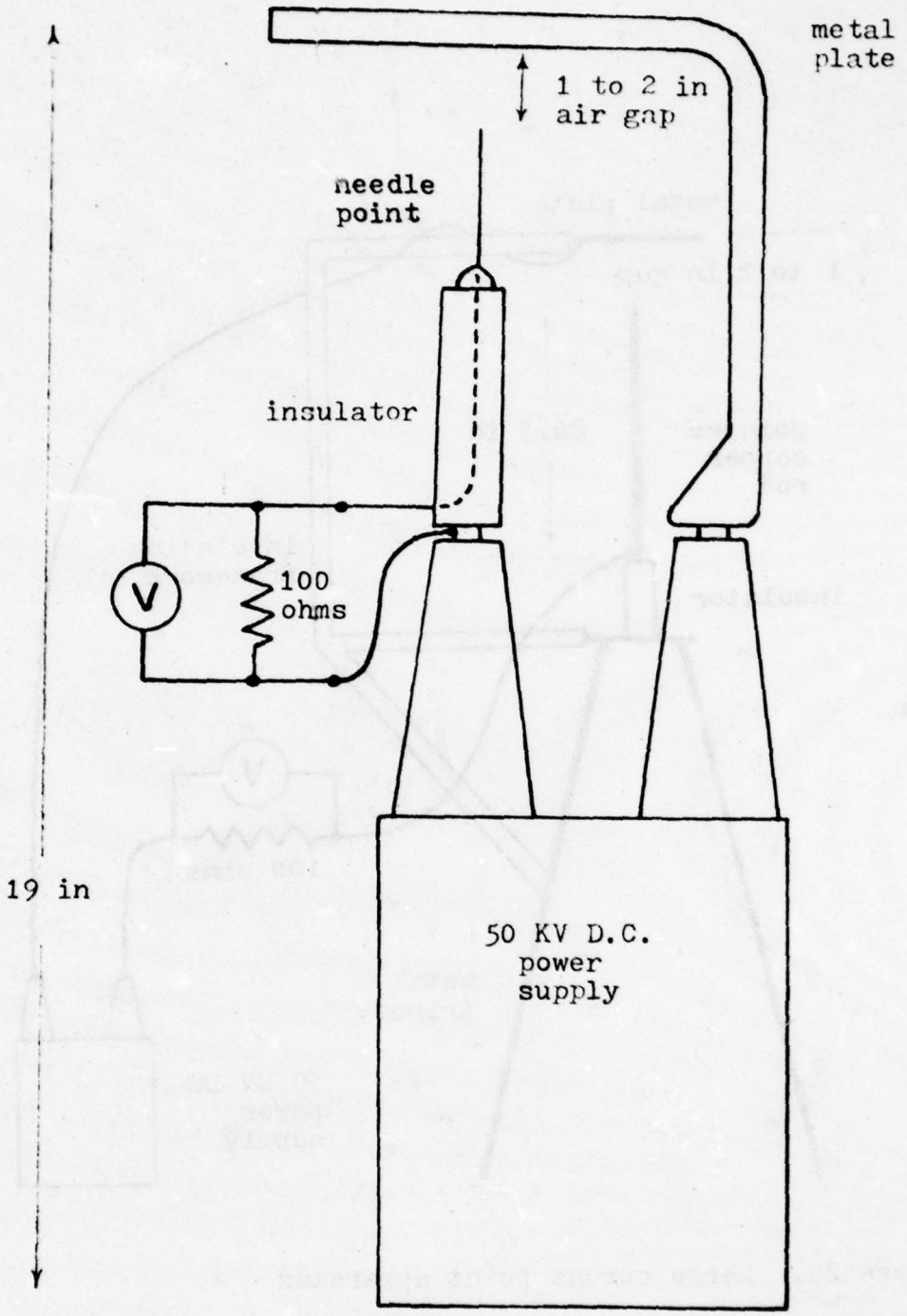

Figure 19. Compact corona point apparatus

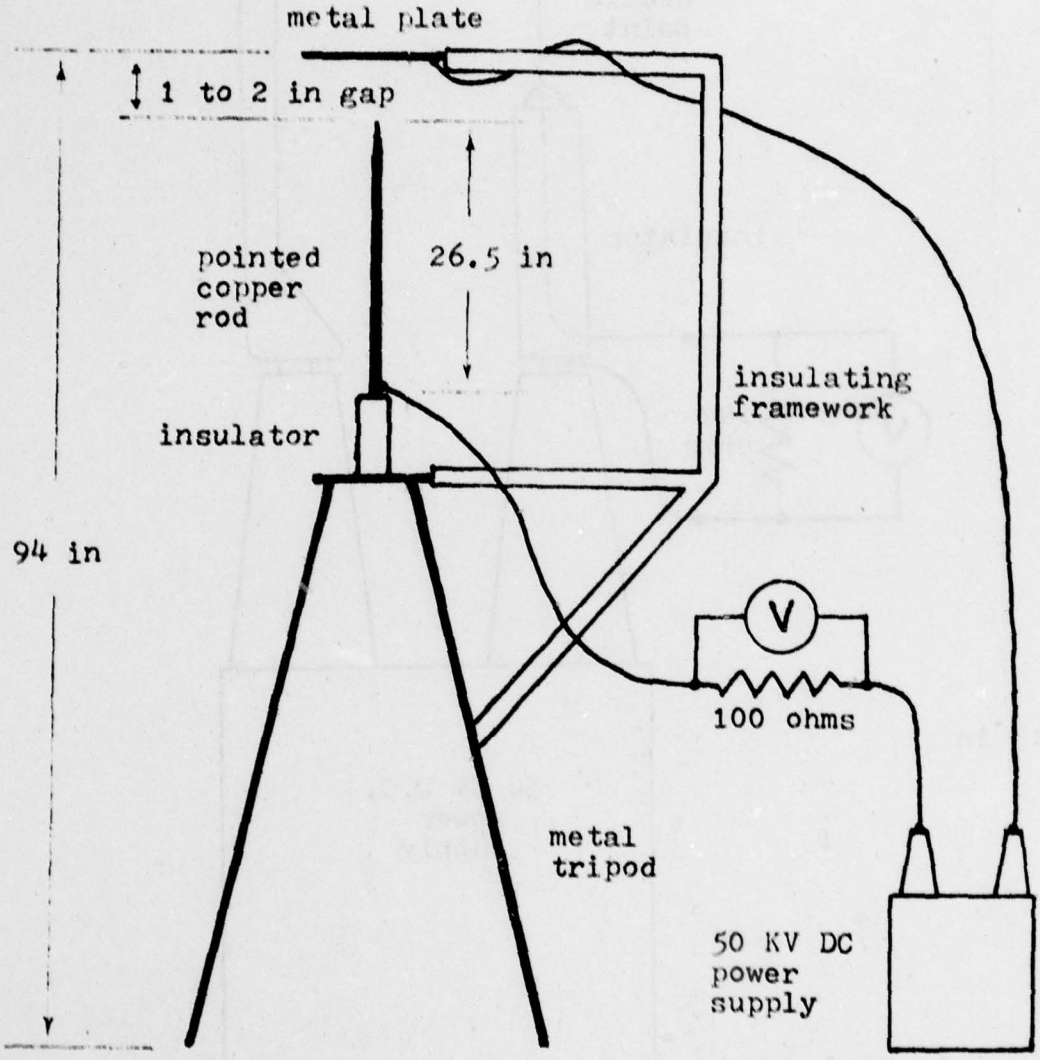

Figure 20. Large corona point apparatus

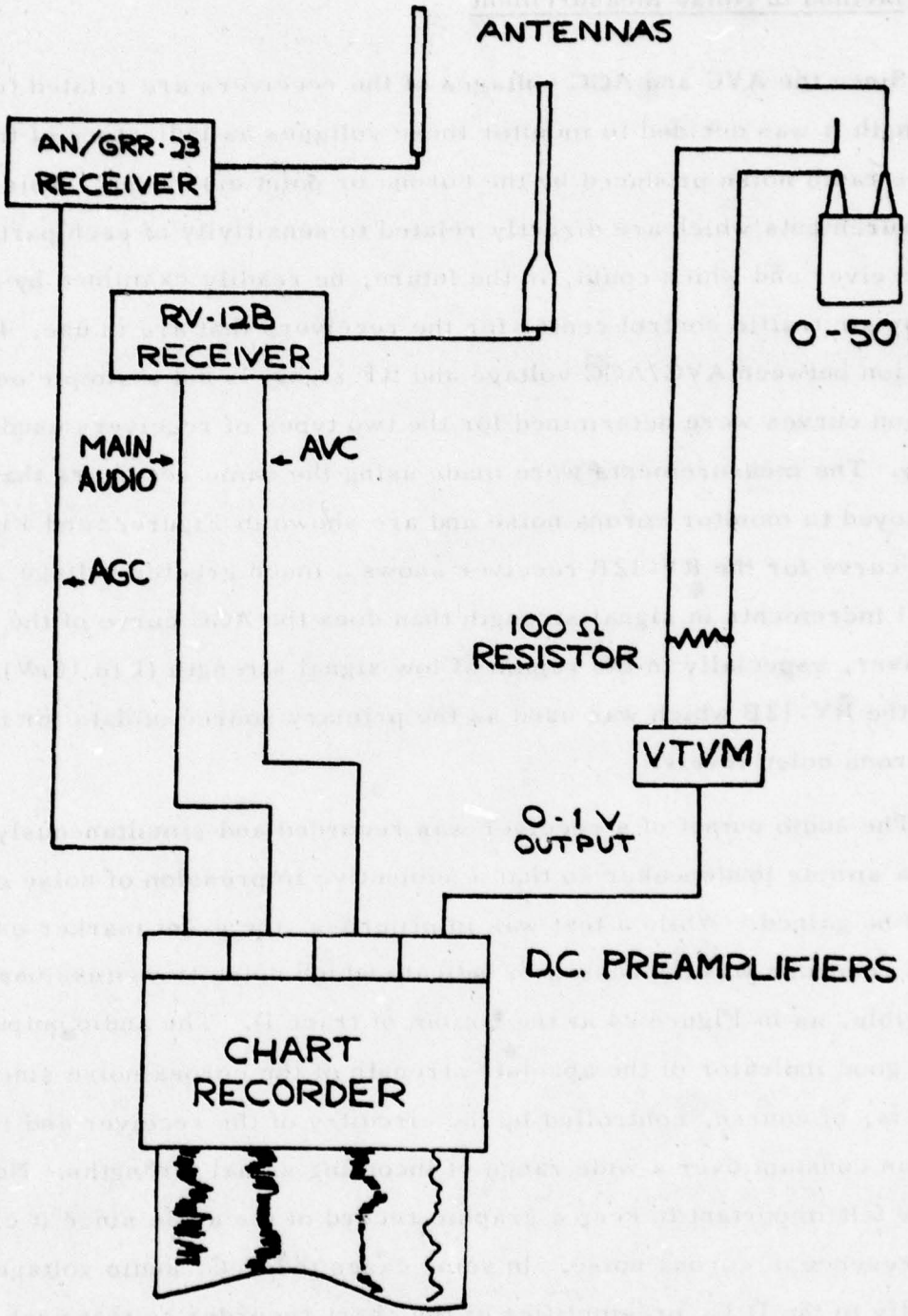

Figure 21. Block diagram of a typical data gathering arrangement

5.2 Method of Noise Measurement

Since the AVC and AGC voltages of the receivers are related to RF signal strength it was decided to monitor these voltages as indicators of the intensity of the radio noise produced by the corona or point discharge. This provides measurements which are directly related to sensitivity of each particular type of receiver and which could, in the future, be readily examined by a technician at any air traffic control center for the receivers that are in use. Because the relation between AVC/AGC voltage and RF signal is not a simple one, calibration curves were determined for the two types of receivers used in this study. The measurements were made using the same receivers that were employed to monitor corona noise and are shown in Figure 22 and Figure 23. The AVC curve for the RV-12B receiver shows a much greater voltage swing for small increments in signal strength than does the AGC curve of the AN/GRR-23 receiver, especially in the region of low signal strength (1 to 10μV). Therefore, it is the RV-12B which was used as the primary source of data for the comparison of corona noise levels.

The audio output of a receiver was recorded and simultaneously monitored with a simple loudspeaker so that a subjective impression of noise characteristics could be gained. While a test was in progress, the event marker on the strip chart recorder was depressed to indicate which noise transmissions were intelligible, as in Figure 24 at the bottom of trace D. The audio output is not a good indicator of the absolute strength of the corona noise since the output level is, of course, controlled by the circuitry of the receiver and is supposed to remain constant over a wide range of incoming signal strengths. Nonetheless, it was felt important to keep a graphic record of the audio since it clearly shows the presence of corona noise. In some cases the A.C. audio voltage was fed directly to the D.C. preamplifier of the chart recorder so that peak voltages could be recorded, in other cases a simple full-wave rectifier was inserted between the audio output and the input of the strip chart preamplifier in order to obtain a record of the loudness of the audio output.

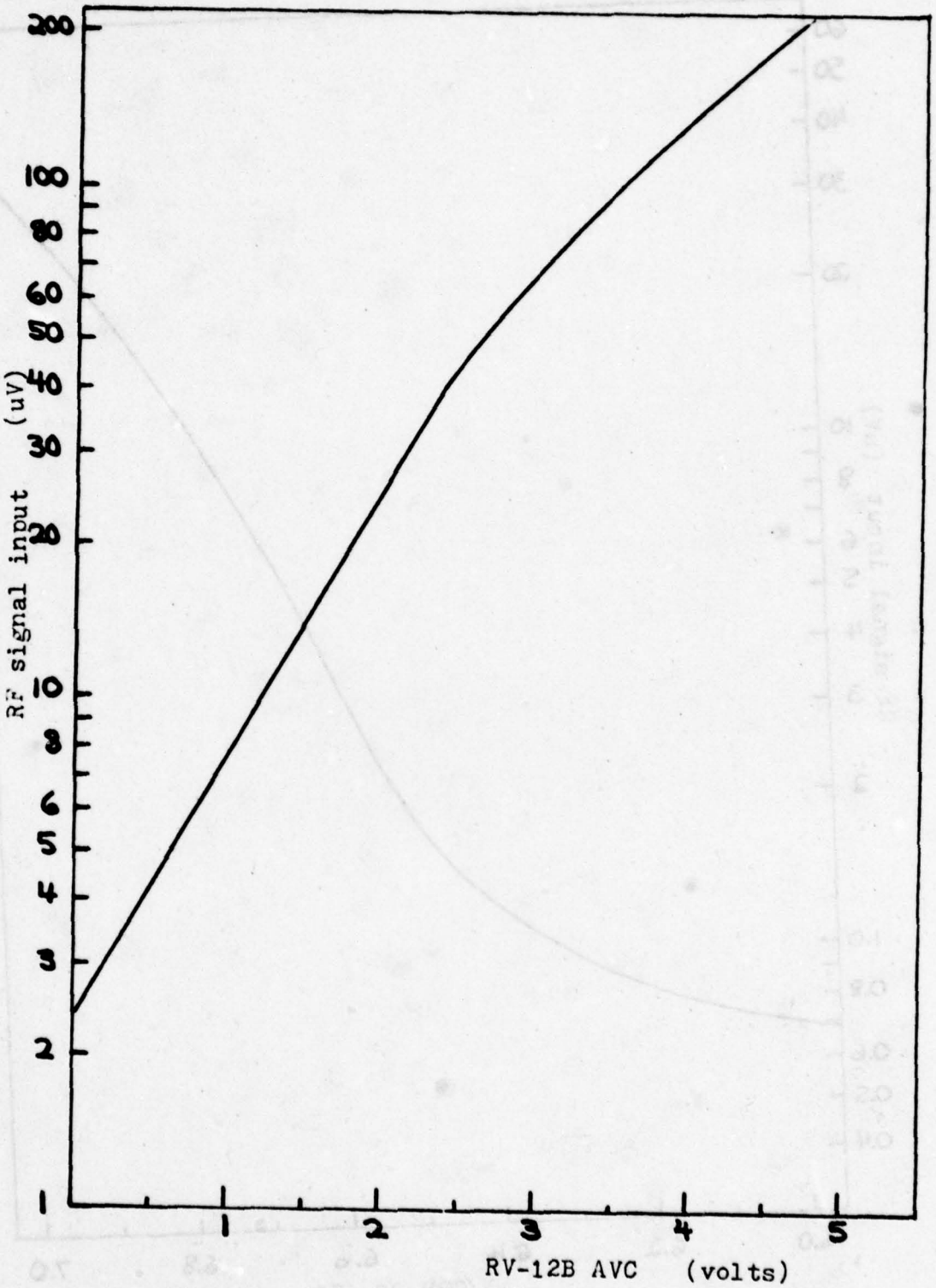

Figure 22. AVC voltage calibration for the RV-12B receiver

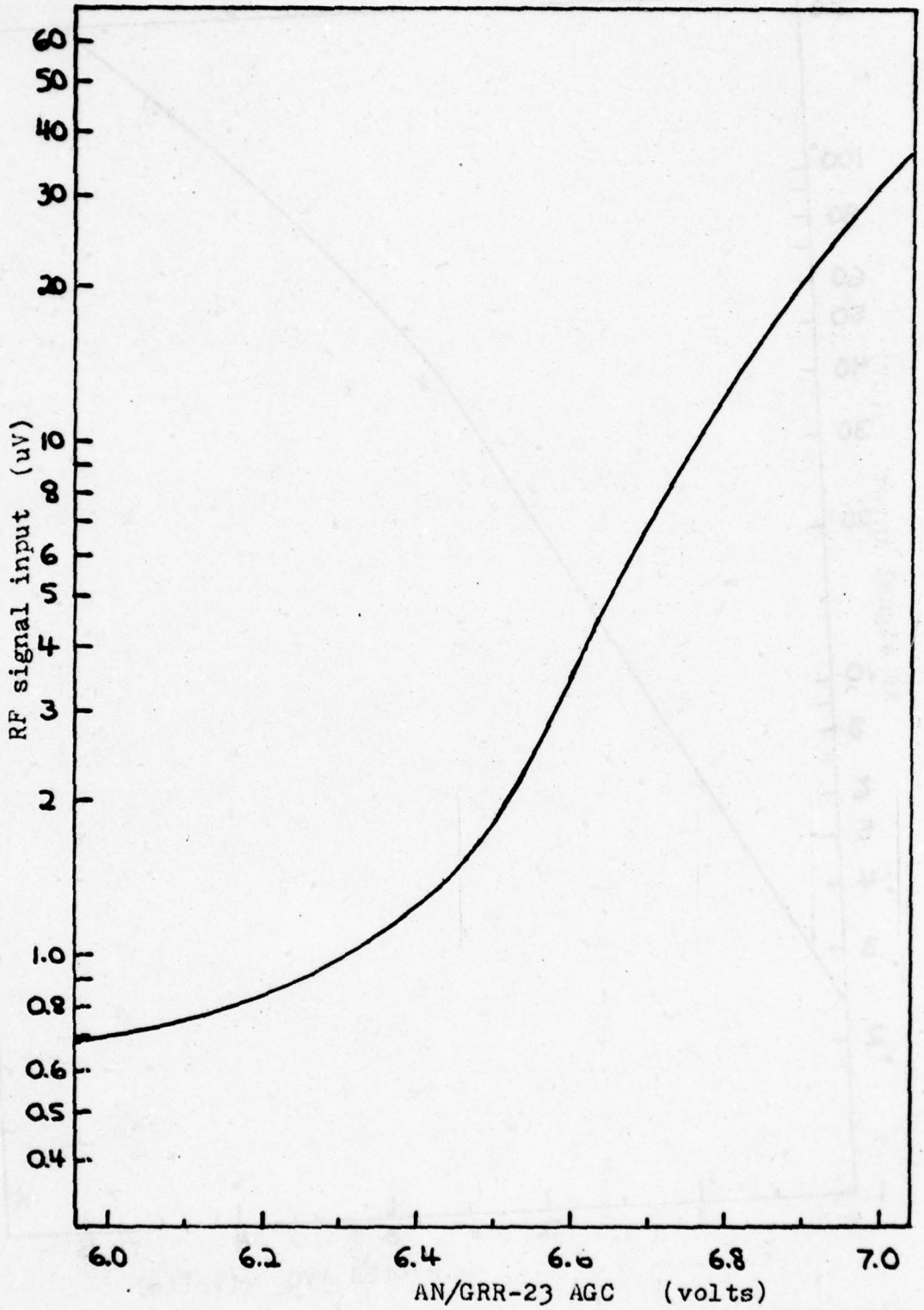

Figure 23. AGC voltage calibration for the AN/GRR-23 receiver

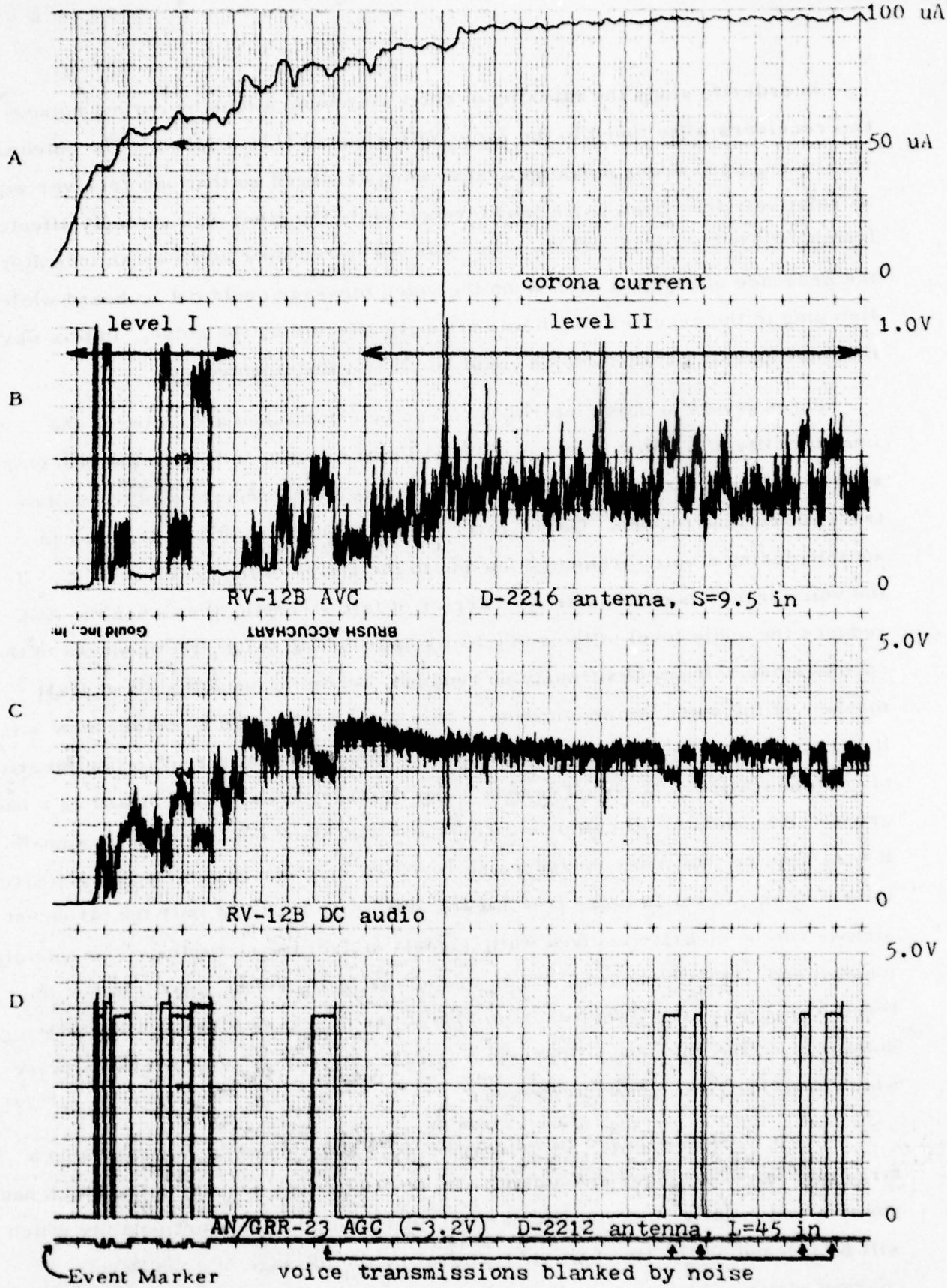

Figure 24. Strip chart record showing level I and II noise
S & L refer to dimensions shown in Figure 18A.

In order to study the masking of voice communications by corona noise, two receivers were tuned to the same VHF channel (124.1 MHz). The antennas, receivers, and corona noise apparatus were arranged so that one receiver would be relatively free from noise interference while the other was strongly affected (compare Figure 24, B and D). The noise-free receiver acted as an indicator of the presence of a signal even when the voice message could not be heard while listening to the receiver which was strongly affected by the noise. In this way, the total loss of a transmission could be clearly documented.

Three levels of noise interference can be established according to the intelligibility of a voice message. Level I corona noise will open the receiver squelch circuit but will not cause any difficulty in the reception of the voice-transmitted information. Often, level I noise is so weak that it becomes inaudible during a voice transmission due to the action of the receiver AGC. If the voice transmission has an RF carrier of fair strength, then when the AGC reduces the audio level of the voice to its appropriate value, the loudness of the corona noise will simultaneously be reduced, becoming inaudible or at least masked by the voice communication. This level I noise can be bothersome since it will open the squelch on a receiver, but it poses no real threat to the integrity of communications. Level II corona noise is strong enough to be heard as a background component of all communications and will blank out the weakest signals. It may require that many messages be repeated in order to clearly relay desired information. Level III noise (see Figure 39B) is so high that only the strongest signals can be clearly received while signals of average strength are completely masked and cannot be heard. There are no distinct dividing lines between the three levels since the transition from one to the next is gradual and depends somewhat on the subjective impressions of the listener as to that level of noise which contributes serious interference.

Corona noise was heard in conjunction with voice communications using a large number of receiver and antenna combinations with corona points which had positive and negative electrical polarity. (It is the positive point polarity which will be induced on the tip of an air terminal by the passage of a negatively charged cloud.) The horizontal distance between the corona point and various

antennas ranged from 7 inches to 12 feet. Figure 24 is a typical recording and contains examples of serious interference due to level II noise and minimal interference due to level I noise, both produced by a positive point discharge. Corona current from 0 to 100μA is recorded on the top trace (A) while the AGC level recorded in the bottom trace (D) gives a definite marker for all voice communication on the 124.1 MHz channel which is common to both of the receivers used during this test. Notice that the AGC of this receiver (AN/GRR-23) is not visibly affected by the corona noise and that the event marker immediately below the AGC trace is not depressed for every case in which the AGC level indicates a voice signal. The audio output of the other receiver (RV-12B) is recorded by trace C and was used by the listener to decide when to depress the event marker. Any case in which an AGC level of 3.5V to 4V in trace D shows a signal without a corresponding notch in the event marker, is a case in which the voice transmission was masked by corona noise. The AVC level of the RV-12B receiver is recorded by trace B and shows barely discernable changes due to the presence of a signal while the noise is in the level II region. In the level I region the AVC increases when voice signals stand out clearly above the noise which is near the baseline of the trace. When examining Figure 24, it is important to note that all of the AGC increases shown in trace D are due to voice transmissions.

Noise in the level I region increases the AVC baseline by less than 0.1V, is heard in the background, but does not impair the clarity of a voice transmission. Level III noise corresponds to AVC increases of more than 0.5V and renders the channel useless for reliable communication. In the intermediate region of level II (0.1V to 0.5V increase in AVC), the corona noise causes serious interference which demands that a message be repeated before it can be clearly understood.

5.3 Results of Noise Measurements

5.3.1 Introduction

Because of the differences in the physical process of discharge, the positive and negative point discharges will be discussed separately. In each case data will be presented to show the dependence of noise interference on corona current and distance between the corona point and receiving antenna. The use of the AVC voltage of the RV-12B receiver as a measure of noise level produces a chart record which closely corresponds to the subjective aural impression obtained when listening to the audio output of either the RV-12B or the AN/GRR-23 receivers. This is especially true when the chart recorder preamplifier is adjusted so that its D.C. offset cancels the quiescent AVC voltage (about 0.37V) which exists even when no signal or corona noise is present. This is not unexpected since the AVC voltage is related to the logarithm of signal strength (see Figure 22),in much the same way that the human ear responds logarithmically to different intensities of sound. The AGC voltage of the AN/GRR-23 receiver is useful for a different purpose, since it jumps suddenly from 3.2V to 6.5V as its threshold is reached and then increases by only another volt or so over a very broad range of signal strengths. This behavior allowed it to function nicely as a monitor for the presence of signals which can be observed as clear rectangular steps in the chart recorder trace, even when the same signals cannot be seen in the trace of the AVC from the RV-12B. If a signal did not produce a visible, rectangular step in the AGC trace, it could not be heard above the corona noise when listening to the output of the AN/GRR-23. On the other hand, many signals which caused a clear increase in the recorded trace of the RV-12B AVC voltage could not be heard in the audio output of that receiver. Generally, a signal which did not at least double the amplitude of the recorded trace of RV-12B AVC voltage would not be even marginally useful for voice communication through that receiver.

In order to record noise even at the lowest levels, both receivers were operated with the squelch controls turned off. The bias controls of the chart recorder preamplifiers were adjusted so that quiescent state AVC and AGC voltages, ambient noise, and internal receiver noise do not appear as part of the recordings.

5.3.2 Corona Noise Due to A Positive Point

The maximum corona current observed for a positive point discharge was close to 100μA. When this upper limit was reached, arcing between the point and plate would begin, typically at an applied voltage of 30kV with an air gap of one inch between the point and plate. Larger gaps between the point and plate would allow higher applied voltages, but arcing would still take place at about the same maximum current. As expected, the noise level heard in the receivers would increase as the corona current increased.

To show the relation between noise and corona current, strip chart records were analyzed on a point-by-point basis, measuring an AVC voltage and the corresponding corona current and plotting the results as in Figure 25. This graph does not include a constant D.C. offset of 0.372V which is the quiescent value of the AVC voltage. The same receiver-antenna combination (RV-12B, D-2216) was analyzed for three different distances from the corona point. The noise versus current relation is the same not only for these three distances, but for all tested distances and receiver-antenna combinations, although the actual AVC voltages may vary greatly from one combination to another. Corona currents below 40μA would barely perturb the quiescent AVC level indicating that no appreciable noise is being generated as far as a typical communications receiver is concerned. Listening to the audio outputs of the receivers confirms this since it was hard to distinguish corona noise from ambient background noise until corona currents began to exceed 25μA.

As can be seen in Figure 26, the effect of distance between receiving antenna and corona point is important in determining the resultant noise level at the receiver. Here again, the AVC voltage is taken as the measure of noise level and indicates that serious noise interference is to be expected whenever a positive point discharge occurs within 24 inches of a receiving antenna. The curves shown in this figure were derived from recorded data on a "worst case" basis, i.e., the maximum noise-induced AVC voltage was used to represent the noise level at each distance. Some data was obtained at distances greater than 50 inches, but it was difficult to obtain reliable measurements at these distances since the noise

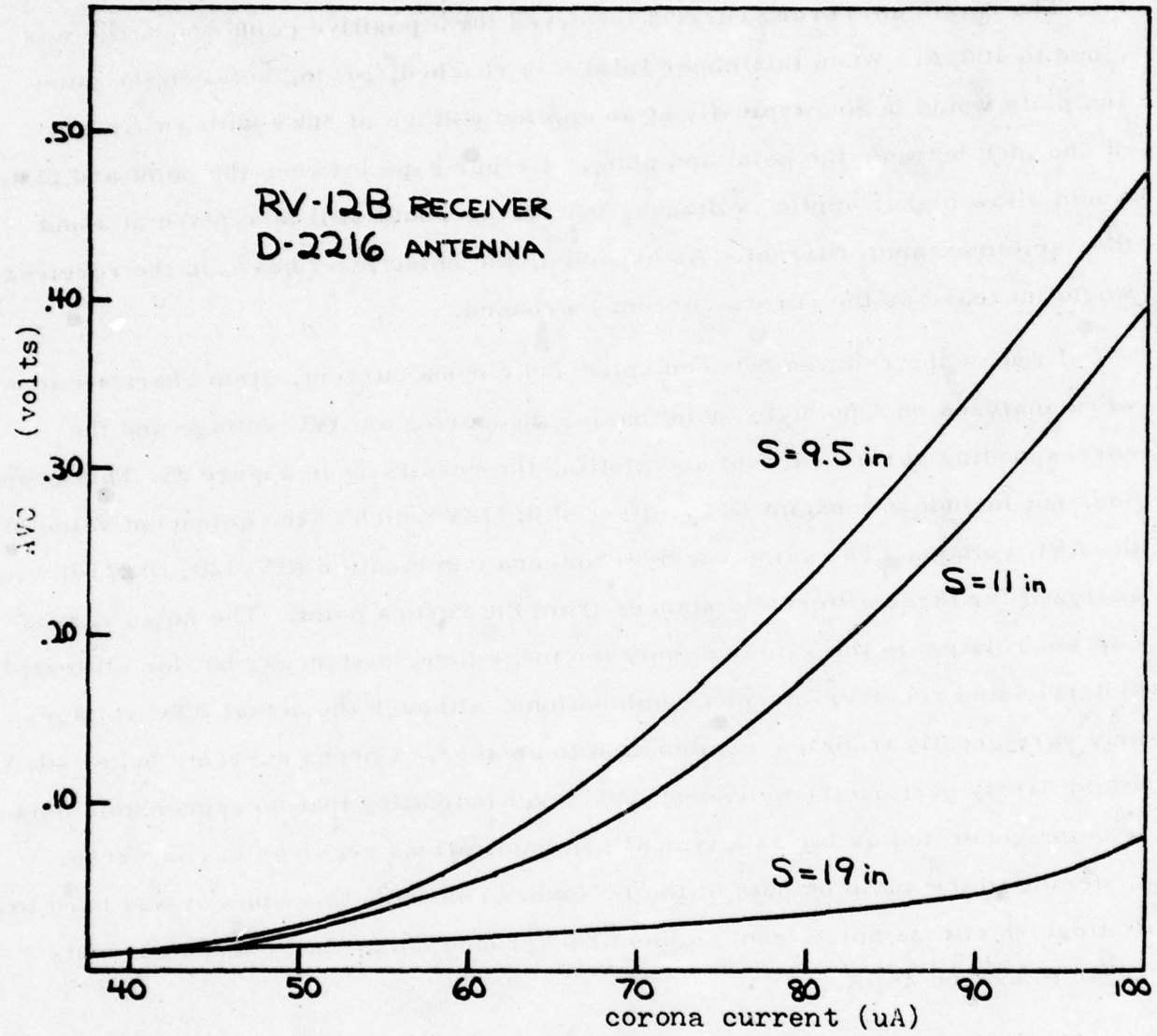

Figure 25. Noise level vs. corona current for a positive point at three distances

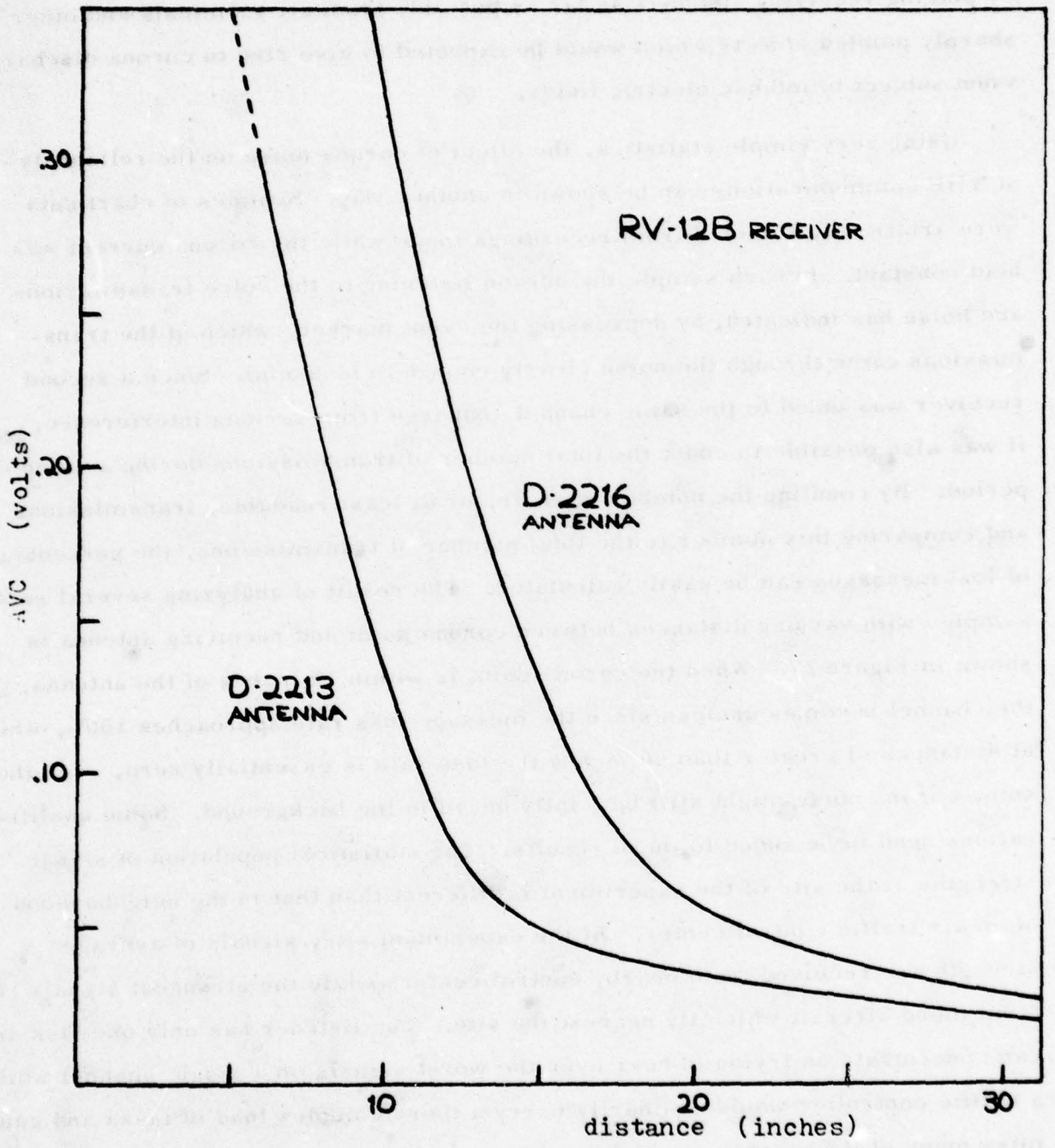

Figure 26. Noise level vs. distance using two different antennas and a positive point discharge

level was so low. Thus, it is seen that some noise reduction can be achieved by placing receiving antennas as far as possible from air terminals and other sharply pointed objects which would be expected to give rise to corona discharge when subject to intense electric fields.

Using very simple statistics, the effect of corona noise on the reliability of VHF communications can be shown in another way. Samples of chart data were arbitrarily selected from recordings made while the corona current was held constant. In each sample the person listening to the voice transmissions and noise has indicated, by depressing the event marker, which of the transmissions came through the noise clearly enough to be useful. Since a second receiver was tuned to the same channel, but free from serious interference, it was also possible to count the total number of transmissions during a sample period. By counting the number of clear, or at least readable, transmissions and comparing this number to the total number of transmissions, the percentage of lost messages can be easily calculated. The result of analyzing several such samples with varying distances between corona point and receiving antenna is shown in Figure 27. When the corona point is within 10 inches of the antenna, the channel becomes useless since the message loss rate approaches 100%, while at distances of greater than 50 inches the loss rate is essentially zero, even though some corona noise might still be faintly heard in the background. Some qualifications need to be added to these results. The statistical population of signal strengths at the site of the experiment is different than that in the neighborhood of an air traffic control center. At the experiment site, signals of average strength are received from nearby control centers while the strongest signals come from those aircraft which fly nearest the site. The listener has only one task and can concentrate on trying to hear even the worst signals on a single channel while a traffic controller would ordinarily carry a more complex load of tasks and could miss many of the messages which have marginal intelligibility in a background of severe corona noise. Hence, these lost-message statistics should not be assumed to apply quantitatively at different locations unless it is first established that the statistical populations of weak and strong signals are the same at each location.

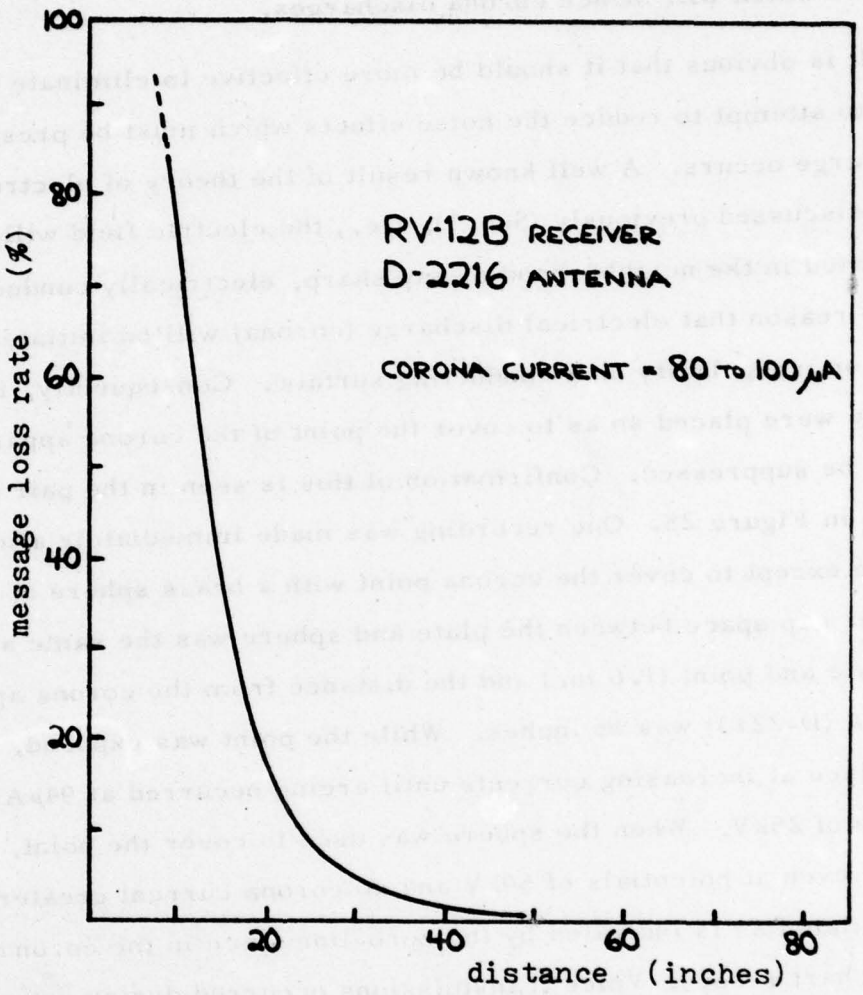

Figure 27. Message loss rate as a function of corona point distance from antenna

The qualitative result , however, remains unchanged and is quite simple: If corona discharge cannot be eliminated, some relief from the problem of noise interference can be obtained by judicious placement of antennas with respect to objects which will induce corona discharges.

It is obvious that it should be more effective to eliminate corona discharge than to attempt to reduce the noise effects which must be present whenever the discharge occurs. A well known result of the theory of electrostatic fields has been discussed previously (Sec. 3), i, e., the electric field will be concentrated in the neighborhood of any sharp, electrically conducting object. This is the reason that electrical discharge (corona) will be initiated at the sharpest point or irregularity on a conducting surface. Consequently, if a conducting sphere were placed so as to cover the point of the corona apparatus, the discharge would be suppressed. Confirmation of this is seen in the pair of chart records shown in Figure 28. One recording was made immediately after the other with no change except to cover the corona point with a brass sphere of one inch diameter. The air gap space between the plate and sphere was the same as it was between the plate and point (1.6 in.) and the distance from the corona apparatus to the antenna (D-2213) was 45 inches. While the point was exposed, corona discharge took place at increasing currents until arcing occurred at 94μA with an applied voltage of 25kV. When the sphere was used to cover the point, arcing did not occur, even at potentials of 50kV and no corona current greater then 2μA could have existed as is indicated by the zero-line trace in the corona current section of the chart record. Voice transmissions occurred during both tests and are clearly indicated by the tall, off-scale excursions in the AVC trace.

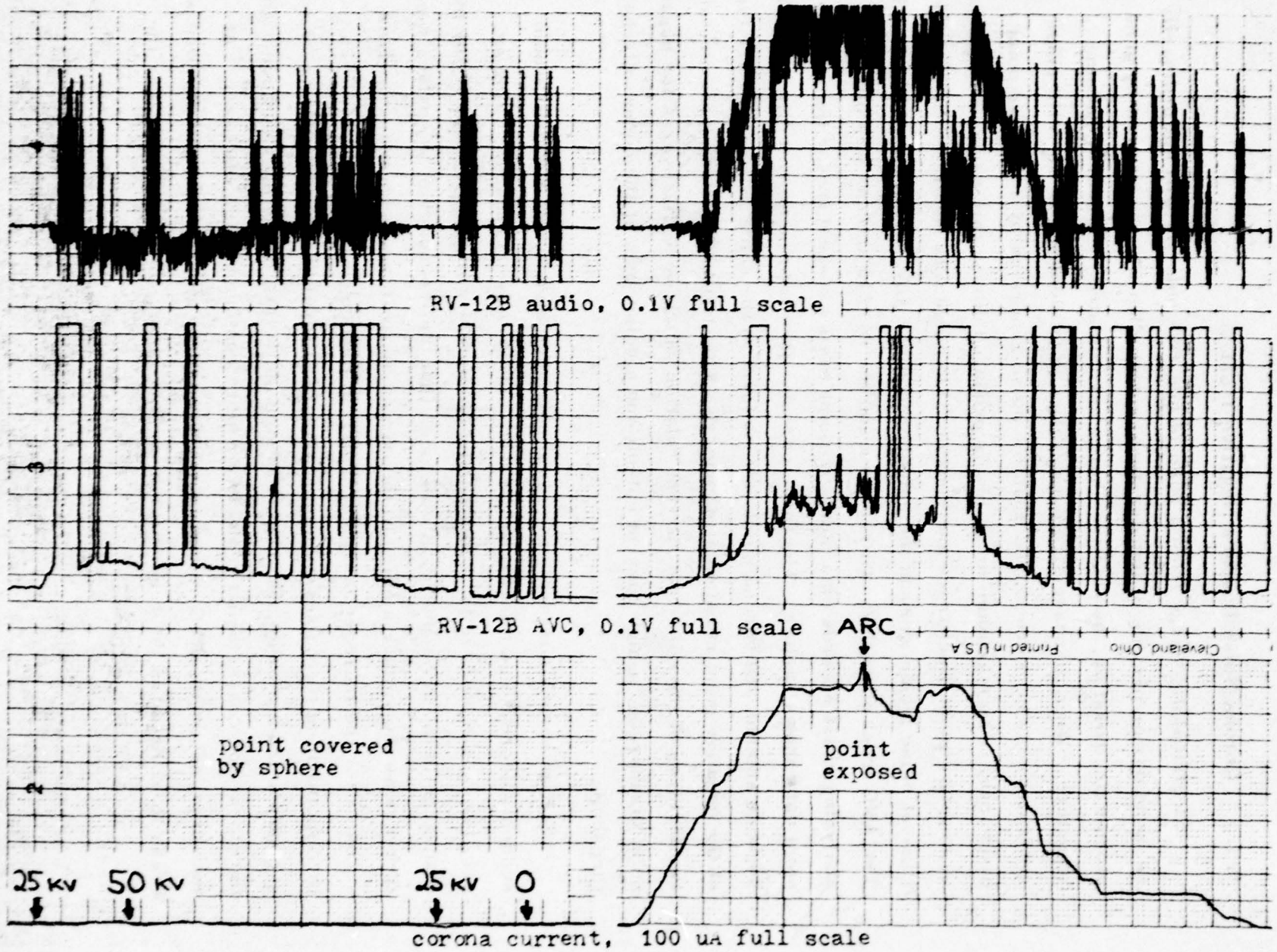

Figure 28. Noise reduction by placing a sphere over the corona point

5.3.3 Corona Noise Due to a Negative Point

Electrical discharge from a point of negative polarity will not ordinarily be found during periods of thunderstorm activity but may be induced by snow-storms or, possibly, by positive charge accumulated by a nearby radome structure. When discharge from a negative point does occur the VHF noise generated may be more intense than the noise generated by a positive point discharge. The maximum noise levels produced during this study were generated by negative point discharges and considerable noise was generated by low currents. Highest noise levels were in the neighborhood of 50μA, as shown by Figure 29. The AVC level of the RV-12B receiver and the D-2213 antenna was plotted by analyzing chart records on a point-by-point basis as was done for the positive point data shown earlier. The three curves, each representing a different distance between antenna and corona point, all conform to the same pattern and are typical of the negative point noise data in general. This figure does not, however, show two features of the noise and current relation which were discovered for negative point discharges, a high current cut-off and a noise peak at the corona discharge threshold.

At high corona currents, the radio noise detected by the receiver would suddenly decrease as the corona current continuously increased. Using an oscilloscope to observe the rapid pulses of current which are typical of any point discharge in the atmosphere, it was found that the frequency of the pulses would increase as the voltage applied to the corona apparatus was increased. This accounts for the increase in average current measured by the VTVM, even though the amplitude of the pulses was decreasing. At a pulse rate of about 2×10^6 per second the front of one pulse begins to step on the tail of the previous pulse and the pulsations cease, being replaced by more continuous flow of charge. At the same instant the AVC voltage would drop to its quiescent level and noise would cease to be heard in the receiver. It is quite clear, therefore, that it is the

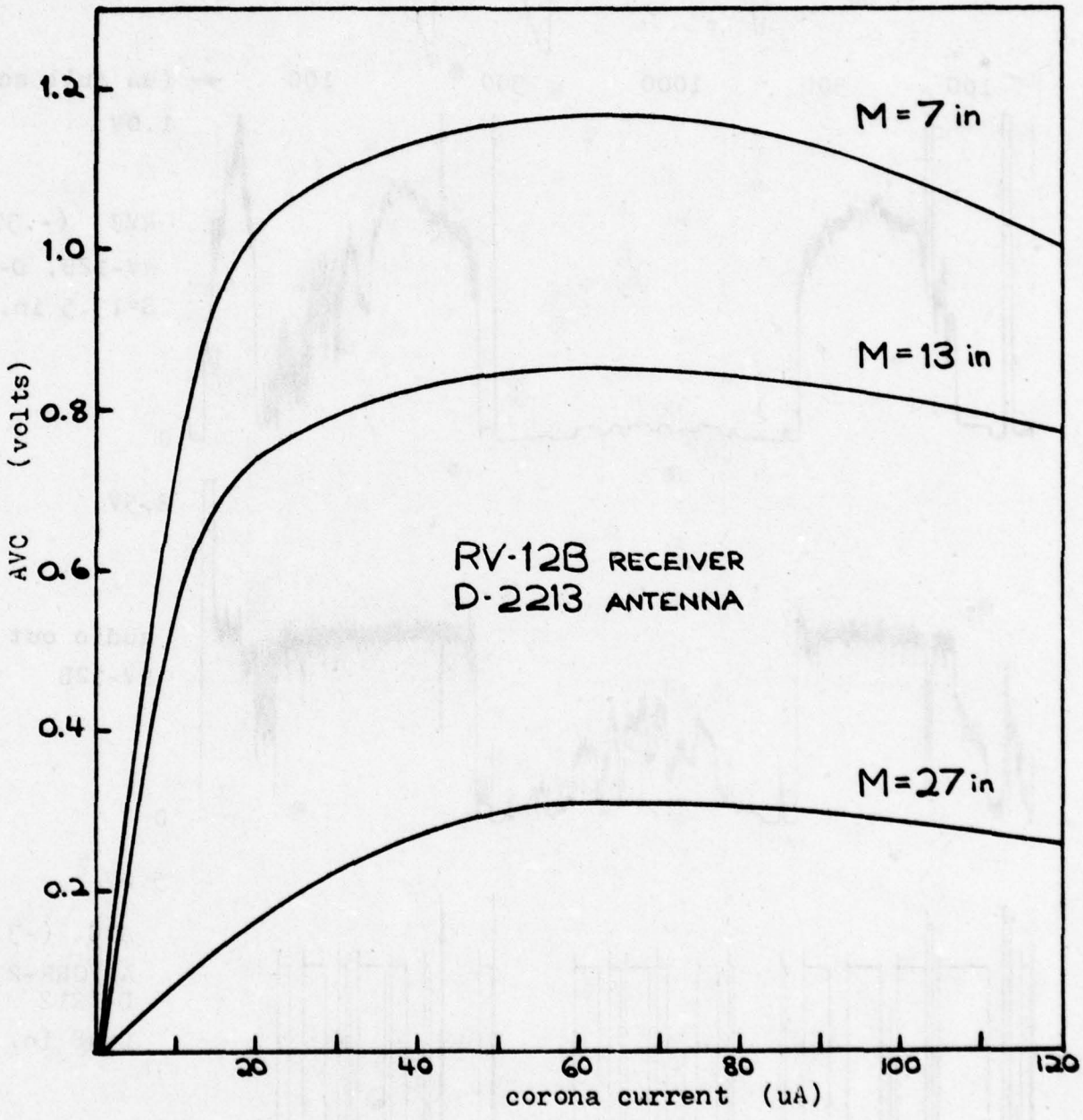

Figure 29. Noise level vs. corona current for a negative point at three distances

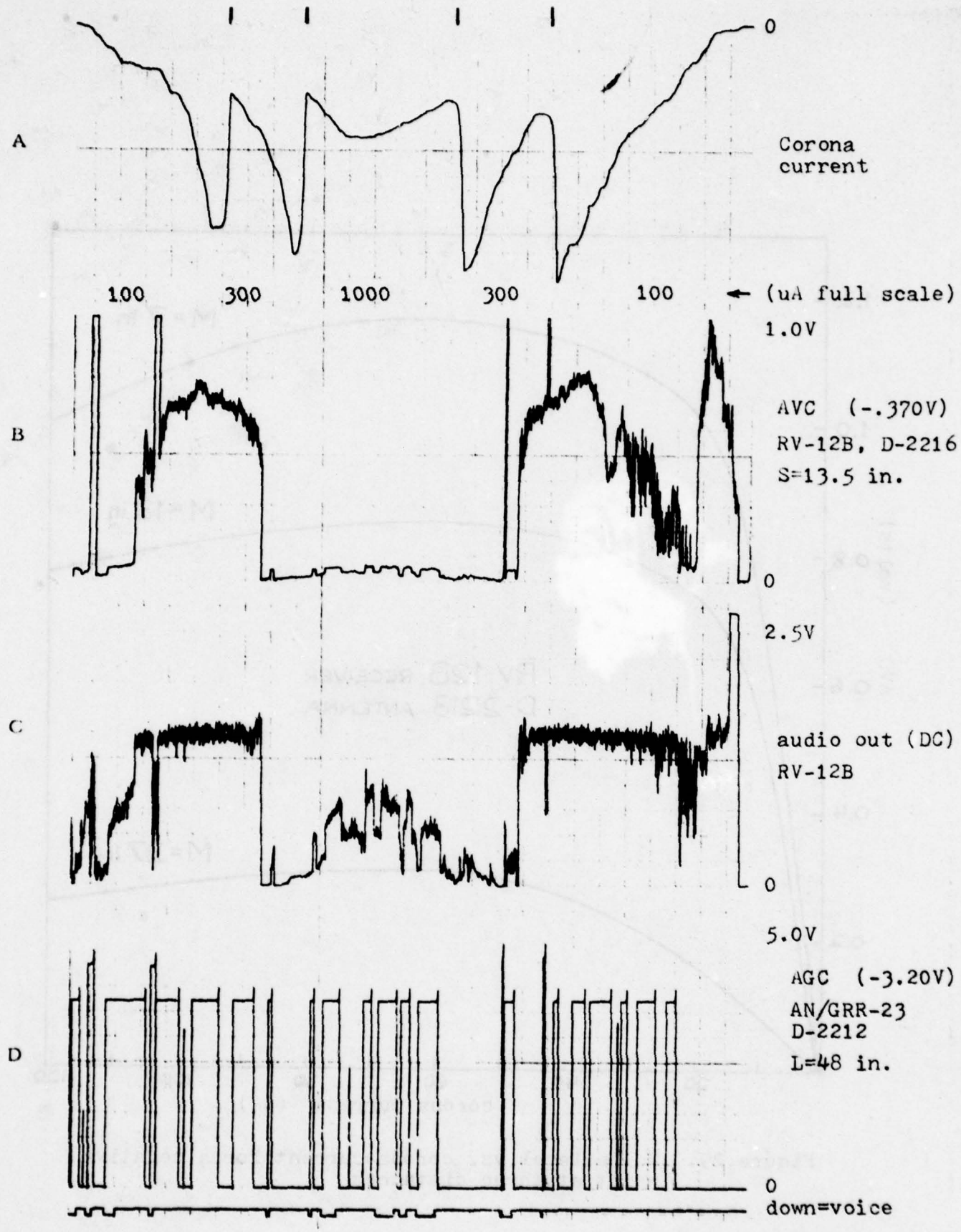

Figure 30. Corona noise from a negative point and voice blank-out due to noise (6-23-78)

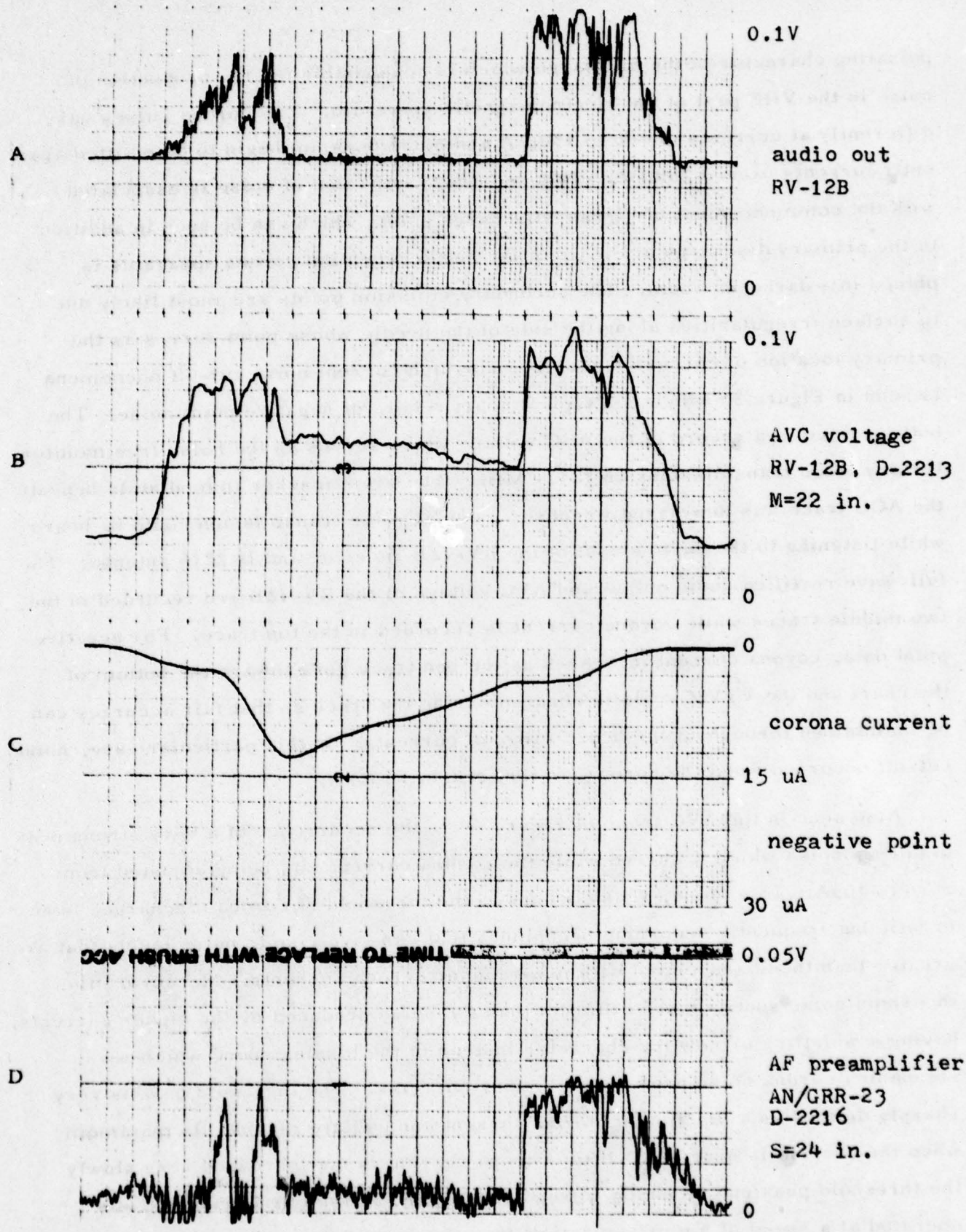

Figure 31. Correlation of threshold peaks with AVC voltage, chart speed = 5 mm/s (5-31-78)

pulsating character of the discharge which is responsible for the production of noise in the VHF part of the electromagnetic spectrum. The corona pulses vary differently at currents of 100 to 150μ A and noise does not begin to be emitted again until currents exceed 200μ A. This secondary emission of noise is associated with the commencement of "fresh" discharge points which can be seen in addition to the primary discharge at the tip of the needle when the corona apparatus is placed in a darkened room. The secondary emission points are most likely due to surface irregularities along the side of the needle whose point serves as the primary location of corona discharge. The high current noise cut-off phenomena is seen in Figure 30 which is a typical chart record of negative point noise. The bottom trace is a record of the AGC voltage which serves as the noise free monitor for any voice transmissions on 124.1 MHz. The event marker immediately beneath the AGC trace was depressed whenever a useful voice transmission could be heard while listening to the audio output of the RV-12B receiver and D-2216 antenna. The full-wave rectified audio output and AVC voltage of the RV-12B are recorded in the two middle traces while corona current is recorded in the top trace. For negative point data, corona current increases as the pen trace goes toward the bottom of the chart and the VTVM scale is changed during the trace so that fair accuracy can be maintained throughout the broad range of currents. In this particular case, noise cut-off occurred when the corona current reached 130μA.

Also seen in the AVC trace of Figure 30 is the occurrence of a very strong peak in corona noise which occurred while the corona current was being adjusted from zero to 10μA. This noise, which occurs in the threshold of corona discharge, is an erratic but frequently occurring phenomena that can give rise to noise levels that are greater than those associated with much higher corona currents. Moreover, the threshold noise sounds much different than the noise produced by the higher currents, having a whistling or howling character instead of the hissing sound which accompanies corona noise produced by higher currents. The threshold peak is very sharply defined as a function of corona current and usually reaches its maximum when the current is near 4μA. If the corona current is not increased very slowly the threshold peak can be easily missed. In Figure 31 the chart recorder was operated at a speed of 5 mm/sec rather than the usual 0.5 mm/sec to obtain

better time resolution of the correlation between the AVC and peak audio voltages in the threshold noise region. The phenomenon was not confined to any one combination of receiver, antenna, and corona point apparatus and therefore seems to be a consequence of low current discharges rather than an artifice of the initial action of a receiver's AVC circuitry. Corona discharge pulses have greater amplitudes at low current levels and this may be related to the exceptionally high noise level which is produced occasionally between 0-10 μA. Wind speed and other local changing conditions could be the reason why the phenomena is not always present.

As was seen before with positive point data, the intensity of noise from a negative point varies inversely with the distance between the corona point and receiving antenna (D-2216) as shown in Figure 32. This graph was prepared by finding the maximum AVC voltage for currents between 20 and 100μA for each of several distances between corona point and antenna. The AVC voltage for the threshold noise peak was ignored because of its erratic character, but threshold noise also varies with distance in much the same manner. As with the noise from positive point discharges, the noise level is very low when the distance between point and antenna is greater than 50 inches. Likewise, placing a 1 inch diameter sphere on top of the corona point inhibits the discharge process so that no noise is produced as seen in Figure 33. In this record, the two top traces are from the RV-12B receiver and show its audio output and AVC voltage. The bottom trace is a record of the audio preamplifier output from the AN/GRR-23 receiver which was operated with the squelch circuit turned on. The corona point was at a distance of 12 inches from the D-2213 antenna which was feeding the RV-12B and 35 inches from the D-2216 antenna which was connected to the AN/GRR-23.

Since the noise produced by negative point discharges was generally stronger and more stable than that from positive points, it was used to study the variations in noise level which could be produced by most of the many possible combinations of receiver, antenna, and corona point position. Figures 34 through 38 show some of the many ways in which the corona noise level at the receiver is influenced by the relative positions of the corona point and antennas. In all of these recordings the horizontal distances between antennas and corona points were kept as nearly constant as possible while the vertical position of the point was changed relative to the antenna. This was accomplished by moving both the corona point and the antenna

up and down. The distances referred to are shown in Figure 18 and, in addition, the straight line distance between the tops of antennas D-2216 and D-2213 are given as d_s and d_m, respectively. These distances can be compared directly to those shown in Figures 3a, 3b, and 3c. In the first three of this series of recordings, Figures 34, 35, and 36, the corona point is moved up and antenna D-2216 is moved down so that the vertical position of the point goes from the middle of the antenna to a position about 14 inches above the top of the antenna. Since the maximum sensitivity of a dipole antenna lies in a plane perpendicular to the dipole and passing through the middle of the dipole, the noise received by the antenna is seen to decrease as the point is moved from the middle position to the top position. Hence, the maximum noise induced AVC level in the RV-12B receiver is decreased from 1.0V in Figure 34 to 0.7V in Figure 36. Without changing the corona point and antenna locations, the antenna connections to the receivers were interchanged so that the performance of different combinations of receiver and antenna could be evaluated by comparing the records shown in Figures 37 and 38 to those of the three previous figures. In all of the combinations of receiver, antenna, and point location which were surveyed during this study, no cases were observed which were contrary to the pattern shown here. The greatest variation that could be achieved has been seen in many of the previous figures where the AN/GRR-23 receiver was used with the D-2212 antenna to produce the relatively noise-free combinations which served as a monitor for the presence of signals which could not be detected in another receiver due to corona noise. The reason for the small amount of noise input to the D-2212 antenna is the placement of the corona point in a null region of the vertical gain pattern of this antenna. Moving the corona point toward the region of maximum response was found to increase the noise received by the D-2212 antenna, just as it was for the other antennas. None of the data presented in this report should be construed as an evaluation of antenna performance or an endorsement of any particular antenna design.

Notice also in Figures 34 through 38, that the levels of corona noise are not perfectly reproducible. This is characteristic of the erratic nature of the discharge process itself which gives data that are "notoriously nonrepeatable" (3). The

threshold peaks are missing in the AVC trace of Figure 34, but give rise to the highest AVC levels recorded in Figure 38. The presence of the threshold peaks in many of the audio output traces is an indication of the presence of this low-current phenomena, but cannot be taken as a measure of its strength in competition with incoming voice signals. Rather, the audio peaks indicate the failure of the AVC circuit to function optimally when the noise level is low. In other recordings, however, the threshold noise peak can give rise to the maximum perturbation in AVC level as was seen in Figure 30.

Noise interference from a negative point discharge was studied as a function of corona current by keeping the current adjusted to a constant value for minutes at a time and listening to the combined noise and voice message in the audio output of the RV-12B receiver while the AN/GRR-23 acted to indicate the presence of voice which could not be audibly detected. Currents from 8 to 10μA produced level I noise which could be heard as a background to an otherwise clear message and produced an increase in AVC level of only 0.05V, as seen at the left side of Figure 39. In the middle of this figure, currents range from 10 to 25μA and produce level II noise which caused great difficulty in understanding the content of any message even though the presence of a voice was heard in every case but one. At the right, currents are between 42 and 45μA and produce level III noise which blanked out communications almost completely and even elevated the AGC baseline of the usually noise-free AN/GRR-23 and D-2212 receiver-antenna combination. The event marker was depressed whenever voice was heard, even if a message could not be clearly understood. In one case, which is marked by an asterisk (*) in the level III period, the listener became confused while trying to indicate even the most marginal presence of a voice. While straining to hear anything at all, the voice marker was kept down for a few seconds after the signal itself had ceased. In the middle of the transmission the marker was released as the noise momentarily covered the voice completely. At the extreme right, an exceptionally strong signal broke through the noise quite clearly.

The highest noise level produced during the course of this study (except for threshold peaks) pushed the AVC level of the RV-12B up to 1.63V at which

time the corona current was 50μA. Antenna D-2216 was placed 10 inches from the corona point which was negative. According to the calibration for the RV-12B (Figure 22), an RF input of 16μV, 30% modulated with 1000 Hz, would be needed to produce an AVC level the same as that from the corona noise. The highest noise level for a threshold peak occurred at a corona current of 5μA with the corona point 10 inches from antenna D-2213. Here, the AVC level went to 1.75V, corresponding to an RF signal of 18.5μV. Other exceptionally high noise levels were found to correspond to corona currents of 14, 37 and 65μA. Hence, the maximum noise level is not adequately predicted simply by measuring the corona current and may be more dependent on factors related to the pulsating character of the discharge. A Fourier analysis of the frequency components in different pulse shapes might be revealing since it is suspected that pulses in the threshold region have shorter rise times and longer decay times than those in the high current region. The time between successive pulses is on the order of a microsecond, decreasing and becoming more regular as the average current increases. Thus, if the attack and decay time constants of a particular receiver are on the order of 100 milliseconds, something on the order of 100,000 pulses of corona noise could be received while the AGC circuit of the receiver is turning itself on. It is conceivable that bursts of several thousand noise pulses slip through the noise limiting circuits of a receiver and that in the threshold region of corona discharge, the bursts are separated by sufficient time for the AGC to turn itself off during quiet periods. If this is the case, the noise limiting ability of the circuit would be effectively destroyed. On the other hand, the threshold noise peaks could be explained by supposing that the noise pulses produced in this domain are particularly rich in the high frequency part of the spectrum to which the receiver is sensitive. Further study will be necessary to answer these questions. It is quite clear, however, that there is no need to look for the maximum corona currents when trying to find serious noise interference due to a negative point discharge. The greatest noise levels found in this study were produced by currents under 100μA which is much less than the 500μA maximum which was frequently obtained. It is in this respect that the noise from a negative point discharge is most different from that due to a positive point which was only seen to increase as the corona current increased.

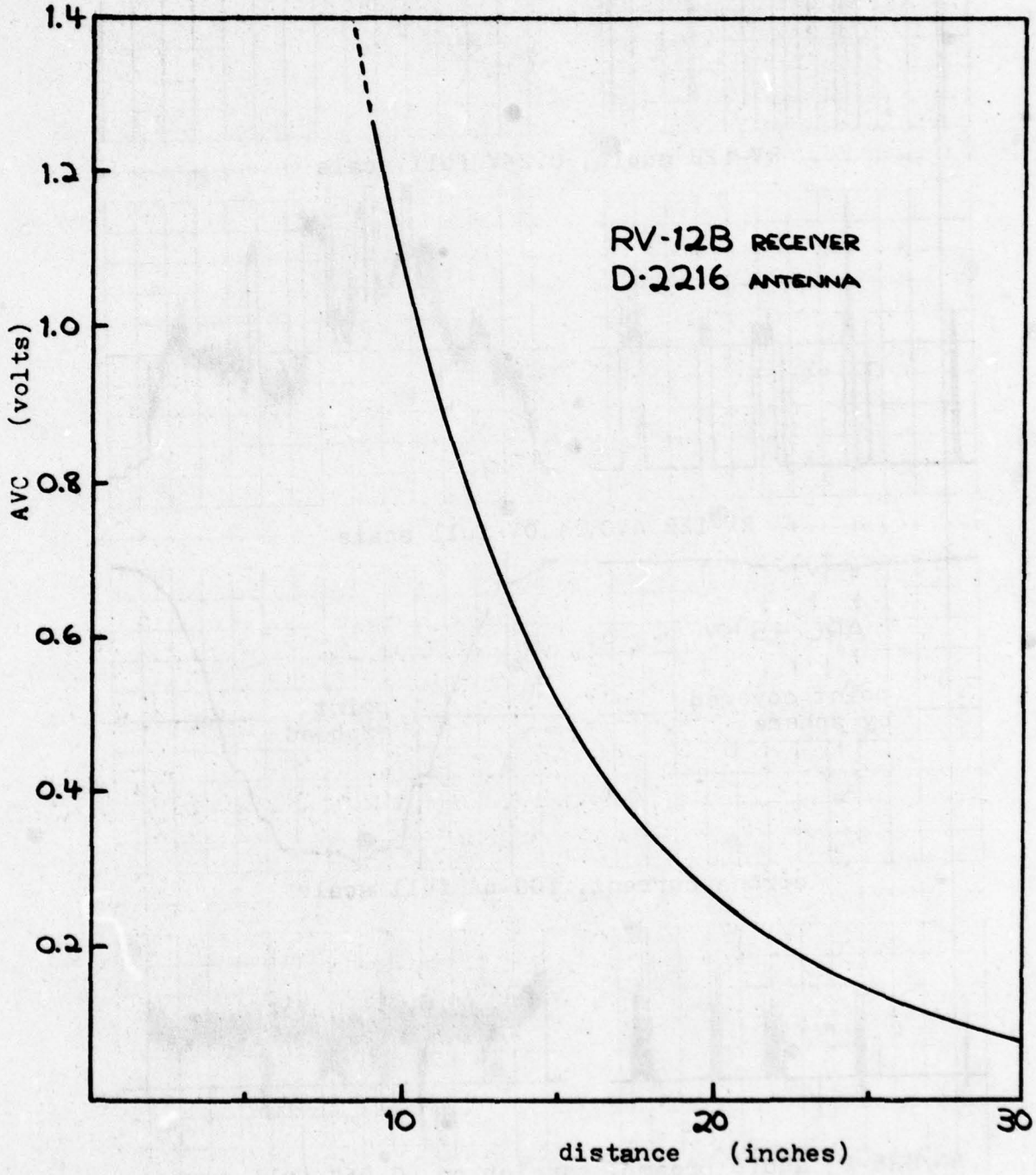

Figure 32. Noise level vs. distance for a negative point discharge

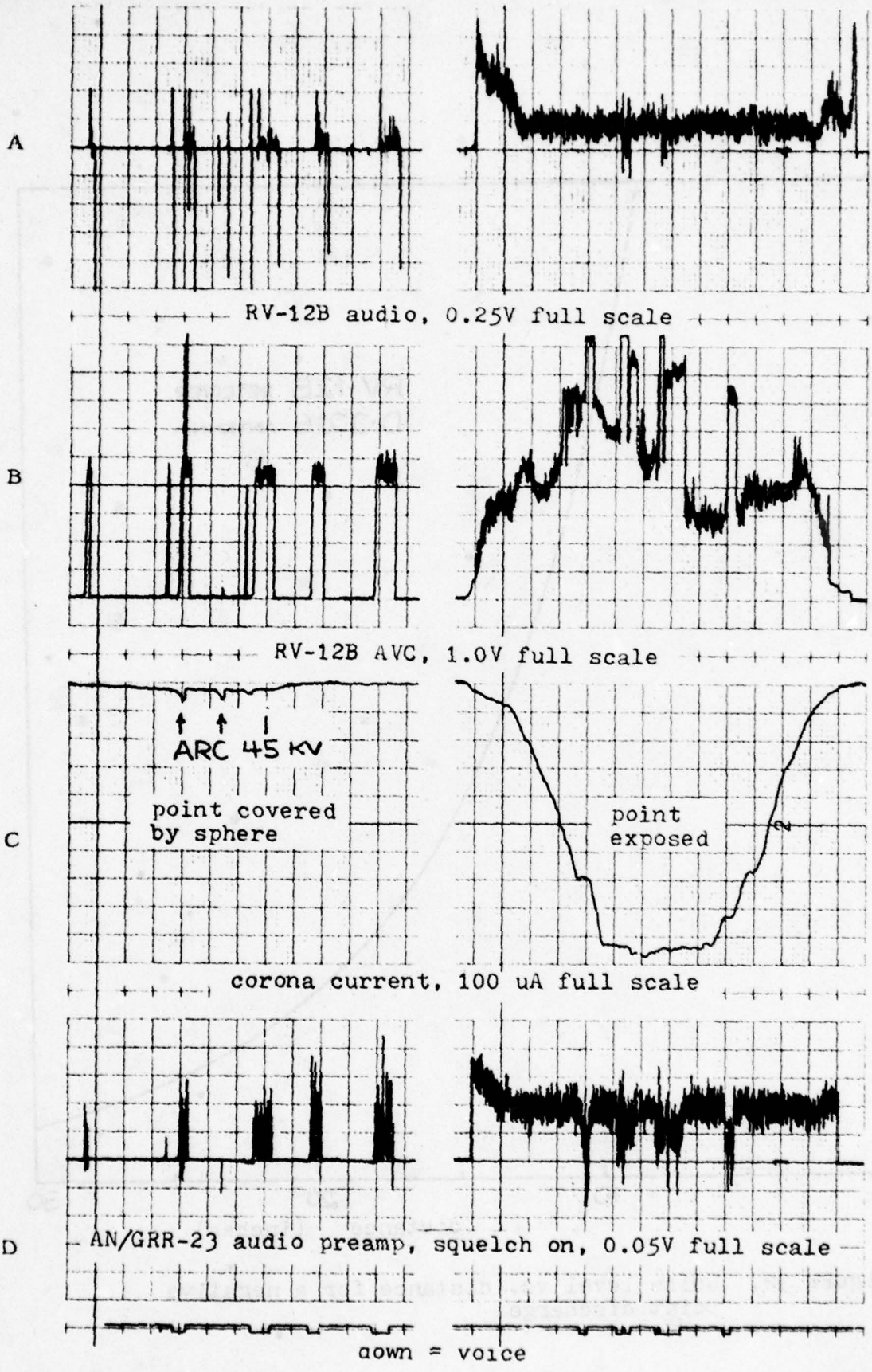

Figure 33. Noise reduction by placing a sphere over the corona point

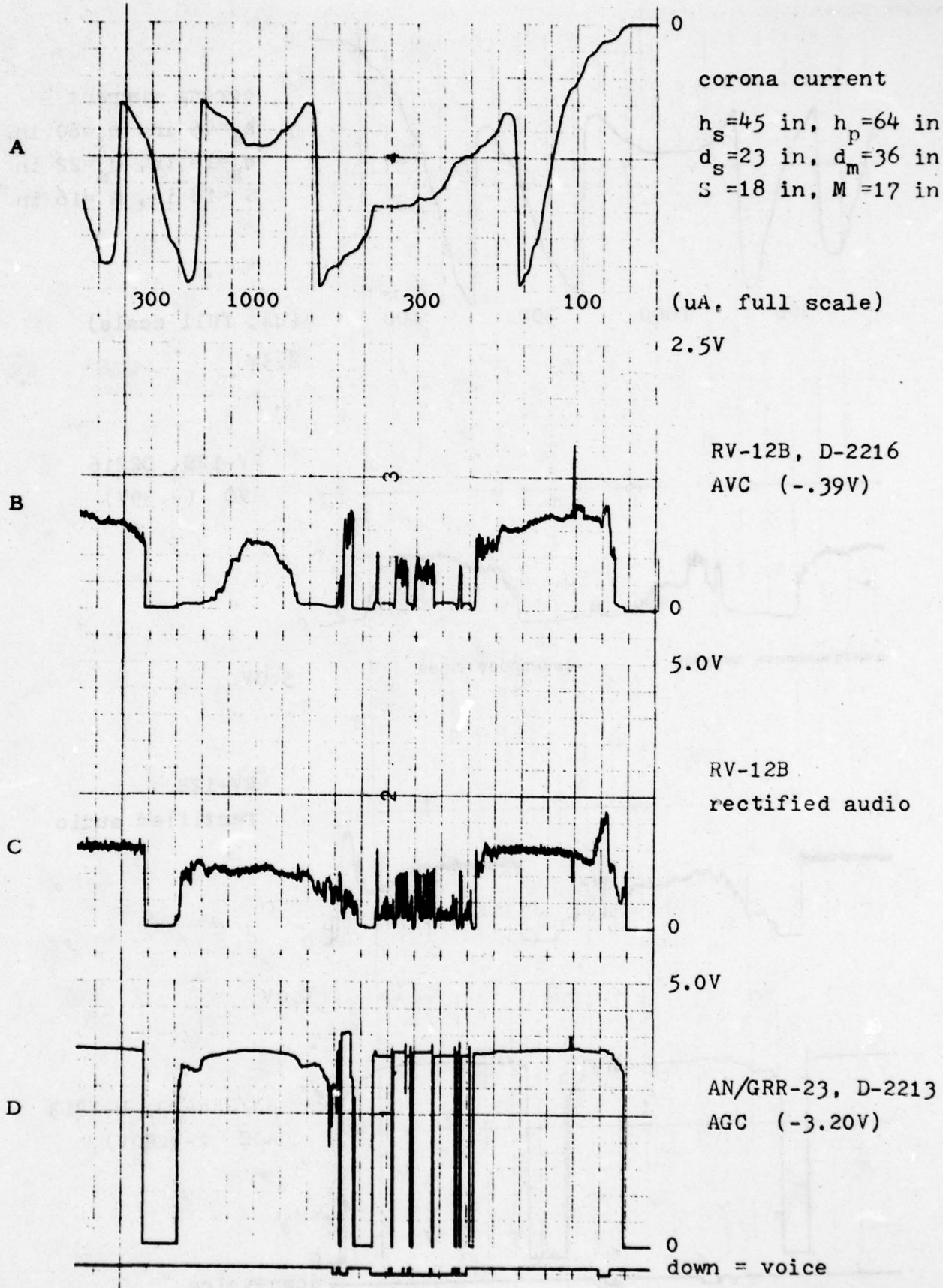

Figure 34. Dependence of noise on position of point

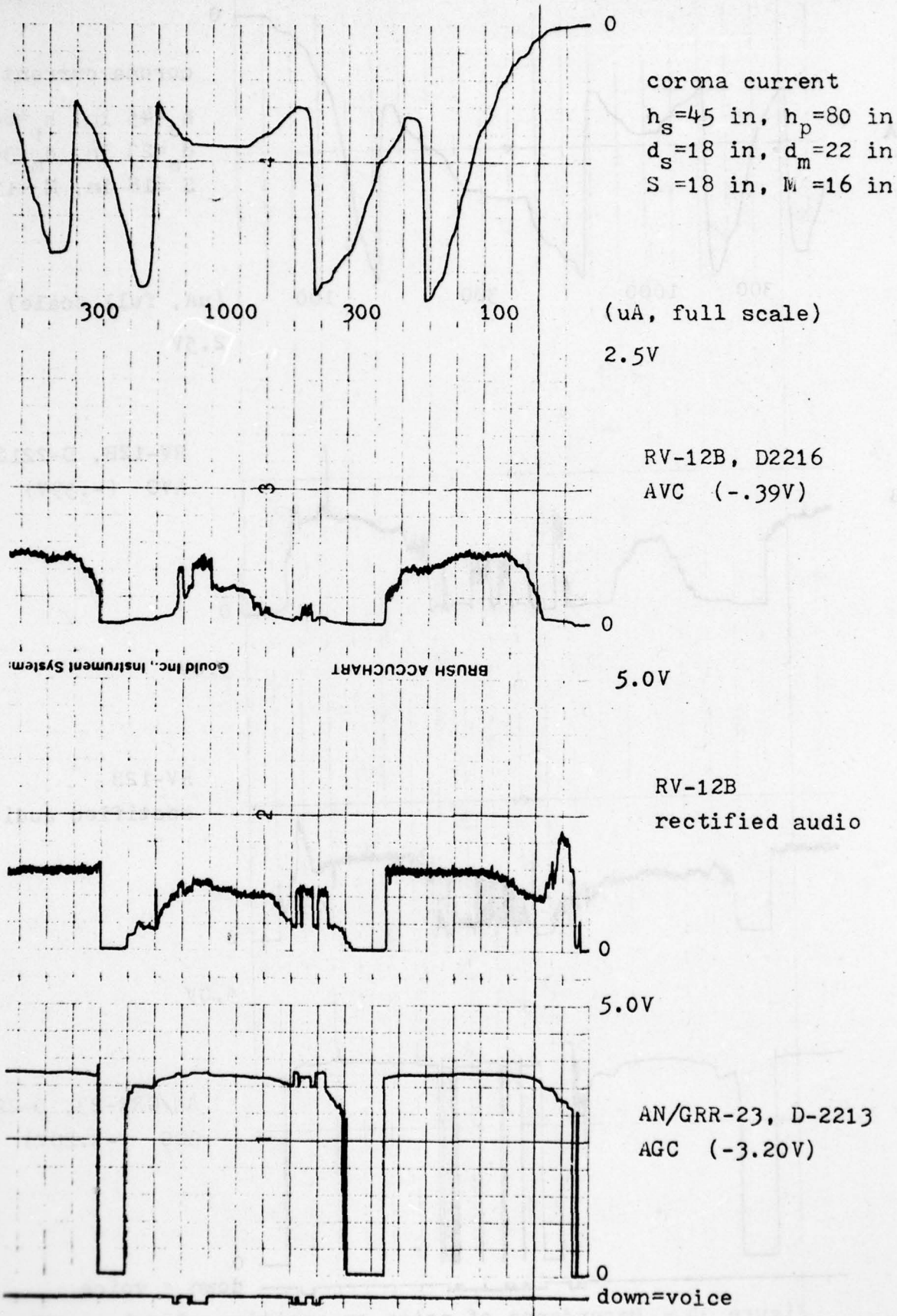

Figure 35. Dependence of noise on position of point, h_p increased

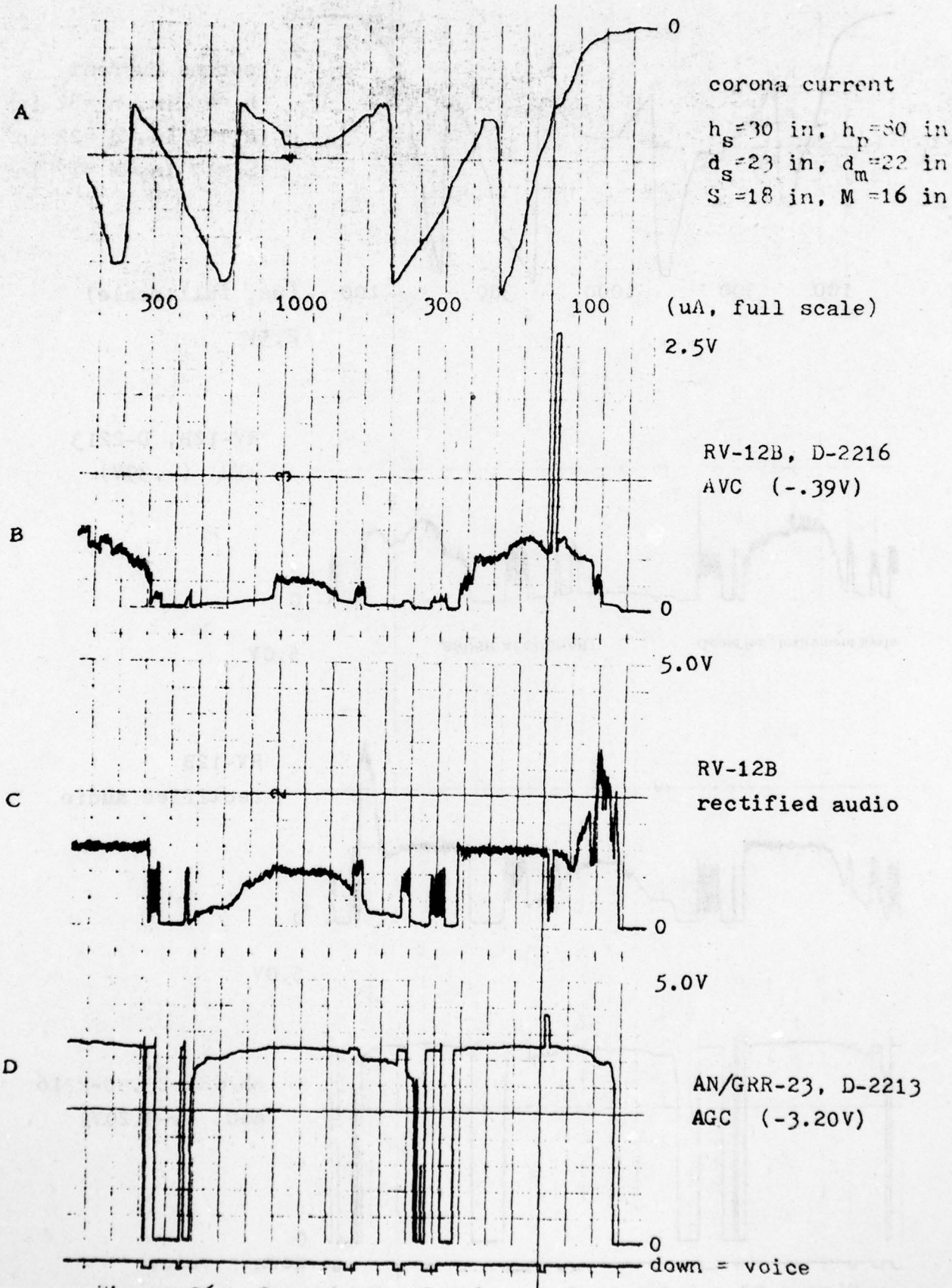

Figure 36. Dependence of noise on position of point, h_s decreased

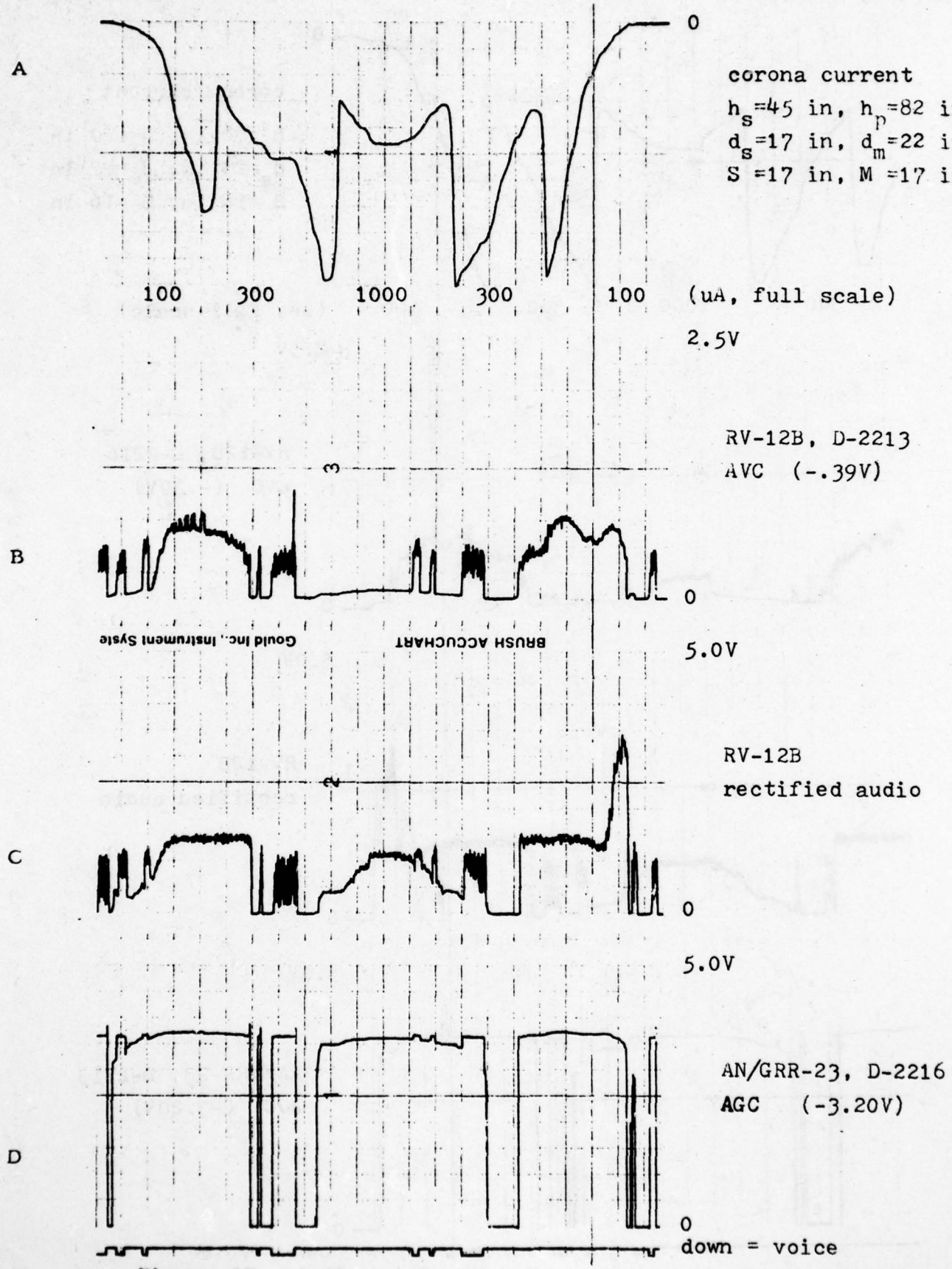

Figure 37. Antennas interchanged, compare to Fig. 35

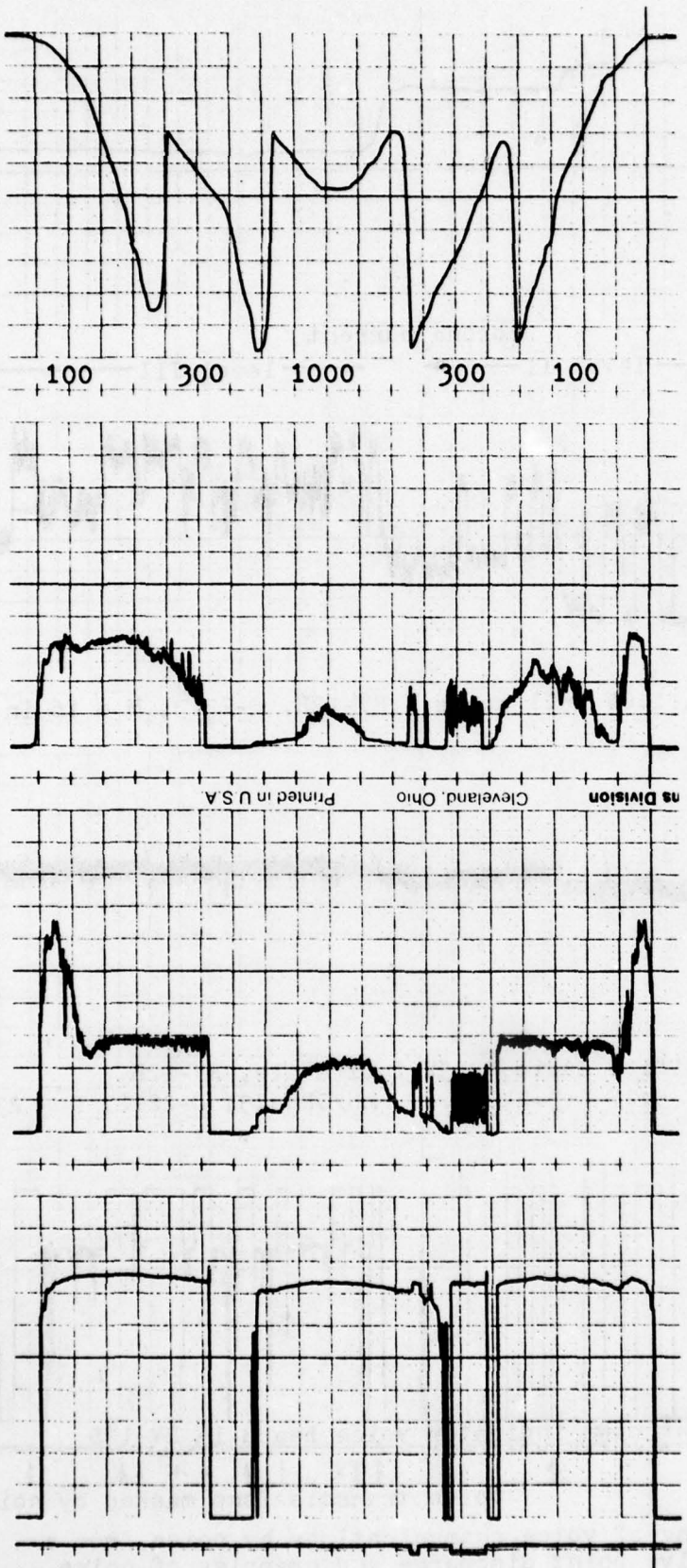

Figure 38. Antennas interchanged, compare to Fig. 34

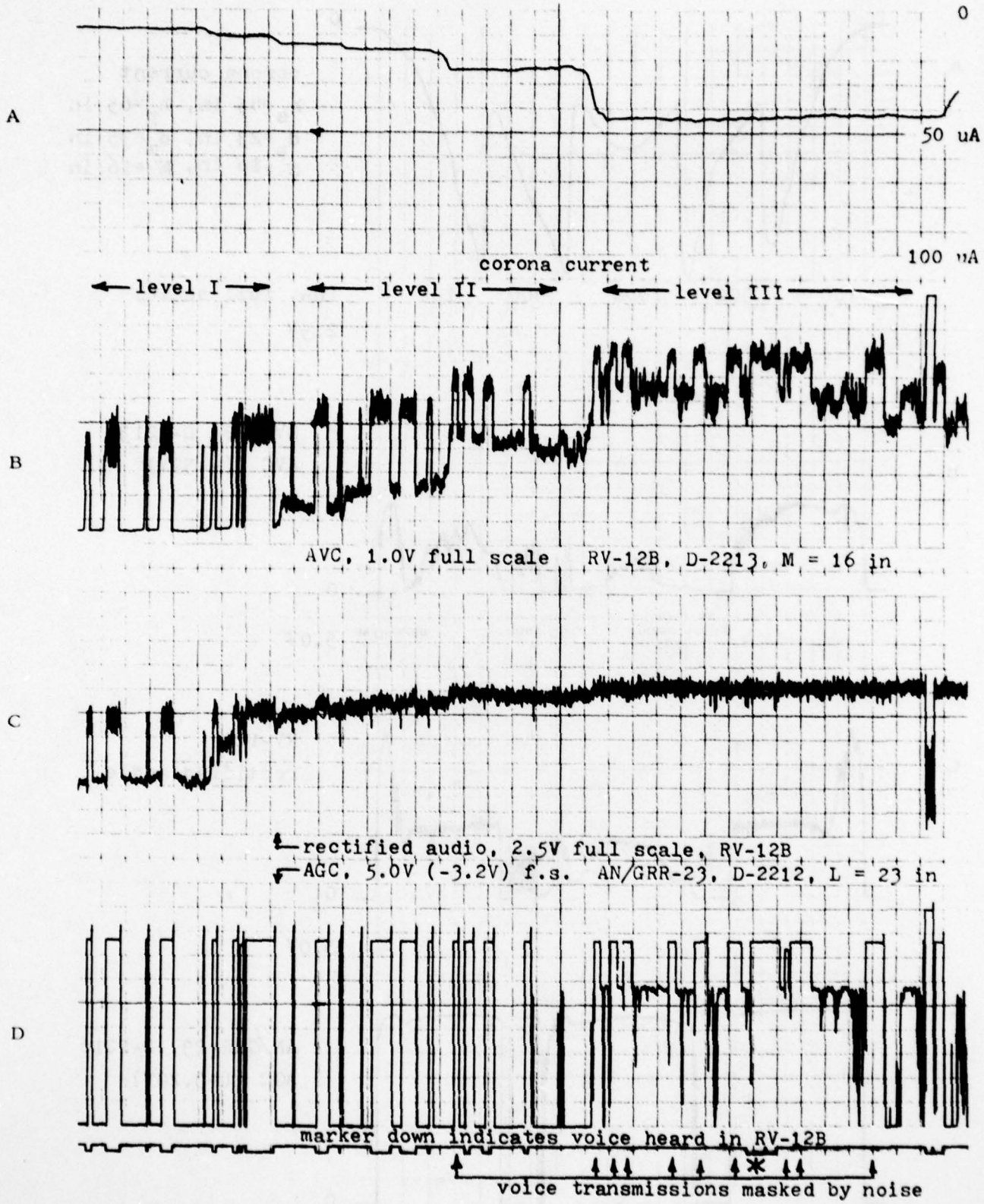

Figure 39. Masking of voice communications by noise from a negative point discharge and examples of noise levels I, II, and III

5.3.4 Other Effects

The erratic nature of the noise due to corona discharge is due to the multitude of factors which can influence either the discharge itself or the transmission of the noise from corona point to receiving antenna. Since it is difficult, if not impossible, to control all of these factors simultaneously, the results of any experiment are hard to reproduce with high accuracy. This study was extended so that some of these factors such as the polarization of corona noise radiation and the effect of the dimensions of a corona point apparatus on the emission of noise could be examined, at least briefly. The fact that wind plays an important role in the corona process is well known, but no attempt was made to construct wind tunnel experiments to monitor corona current changes with wind speed which will affect the radio noise. However, simple measurements of wind speed were made in the vicinity of the corona point. During most of the noise measurements winds ranged from 0 to 5 miles per hour, but in the experiment where the highest level of threshold noise was recorded, winds were gusting up to 15 mph. Exceptionally strong winds did not occur during any of the measurement periods.

The polarization of the corona discharge radiation was examined by detaching the smallest dipole antenna from its mount and rotating the antenna from its mount and rotating the antenna in a vertical plane about an axis which was perpendicular to the longest dimension of the antenna and passed through its center. As seen in Figure 40, the noise level dropped nearly to zero when the antenna was horizontal, indicating that the noise radiation is strongly polarized in the vertical direction. This is not too surprising since the electric field of the corona point apparatus has a primarily vertical orientation. However, it is hard to see how this effect could be employed for noise reduction purposes since it is expected that mounting antennas horizontally would decrease their ability to receive voice communications as much as it would decrease noise. This experiment was performed with the corona point shown in Figure 19 which has a very short electrical length thus, leading to a small effect on the polarization.

The efficiency with which corona noise is transmitted from point to antenna can be influenced by the effective electrical length of a lightning rod, the presence

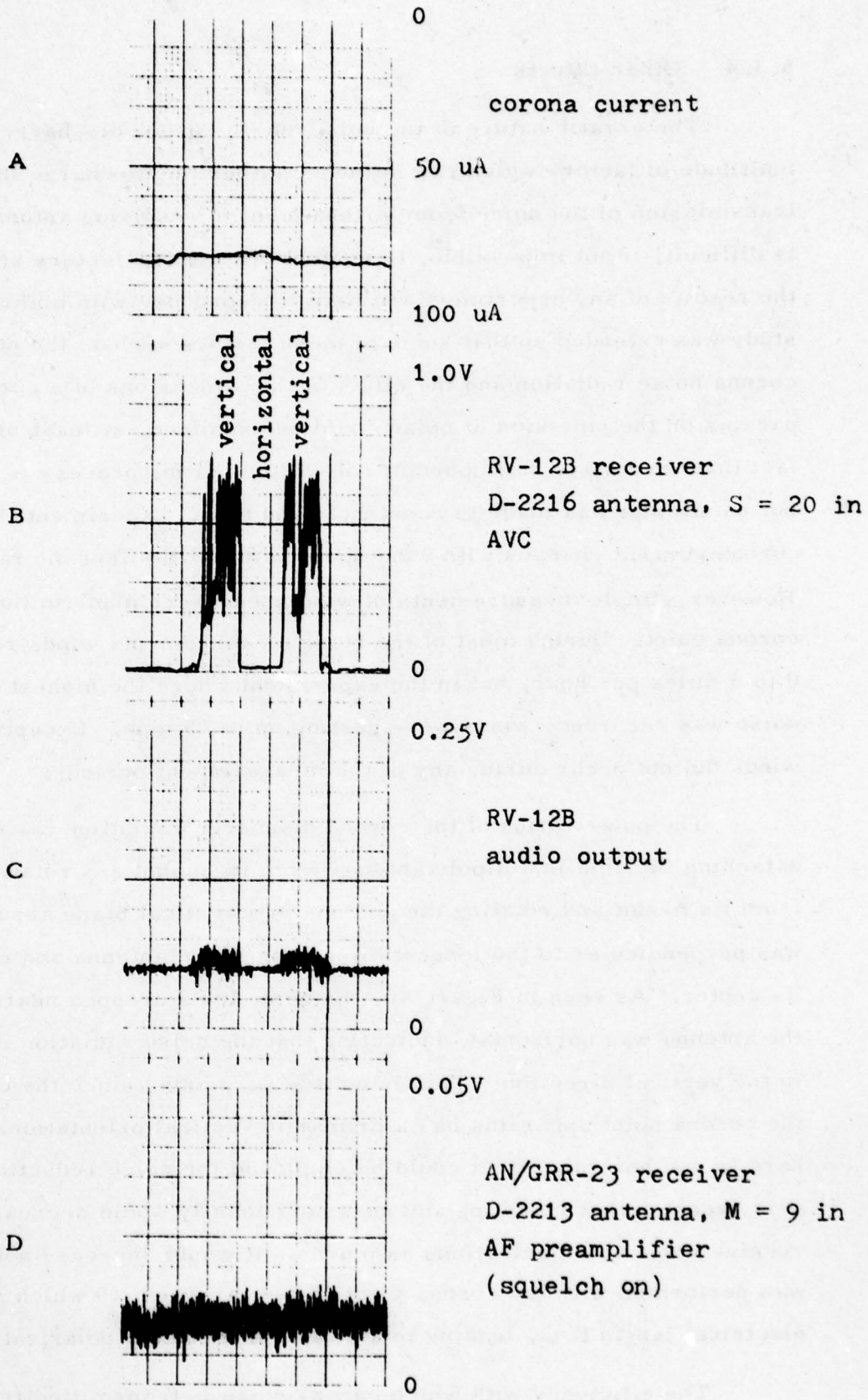

Figure 40. Polarization of radio noise from a corona discharge

of nearby electrical conductors, and the arrangement of wires which serve to ground the corona point structure. These effects were discovered using the large corona point apparatus. The possibility of such effects was first considered when it was noticed that the section of lightning rod which serves as the corona point in the large apparatus measured approximately a quarter wavelength long. The rod has a length of 26.5 inches and the radiation for which the receivers were tuned has a frequency of 124.1 MHz giving

$$\lambda = c/f = 2.42\text{m} = 97.2 \text{ in.}, \quad \lambda/2 = 47.6 \text{ in.}, \text{ and } \lambda/4 = 23.8 \text{ in.}$$

Hence, it was quite simple to use the common practice of placing a ground plane reflector at the base of a quarter-wave antenna to convert it to an efficient half-wave dipole. Two pieces of steel channel were placed on the corona point tripod at the base of the rod, being arranged at right angles to each other and lying in a plane perpendicular to the rod so that they would serve as a ground plane reflector for noise radiation emitted by the corona discharge. This arrangement might be thought of as simulating the structural steel of a building on which a lightning rod has been mounted and it produced a noticeable increase in the level of noise received by the RV-12B. This is shown in Figure 41 which has, for comparison, a noise and current recording which was made without the reflector and with the ground lead attached to the middle of the rod in order to further shorten its effective radiating length. To further study these effects, a series of tests were carried out in which precautions were taken to insure that the position of every electrical element in the corona point apparatus was carefully controlled, including the instrument leads. Electrical current pulses which are due to the pulsating nature of the corona discharge are carried to ground through the length of the rod, a 100 ohm dropping resistor which allows a VTVM to measure corona current, and then back to the high voltage power supply which is also grounded to the metal corona point tripod that stands uninsulated on the earth. This simulates the grounding circuit of a lightning rod installation (although for good protection the inductance to ground should be as low as possible). The more interesting results from the series of tests are presented in Figure 42. A comparison of sections A and B of this figure shows again the effect of removing the ground plane reflector, all other elements remaining the same. The dramatic difference between

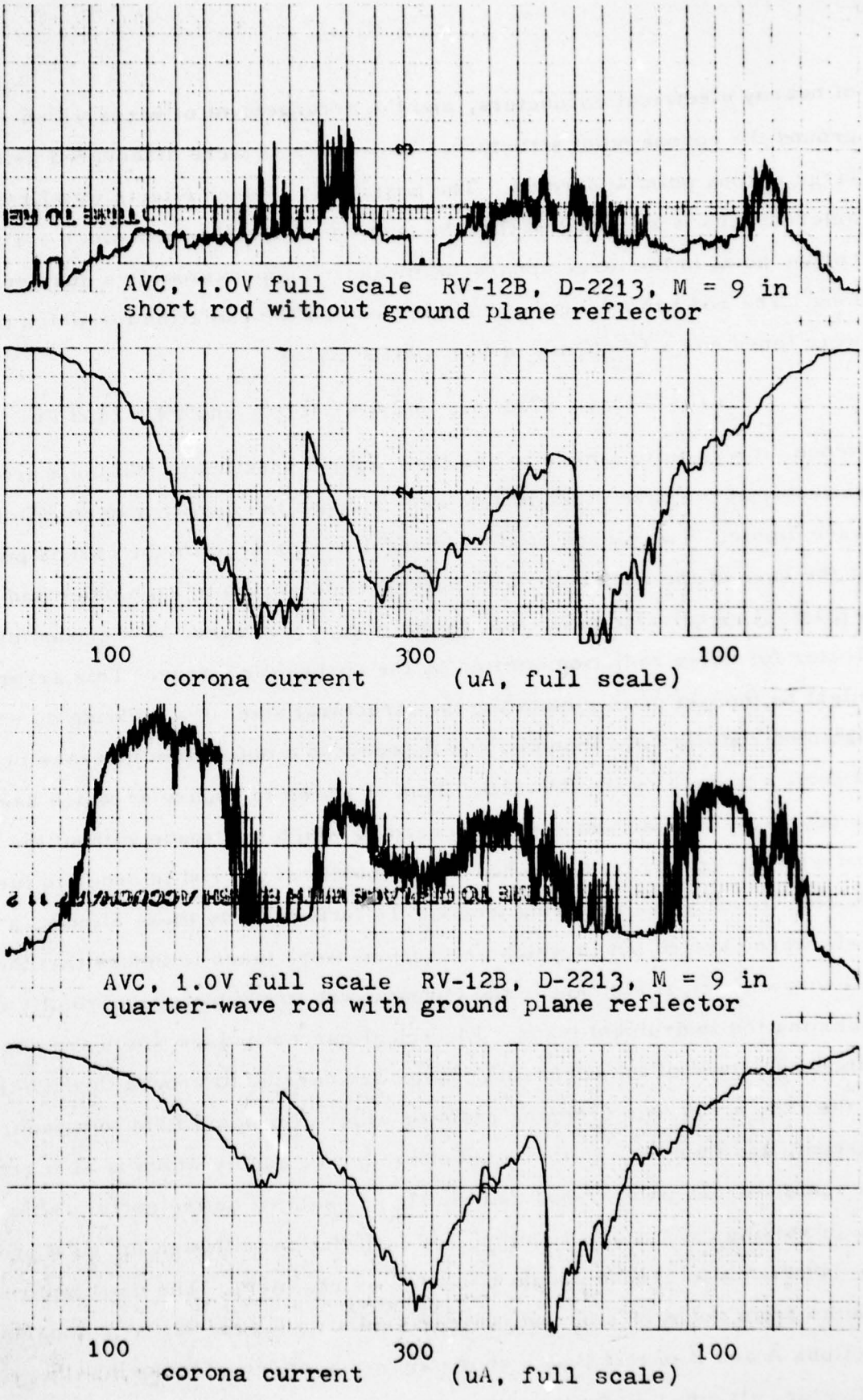

Figure 41. Comparison of different corona noise radiating geometries

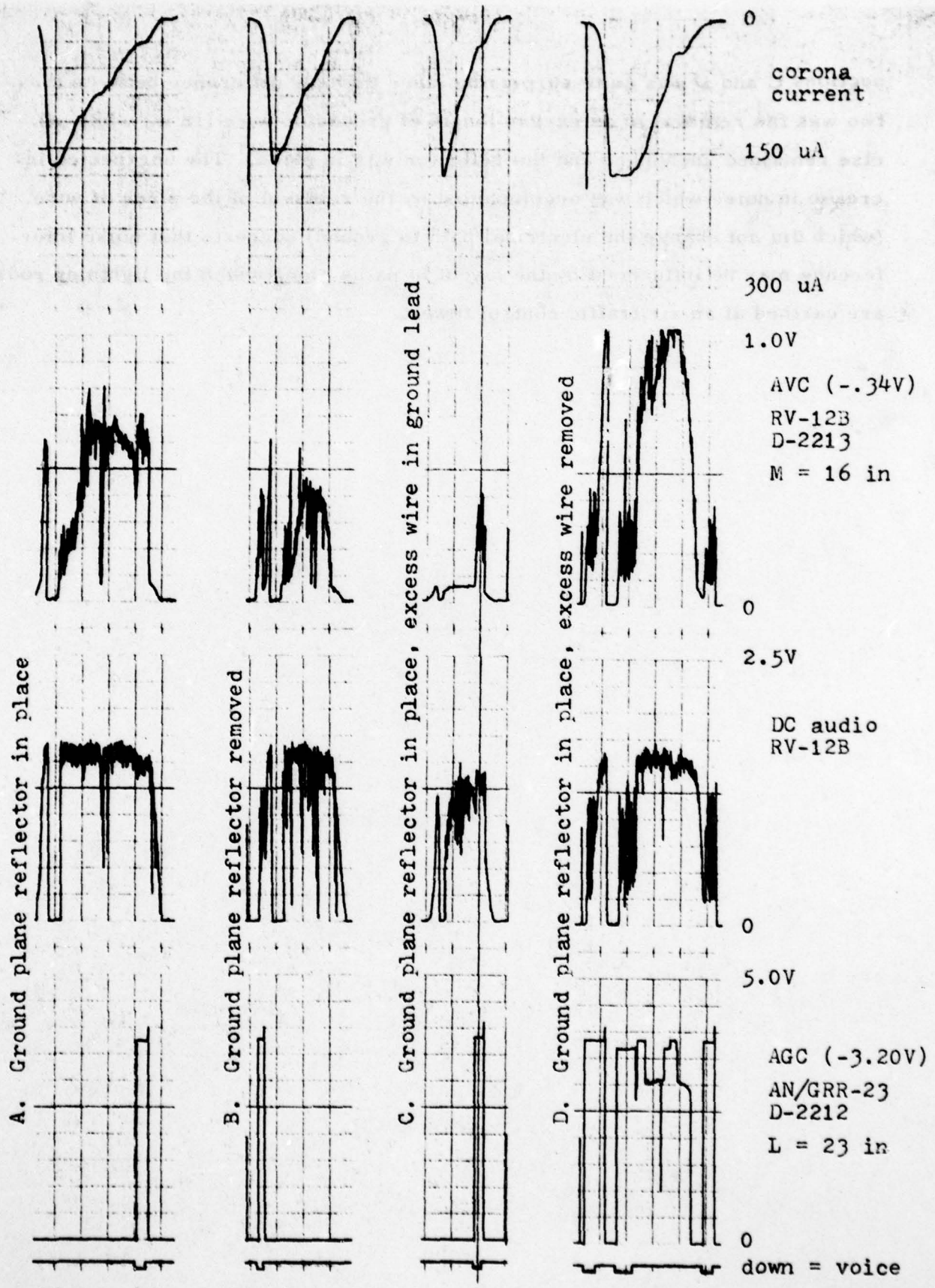

Figure 42. Radiative effects related to length of rod and placement of ground leads

sections C and D was quite surprising since the only difference between these two was the removal of an excess length of grounding wire (18 in) while all else remained unchanged and the reflector was in place. The unexpected increase in noise which was accompanied by the removal of the piece of wire (which did not change the electrical path to ground) suggests that noise interference may be influenced by the layout of paths along which the lightning rods are earthed at an air traffic control tower.

6.0 CONCLUSIONS

6.1 General

The VHF noise problem has been investigated in detail theoretically and experimentally, both on site and in the laboratory. There is little doubt that the noise emanates from corona discharge in the near vicinity of the VHF antennas. The prime originators of the corona discharge are the nearby lightning rods, but some small effect probably comes from the radome during very dry icy conditions. The fact that corona discharge is a broadband radiator of RF noise indicates that as long as the discharge is there a receiver will monitor it if the signal strength is high enough. The corona source must, therefore, be removed or the antennas moved far enough away from the noise to make the effect minimal.

The theoretical approach indicated that a 4 inch sphere on top of the Logan Tower lightning rods would eliminate them from going into corona on all but direct strike occasions. This was carried out successfully on the tower, since which time the problem has gone away, except on one occasion where slight noise was recorded possibly due to corona or streamers on the radome structure or its support ladder. The addition of the sphere to the tip of the lightning rod is shown to retain the lightning protection capabilities.

The experimental results supported this theory and showed several other interesting facts which are discussed below.

Most of the tests were performed on the RV-12B receiver because of the unit's ability to monitor smaller increments of signal strength at the AVC output. Even though the AN/GRR-23 receiver had a more sophisticated noise suppression system, the final noise received from corona was found to be the same in both systems and would lead to the same amount of trouble for a controller communicating with an aircraft (see Figure 31).

Antenna length and type would not effect the corona noise to signal ratio, as it is a genuine broadband transmitter that is being received by an antenna in its designed frequency band. The antenna should not, however, have a pointed top as

this would enhance corona generation. As expected, the distance of antenna to corona source is related to the noise intensity.

The corona discharge under a thundercloud is generally from a positive point, whereas that under blowing snow and ice conditions is from a negative point. The experiments showed that significant noise was generated below 100 μ A which had surprising characteristics. For a negative point, it was not uncommon to get severe noise for very low corona currents between 1 and 10 μ A. As the current increased this whistling or howling noise suddenly dissapears and is gradually replaced by the more characteristic hissing sound at higher currents, which again suddenly stopped somewhere above 100μ A. For a positive point, the noise level tended to increase directly with increasing corona current as one may normally expect.

Experiments with the radome material indicated that in dry weather an extremely large charge may reside on its surface for long periods, especially during blowing snow conditions because ice and snow is very highly charged. A highly charged radome will lead to high electric fields in the immediate vicinity hence, corona may form and streamers may constantly pass over the radome surface.

Further tests showed that a corona generator with an electrical length related to the frequency wavelength by $\lambda/4$, $\lambda/2$, or λ, can give rise to larger noise signals. A lightning rod of length $\lambda/4$ = 23.8 inches would, therefore, be of length $\lambda/4$ at 124 MHz. The electrical pulses traveling in this rod caused by the corona, cause it to act as an antenna giving increased noise problems. It was also found that the corona noise tended to be vertically polarized, probably due to the horizontal field lines on top of the tower.

The more detailed conclusions are as follows:

6.2 Corona Current and Noise Level

Serious noise interference was produced by the corona discharge at positive and negative points. Level II and level III noise can be caused with either positive or negative currents of less than 150 μA. In the positive point case, noise levels

increased directly (but not linearly, e. g., Figure 25) as the corona current increased. In the case of negative point discharge (Figure 29), the current/noise relationship is more complicated. Noise levels reach a maximum in the neighborhood of 60μA and decrease slightly as current increases to 100μA. At a current above 100μA, a sudden decrease or cut-off of corona noise occurs in the negative point case. The precise current at which this cut-off takes place varied from one test to another, but was usually found between 100μA and 150μA. As negative point discharge currents increased from 5μA to 10μA, a sudden peak was intermittently found in the noise level. This threshold peak would sometimes produce greater noise than that due to currents of 50μA to 100μA. The noise cut-off and threshold peak phenomena are not shown in Figure 29 (which presents the average result of many tests) but can be clearly seen in trace B of Figure 30 as well as many of the other chart recordings. Because of the threshold peaks and noise cut-off phenomena, there is no simple relation between corona currents and resultant noise levels.

6.3 Distance from Corona Point to Antenna and Noise Level

Noise from any source will decrease in intensity as the distance between the source and receiving antenna is increased. The manner in which this decrease takes place ($1/d$) is shown by Figures 26 and 32 which are drawn from positive point and negative point data, respectively. The noise-induced AVC voltage decreases by 50% (from 0.30V to 0.15V) as the distance between a positive point discharge and antenna D-2216 increases from 10 inches to 15 inches (Figure 26). Likewise, for a negative point (Figure 32), a 50 % decrease (from 1.0V to 0.5V) is seen when the distance increases from 10 inches to 15 inches. This is the $1/d^2$ relationship.

In both cases, when the distance exceeds 25 inches the curves level out, indicating that only small additional decreases can be obtained by further increases in distance. Distances greater than 25 inches, however, have reduced the noise to level I (less than 0.1V) in all test cases.

6.4 Radius of Curvature of the Corona Point and Noise Level

On the basis of electric field theory, Section 3.0 predicts that a blunt or rounded point will always be surrounded by a less intense electric field than a sharper point under similar conditions. Therefore, higher ambient fields will

AD-A072 057 ATLANTIC SCIENCE CORP INDIAN HARBOUR BEACH FL F/G 17/2.1
AN INVESTIGATION INTO THE NOISE INTERFERENCE PROBLEMS AT LOGAN --ETC(U)
APR 79 B J LIPOFSKY, R B BENT, S K LLEWELLYN DOT-FA77WAI-774
UNCLASSIFIED FAA-RD-79-58 NL

2 OF 2
AD
A072057

END
DATE
FILMED
9-79
DDC

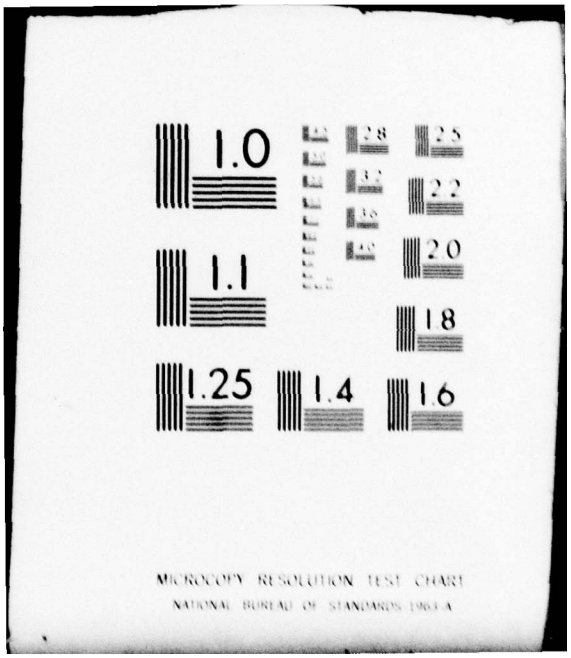
1.0
1.1
1.25
1.4
1.6
2.8
3.2
3.6
4.0
2.5
2.2
2.0
1.8
MICROCOPY RESOLUTION TEST CHART
NATIONAL BUREAU OF STANDARDS 1963-A

be required to initiate the discharge when the radius of curvature of the point is increased. These predictions are clearly shown to be true by Figure 28 (for a negative point) and Figure 33 (for a positive point). In both of these figures two tests are shown side-by-side. Trace C in both figures shows that the discharge is suppressed by placing a metal sphere with radius 0.5 inches (1.27 cm) over the needle point which had previously produced discharge currents of 100 μA. Since the discharge is suppressed, the noise associated with it is also reduced as shown by the recorded AVC voltage, trace B in both figures. The field strength during these tests went as high as 10^6 V/m (50kV across a 2 inch gap) without initiating discharge at the sphere. (Some corona discharge was produced at other less-rounded points on the high voltage equipment.)

6.5 Further Investigation Suggested by this Study

Corona discharge can occur at any sharp point, not just at the tips of lightning rods. If the recommendations of the previous section do not result in the reduction of noise problems at a particular site, it could be that corona discharge is occurring at unsuspected points. Thus, some means for finding corona sources must be developed. Optical methods relying upon the excitation of the ionized air during a discharge could accomplish this and allow for point-by-point location of corona noise sources.

The pulsating nature of the discharge is an important factor in the creation of radio noise. A typical pulse in the discharge process has a rise time of 10 nanoseconds which means that a Fourier analysis of the pulse shape would show frequency components in the region of 100 MHz.

Not only the distance between corona point and receiving antenna, but the entire geometry of the lightning rod, grounding leads, and building structure needs to be considered in more detail. Results discussed in Section 5.3.4, Other Effects, indicate that an entire lightning protection system may be considered to be an antenna for broadcasting corona noise. A study of corona noise as a function of lightning rod length and ground lead design might lead to the discovery of new methods for corona

noise suppression. The data presented in Figure 42 show that the coupling of corona noise from source to receiving antenna can be modified by a factor of 10 or more when minor changes are made in the geometry of conductors which are near the corona point. At the same time, however, the data show that this aspect of the problem is exceptionally complex.

The effects of the radome material in collecting charge and causing nearby structures such as radome, ladder or lightning rods to go into corona is significant.

Experiments should be performed with various radome surfaces with a view to reducing significantly the electrical charge causing the problem.

7.0 GENERAL RECOMMENDATIONS

These recommendations are given to assist not only improvement of the Logan Airport problem, but also to assist in the design of new installations or the removal of noise problems at other sites.

The noise problems have been shown to be caused by corona discharge or streamers which occur in the presence of high electric fields. The taller the structure on which the antennas are installed, the more likely the noise will occur. If there is a radome nearby, this also can become highly charged and lead to corona or streamer noise. Ideally, therefore, the antennas should be mounted on as low a structure as is feasibly allowable and not too close to a radome surface. The results show that the antennas should be placed at least 4 feet away from a corona source such as a lightning rod or the radome surface, in order for the interference to be kept to a minimum acceptable level. If it is impossible to attain the 4 foot distance, then the corona should be removed by reducing the radius of curvature at the source. For example, a 4" diameter sphere on the tip of a lightning rod at 300 feet will successfully remove the corona on all but very close lightning occasions. The lower the structure the smaller the radius of curvature required. It is also shown that such a blunt point will not distract the rods capabilities of being a good lightning protection device.

If lightning rods and their vertical ground leads have to be placed close to the antennas, then their effective vertical length should not be related to the electrical lengths of the VHF frequency (23.8 inches = $\lambda/4$ at 124 MHz).

Different types of antennas will not eliminate the noise which is an actual broadband transmission in the receiver band. The sophisticated noise limiting circuitry of the GRR-23 receiver did not cause any appreciable lowering of the noise signal again probably because of its high frequency components.

Corona noise occurring under positive electrical fields such as blowing snow conditions, is likely to lead to more severe VHF noise than that from

regular thunderstorms. The high electric fields may also persist several hundred miles away from the blowing snow in a clear blue sky, as the ions are carried by the wind over appreciable distances in the dry air.

More research is needed to investigate the effects of a highly charged radome, as streamers may be prevalant on the surface for considerable periods of time and corona may occur on nearby structures such as ladders and lattice framework.

8.0 REFERENCES

1. Trichel, G. W., The mechanism of the negative point to plane corona near onset, Phys. Rev. 54, 1078-84, 1938

2. Chapman, S., Corona point current in wind, JGR, 75, 2165-69, 1970.

3. Nanevicz, J. E., D. G. Douglas, Static-electricity analysis program, SAMSO TR 75-44, 1974.

4. Stratton, J. A., Electromagnetic theory, McGraw Hill, N. Y., 1941.

5. Morse, P. M., H. Feshbach, Methods of theoretical physics, McGraw Hill, N. Y., 1953.

6. Moore, C. B., Research into cloud electrification and its modification, Response to RANN Questionaire, 1977.

7. Standler, R. B., The response of elevated conductors to lightning, MS thesis, New Mexico Tech, 1975.

8. Chalmers, J. A., Atmospheric electricity, Pergamon Press, New York, 1967

APPENDIX A

VHF ANTENNAS AND RECEIVERS USED FOR NOISE TESTS

1.2.2 Physical Description.- Refer to section 9 for the physical characteristics of the units.

1.3 REFERENCE DATA.- Table 1-1 lists the reference data on the receivers.

Table 1-1. Reference Data, Radio Receiver, AN/GRR-23 and -24

Characteristic	Requirement
PHYSICAL (vhf or uhf unit)	
Dimensions	3-1/2 inches high, 19 inches wide, 12-1/4 inches deep (standard 19-inch rack or cabinet mounting).
Weight	22 pounds.
Cable requirements	Power cables and a mating plug for J2 supplied with equipment. Antenna and other interconnection cabling supplied by FAA.
ELECTRICAL	
Primary input power	05, 120, 210, or 240 volts ± 10%, single phase, 47 Hz to 240 Hz, 50 watts maximum. If a.c. power fails, a 24-volt lead-acid battery (when supplied) is automatically switched in to provide emergency power for a minimum period of 15 minutes.
FUNCTIONAL	
Vhf frequency range	115.00 MHz to 149.95 MHz with 680 channels spaced 50 kHz apart or 115.00 MHz to 149.975 MHz with 1,360 channels spaced 25 kHz apart.
Uhf frequency range	225.00 MHz to 399.95 MHz with 3,500 channels spaced 50 kHz apart or 225.00 MHz to 399.975 MHz with 7,000 channels spaced 25 kHz apart.
Frequency accuracy, vhf/uhf	Crystal controlled, with the oscillator in a semiconductor proportionally controlled crystal oven. No more than ±0.002% drift from operating frequency after 30 minute warmup.
Sensitivity (vhf and uhf)	With a 3.0-microvolt signal 30% ±5% modulated at 1 kHz. applied to antenna input from a 50-ohm source, an output of 100 milliwatts into a 600-ohm load with a 10:1 signal-plus-noise-to-noise ratio is obtained.
Selectivity (25 kHz and 50 kHz channel spacing)	Attenuation / 25 kHz Bandwidth / 50 kHz Bandwidth 6 dB / 20 kHz min / 36 kHz min 40 dB / 30 kHz max / 62 kHz max 60 dB / 42 kHz max / 70 kHz max 80 dB / 50 kHz max / 80 kHz max
IF output	With a 3.0 microvolt signal 30% modulated, produces a nominal output of 125 mV a.c.
Audio output	Two separate transformer outputs, each providing 100 milliwatts into a 600-ohm resistive load.
Audio frequency response	Not more than +1 dB or -2 dB from 300 Hz to 3000 Hz.
Automatic gain control	Receiver output shall not vary more than 3 dB as a 6-microvolt input signal modulated 30% ±5% increases to 1 volt.

Table 1-1. Reference Data, Radio Receiver, AN/GRR-23 and -24 (con.)

Characteristic	Requirement
Automatic gain control time constant	100-millisecond attack, 100-millisecond decay maximum.
Squelch	Receiver output muted, pending carrier application of not greater than 3.0 microvolts with squelch sensitivity at maximum setting, and not less than 5 microvolts with squelch at minimum setting.
Buffer amplifier	Provides impedance matching and isolation of the crystal filter (FL-1) from the mixer multiplier (A2).
Secure voice capability	Provides compatibility with the TSEC/KY-8, -28, and -38 speech security equipment when wide bandwidth crystal filter is used. Output is available at J2-G on receiver rear apron.
ENVIRONMENTAL	
Operating	Relative humidity: 5% to 95% (±5%) Altitude: 0 to 10,000 ft m.s.l.
Non-operating and storage	Ambient temperature: -62° C to +71° C Relative humidity: 5% to 95% Barometric pressure: 3.4 to 31 inches Hg
WARMUP TIME	30 minutes maximum using crystal oscillator; 5 minutes with oscillator-synthesizer.
IF FREQUENCY	20.6 MHz.
CRYSTALS	Standard type not supplied with equipment; CR-75/4 (holder type HC-6/4) stability to achieve frequency accuracy of ±0.0005%.

1.4 EQUIPMENT AND ACCESSORIES SUPPLIED.- The equipment making up the vhf and uhf receivers is listed in table 1-2.

Table 1-2. Equipment Supplied

Quantity	Item	Dimensions (inches) Height	Width	Depth	Unpacked Weight	Volume	Packed Weight	Volume
1	Receiver, Radio, AN/GRR-23 or -24	3-1/2	21	12-1/4	22 lb	0.52 cu ft	38 lb	3.0 cu ft
1	Power cable, 8006147G1 (included in above assembly)							

SUMMARY SHEET

TYPE RV-12B VHF FIXED-TUNED RECEIVER

1. Frequency range.- 115 to 152 MHz.
2. Number of preset frequencies.- One.
3. Type of frequency control.- Crystal.
4. Type of receiver.- Super heterodyne.
5. Intermediate frequency.- 18.3 MHz.
6. Receiver output.- Main audio output 1.0 watt into 20,000 ohm (or 600 ohm by changing tap) load impedance. Low level output 20 db below 1.0 watt into 600 ohms.
7. Type of reception.- AM
8. Crystal.- Type CR-65/U 24-33 MHz.
9. Squelch.- Open 3 microvolts STV.
10. Antenna input impedance.- 50 ohms unbalanced.
11. Bandwidth. 34 kHz minimum.
12. Tuning.- Crystal and individual alignment to a fixed frequency.
13. Power requirements.- 120 volts, 60 Hz, 86 watts.
14. Electron tube complement.- 4 type 6EH7 pentode; 1 type 6EJ7 pentode; 1 type 12AT7 dual-triode; 3 type 12AU7 dual triode; 1 type 12AX7 dual-triode; 1 type 6BX6 pentode; 1 type 6BQ5 pentode. Fuse complement.- One 1-ampere Slo Blow fuse.
15. Diode complement.- 4 type 1N2359; 3 type 1N903A, 1 type 1N658.
16. Furnished accessories.- Crystal oven; 1 Power cord, 24 inches; 1 Alignment tool.
17. Weight of RV-12B Receiver.- 30 lbs crated; 26 lbs uncrated.

TACO

TECHNICAL APPLIANCE CORPORATION
a subsidiary of
GENERAL INSTRUMENT CORPORATION
1 TACO STREET, SHERBURNE, N.Y. 13460
(607) 674-2211 TWX: 510-281-7440

MULDIPOL (TM) OMNIDIRECTIONAL MULTIPLE DIPOLE COLLINEAR ARRAYS

(patented)

116-150 MHz 225-400 MHz

D-2213 UHF/VHF ANTENNA

Featuring: RUGGED-TRANSPORTABLE-COMPACT-LIGHTWEIGHT-HIGH ISOLATION

The MULDIPOL (TM) Multiple Dipole Collinear Array concept has been especially developed by TACO for ground-air-ground, air traffic control and associated vehicular and base communications applications. This omnidirectional concept employs a unique method of shielding the feed cables to improve radiation pattern characteristics and also achieve a high degree of isolation between discrete elements within a closely spaced array. The result is a small, rugged, easy to install and lightweight package which utilizes minimal space and lends itself to tactical/transportable use in the most hostile environments.

Most applications for these types of antennas demand optimum utilization of space and a high degree of mobility. These requirements are eminently satisfied by the MULDIPOL (TM) concept of collinearly stacking. A minimum of 30 db isolation is realized between any two antenna elements in every MULDIPOL (TM) model, whereas it would require about 20 feet (6.10 m) separation between two horizontally displaced dipoles to achieve similar isolation where normally, on most towers, only 10 or 12 feet (3.05 or 3.66 m) is available.

The low profile (silhouette) of this antenna plus the resulting decrease in the number of antennas required at any one tower site also gives much improved radiation pattern coverage.

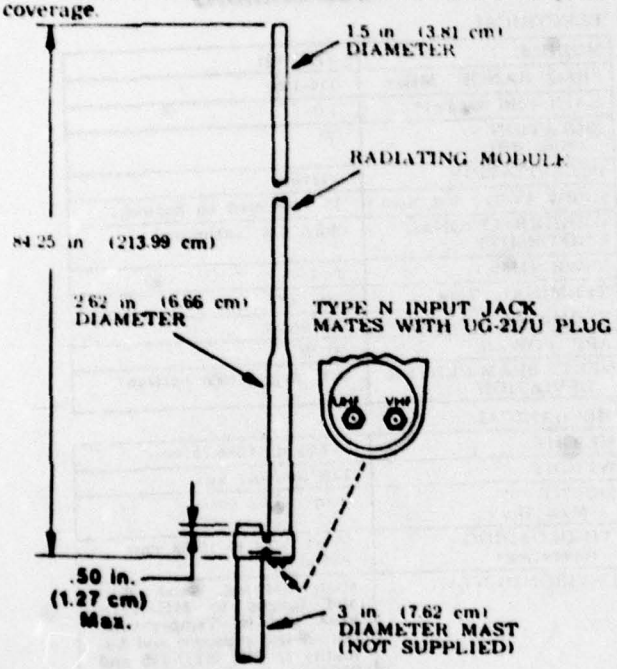

INDEPENDENTLY OPERATING VHF ANTENNA AND INDEPENDENTLY OPERATING UHF ANTENNA IN ONE MODULE. 97

SPECIFICATIONS

ELECTRICAL

MODULE	UHF (1)	VHF (1)
FREQ. RANGE (MHz)	225-400	116-150
* GAIN (dBi @ Fc)*	10	
ISOLATION (Min., dB)	35	
POLARIZATION	Vertical	
HPBW (Vert., deg, Nom.)	75 (centered on horizon)	
OMNIDIRECTIONAL UNIFORMITY	±0.5 dB (azimuth)	
VSWR (Max.)	2:1	
** TERMINAL: Type	"N" (2)	
TERMINAL: Impedance	50-ohms	
APP. POWER	50 W	
VERT. BEAM-CENTER DEVIATION	±10 deg. (from horizon)	

MECHANICAL

HEIGHT:	84.25 in. (213.99 cm)
WEIGHT	10.25 lbs. (4.65 kg)
MOUNT (Mast Dia.)	3 in. (7.62 cm)
WINDLOADING (operating)	65 kt. w/2 in. (5.08 cm) radial ice
ENVIRONMENTAL.	Rain, salt-fog, sand, dust and fungus to MIL-STD-810A and B; Temperature, barometric pressure and humidity to MIL-STD-210 and 210A.
RADOME MATERIAL.	Filament wound fiberglass

* Gain relative to an isotropic source
** Type "HN" available upon request

Rev. D

TACO

TECHNICAL APPLIANCE CORPORATION
a subsidiary of
GENERAL INSTRUMENT CORPORATION
1 TACO STREET, SHERBURNE, N.Y. 13460
(607) 674-2211 TWX: 510-261-7440

MULDIPOL(TM) OMNIDIRECTIONAL MULTIPLE DIPOLE COLLINEAR ARRAYS

(patented)

116-150 MHz

D-2212 VHF/VHF ANTENNA

Featuring: RUGGED-TRANSPORTABLE-COMPACT-LIGHTWEIGHT-HIGH ISOLATION

The MULDIPOL (TM) Multiple Dipole Collinear Array concept has been especially developed by TACO for ground-air-ground, air traffic control and associated vehicular and base communications applications. This omnidirectional concept employs a unique method of shielding the feed cables to improve radiation pattern characteristics and also achieve a high degree of isolation between discrete elements within a closely spaced array. The result is a small, rugged, easy to install and lightweight package which utilizes minimal space and lends itself to tactical/transportable use in the most hostile environments.

Most applications for these types of antennas demand optimum utilization of space and a high degree of mobility. These requirements are eminently satisfied by the MULDIPOL (TM) concept of collinearly stacking. A minimum of 30 db isolation is realized between any two antenna elements in every MULDIPOL (TM) model, whereas it would require about 20 feet (6.10 m) separation between two horizontally displaced dipoles to achieve similar isolation where normally, on most towers, only 10 or 12 feet (3.05 or 3.66 m) is available.

The low profile (silhouette) of this antenna plus the resulting decrease in the number of antennas required at any one tower site also gives much improved radiation pattern coverage.

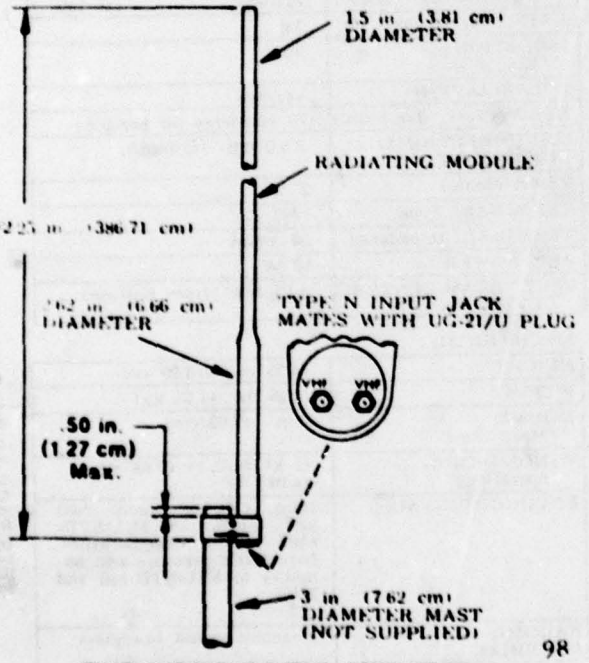

TWO INDEPENDENTLY OPERATING VHF ANTENNAS IN ONE MODULE

98

SPECIFICATIONS

ELECTRICAL

MODULE	VHF (2)
FREQ. RANGE (MHz)	116-150
* GAIN (dBi @ Fc)*	10
ISOLATION (Min., dB)	30
POLARIZATION	Vertical
HPBW (Vert., deg, Nom.)	75 (centered on horizon)
OMNIDIRECTIONAL UNIFORMITY	±0.5 dB (azimuth)
VSWR (Max.)	2:1
** TERMINAL: Type	"N" (2)
TERMINAL: Impedance	50 - ohms
APP. POWER	50 W
VERT. BEAM-CENTER DEVIATION	±10 deg. (from horizon)

MECHANICAL

HEIGHT:	152.25 in. (386.71 cm)
WEIGHT	125 lbs (56.7 kg)
MOUNT (Mast Dia.)	3 in. (7.62 cm)
WINDLOADING (operating)	65 kt. w/2 in. (5.08 cm) radial ice
ENVIRONMENTAL:	Rain, salt-fog, sand, dust and fungus to MIL-STD-810A and B; Temperature, barometric pressure and humidity to MIL-STD-210 and 210A.
RADOME MATERIAL:	Filament wound fiberglass

* Gain relative to an isotropic source
** Type "HN" available upon request

Rev D

TACO

TECHNICAL APPLIANCE CORPORATION
a subsidiary of
GENERAL INSTRUMENT CORPORATION
1 TACO STREET, SHERBURNE, N.Y. 13460
(607) 674-2211 TWX: 510-281-7440

MODEL D-2216 OMNIDIRECTIONAL VHF ANTENNA

(MULDIPOL (TM) CONCEPT)

patented

Featuring: RUGGED–TRANSPORTABLE–COMPACT–LIGHTWEIGHT

This design utilizes the MULDIPOL (TM) concept especially developed by TACO for ground-air-ground, air-traffic-control and associated vehicular and base communication applications.

This VHF Antenna is a halfwave, vertically polarized dipole enclosed in a 1.5 in. (3.81 cm) diameter fiberglass radome. It is a completely sealed, lightweight and simple to install unit. Its low profile produces less pattern deterioration in transmission/reception relative to adjacent antennas on the same tower, such as the types that have been in common use over the past 20 years.

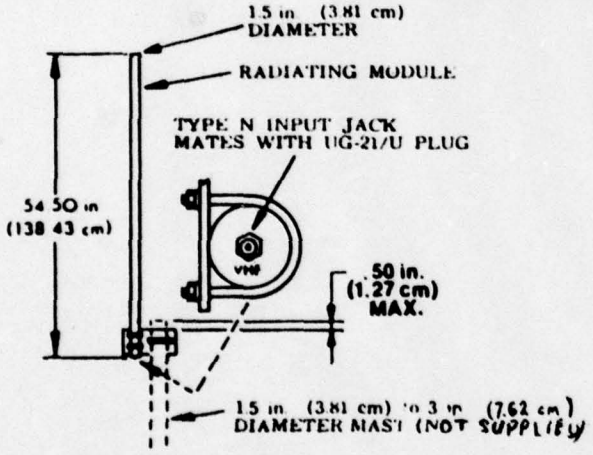

VHF ANTENNA

SPECIFICATIONS

ELECTRICAL

MODULE	VHF (1)
FREQ. RANGE (MHz)	100-156
GAIN (dBi @ Fc)	1.0
POLARIZATION	Vertical, omnidirectional
HPBW (Vert., deg.)	75 (centered on horizon)
OMNIDIRECTIONAL UNIFORMITY	±0.5 deg. (azimuth)
VSWR (Nom.)	2:1
TERMINAL: Type	"N" (1)
TERMINAL: Impedance	50 - ohms
APP. POWER	50 W
VERT. BEAM-CENTER DEVIATION	±10 deg. (from horizon)

MECHANICAL

HEIGHT	54.50 in. (138.43 cm)
WEIGHT	5.5 LBS. (2.49 kg)
MOUNT (Mast Dia.)	1.5 in. (3.81 cm) to 3 in. (7.62 cm)
WINDLOADING (operating)	65 kt. w/2 in. (5.08 cm) radial ice
ENVIRONMENTAL	Rain, salt-fog, sand, dust and fungus to MIL-STD-810A and B; Temperature, barometric pressure and humidity to MIL-STD-210 and 210A.
RADOME MATERIAL	Filament wound fiberglass

*Compared to an isotropic source
**Type "HN" available upon request